



National Library  
of Canada

Bibliothèque nationale  
du Canada

Canadian Theses Service

Service des thèses canadiennes

Ottawa, Canada  
K1A 0N4

## NOTICE

The quality of this microform is heavily dependent upon the quality of the original thesis submitted for microfilming. Every effort has been made to ensure the highest quality of reproduction possible.

If pages are missing, contact the university which granted the degree.

Some pages may have indistinct print especially if the original pages were typed with a poor typewriter ribbon or if the university sent us an inferior photocopy.

Reproduction in full or in part of this microform is governed by the Canadian Copyright Act, R.S.C. 1970, c. C-30, and subsequent amendments.

## AVIS

La qualité de cette microforme dépend grandement de la qualité de la thèse soumise au microfilmage. Nous avons tout fait pour assurer une qualité supérieure de reproduction.

S'il manque des pages, veuillez communiquer avec l'université qui a conféré le grade.

La qualité d'impression de certaines pages peut laisser à désirer, surtout si les pages originales ont été dactylographiées à l'aide d'un ruban usé ou si l'université nous a fait parvenir une photocopie de qualité inférieure.

La reproduction, même partielle, de cette microforme est soumise à la Loi canadienne sur le droit d'auteur, SRC 1970, c. C-30, et ses amendements subséquents.

UNIVERSITY OF ALBERTA

AIR ENTRAINMENT AT FREE OVERFALLS

BY

ALBERT KWAN

A thesis submitted to the Faculty of Graduate Studies and Research  
in partial fulfillment of the requirements for the degree of MASTER  
OF SCIENCE.

IN

WATER RESOURCES

DEPARTMENT OF CIVIL ENGINEERING

Edmonton, Alberta

FALL, 1991



National Library  
of Canada

Bibliothèque nationale  
du Canada

Canadian Theses Service    Service des thèses canadiennes

Ottawa, Canada  
K1A 0N4

The author has granted an irrevocable non-exclusive licence allowing the National Library of Canada to reproduce, loan, distribute or sell copies of his/her thesis by any means and in any form or format, making this thesis available to interested persons.

The author retains ownership of the copyright in his/her thesis. Neither the thesis nor substantial extracts from it may be printed or otherwise reproduced without his/her permission.

L'auteur a accordé une licence irrévocable et non exclusive permettant à la Bibliothèque nationale du Canada de reproduire, prêter, distribuer ou vendre des copies de sa thèse de quelque manière et sous quelque forme que ce soit pour mettre des exemplaires de cette thèse à la disposition des personnes intéressées.

L'auteur conserve la propriété du droit d'auteur qui protège sa thèse. Ni la thèse ni des extraits substantiels de celle-ci ne doivent être imprimés ou autrement reproduits sans son autorisation.

ISBN 0-315-69987-6

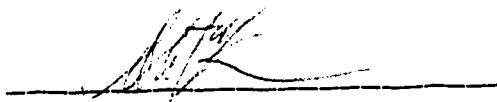
Canada

UNIVERSITY OF ALBERTA  
RELEASE FORM

NAME OF AUTHOR : ALBERT Y. P. KWAN  
TITLE OF THESIS : AIR ENTRAINMENT AT FREE OVERFALLS  
DEGREE : MASTER OF SCIENCE  
YEAR THIS DEGREE GRANTED : FALL 1991

Permission is hereby granted to the University of Alberta Library to reproduce single copies of this thesis and to lend or sell such copies for private, scholarly or scientific research purposes only.

The author reserves all other publication and other rights in association with the copyright in the thesis, and except as hereinbefore provided neither the thesis nor any substantial portion thereof may be printed or otherwise reproduced in any material from whatever without the author's prior written permission.



PERMANENT ADDRESS:

15016 - 63 Street  
Edmonton, Alberta  
Canada  
T5A 2B8

DATED : OCT 01, 1991

THE UNIVERSITY OF ALBERTA

FACULTY OF GRADUATE STUDIES AND RESEARCH

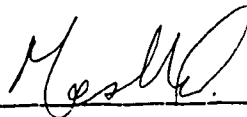
The undersigned certify that they have read and recommend to the Faculty of Graduate Studies and Research for acceptance, a thesis entitled AIR ENTRAINMENT AT FREE OVERFALLS submitted by ALBERT Y. P. KWAN in partial fulfillment of the requirements for the degree of MASTER OF SCIENCE.



Dr. N. Rajaratnam, Supervisor



Dr. P. M. Steffler



Dr. J. H. Masliyah

Date : SEPT 25, 1991

## **ABSTRACT**

Air entrainment downstream of a free overfall is one method for improving water quality. While a good understanding of the hydraulics of flow below overfalls has been developed, a complete understanding of the air entrainment characteristics is far from being realized especially for the plunge pool conditions of free overfall.

Air entrainment characteristics are, in some ways, related to the flow conditions of the free overfall. With this in mind, the current knowledge for both the flow hydraulics and air entrainment characteristics of free overfall were first reviewed. A probe was then built in order to measure the mean air concentrations in the hydraulic jump and plunge pool conditions of a free overfall in a series of laboratory experiments. The maximum air entrainment characteristics were found in the critical hydraulic jump conditions and related to the corresponding Drop numbers. The air entrainment characteristics in the plunge pool conditions were also shown to have unique relationships with the corresponding tailwater depths as well.

## **ACKNOWLEDGEMENTS**

The author would like to thank Dr. N. Rajaratnam for his support, inspiration and guidance in this study. The assistance of Mr. S. Lovell and Mr. M. Jasek in setting up and maintaining the experimental apparatus, especially in developing the air concentration probe, is greatly appreciated. The help of Mr. M. Jasek and Mr. R. Haley in the photographic study and the high speed video work respectively is also greatly appreciated. Special appreciation is given to Mr. O. Aderibigbe for proof-reading this thesis with great patience. Financial support for the author was provided by the Postgraduate Scholarship from the Natural Science and Engineering Research Council. Finally, the author is forever indebted to his wife, Anita, for her encouragement and understanding as well. The arrival of our daughter, Adoria, in conjunction with the completion of this thesis at the same year marks a special occasion to give thanks to God.

## **TABLE OF CONTENTS**

| CHAPTER                                 | PAGE |
|---|------|
| 1. INTRODUCTION                         | 1    |
| 1.1 AIR AND WATER                       | 1    |
| 1.2 FREE OVERFALL                       | 2    |
| 2. HYDRAULICS OF THE FREE OVERFALL      | 4    |
| 2.1 INTRODUCTION                        | 4    |
| 2.2 FLOW CHARACTERISTICS                | 4    |
| 2.2.1 Supercritical Shooting Jet        | 5    |
| 2.2.2 Hydraulic Jump                    | 8    |
| 2.2.3 Plunge Pool                       | 11   |
| 2.2.4 Breaking Surface Waves            | 12   |
| 2.3 AIR ENTRAINMENT CHARACTERISTICS     | 13   |
| 2.3.1 Supercritical Shooting Jet        | 15   |
| 2.3.2 Hydraulic Jump                    | 17   |
| 2.3.3 Plunge Pool                       | 19   |
| 2.3.4 Breaking Surface Waves            | 22   |
| 2.4 CONCLUSIONS                         | 23   |
| 3. EXPERIMENTAL ARRANGEMENT             | 25   |
| 3.1 INTRODUCTION                        | 25   |
| 3.2 EXPERIMENTAL EQUIPMENT              | 25   |
| 3.2.1 Flume Setup                       | 26   |
| 3.2.2 Air Concentration Probe           | 29   |
| 3.3 MEASUREMENT TECHNIQUE               | 33   |
| 3.3.1 General Measurements              | 33   |
| 3.3.2 Probe Calibration                 | 33   |
| 3.4 CONCLUSIONS                         | 39   |
| 4. EXPERIMENTS AND EXPERIMENTAL RESULTS | 41   |
| 4.1 INTRODUCTION                        | 41   |
| 4.2 EXPERIMENTAL WORK                   | 41   |
| 4.2.1 Flow Characteristics              | 42   |
| 4.2.2 Air Concentration Measurements    | 43   |
| 4.3 EXPERIMENTAL RESULTS                | 45   |
| 4.3.1 Flow Characteristics              | 51   |
| 4.2.2 Air Concentration Results         | 51   |
| 4.4 CONCLUSIONS                         | 55   |



|   |     |
|---|-----|
| 5. ANALYSIS OF EXPERIMENTAL RESULTS           | 72  |
| 5.1 INTRODUCTION                              | 72  |
| 5.2 FLOW CHARACTERISTICS                      | 72  |
| 5.2.1 Plunge Pool                             | 73  |
| 5.2.1.1 Jump beginning depth                  | 74  |
| 5.2.1.2 Jump beginning length                 | 77  |
| 5.2.2 Bed hitting length                      | 77  |
| 5.2.3 Breaking Surface Waves                  | 82  |
| 5.3 AIR ENTRAINMENT ANALYSIS                  | 82  |
| 5.3.1 Hydraulic Jump                          | 84  |
| 5.3.1.1 Maximum mean air concentrations       | 85  |
| 5.3.1.2 Air entrainment rates                 | 87  |
| 5.3.2 Plunge Pool                             | 89  |
| 5.3.2.1 Maximum mean air concentrations       | 91  |
| 5.3.2.2 Air entrainment rates                 | 93  |
| 5.3.2.3 Mean air concentration profiles       | 98  |
| 5.4 CONCLUSIONS                               | 104 |
| 6. CONCLUSIONS                                | 107 |
| 6.1 REVIEW                                    | 107 |
| 6.2 PRESENT CONTRIBUTIONS                     | 108 |
| 7. RECOMMENDATIONS                            | 110 |
| 7.1 FLOW CHARACTERISTICS                      | 110 |
| 7.2 ENTRAINMENT CHARACTERISTICS               | 110 |
| REFERENCES                                    | 111 |
| APPENDIX : AERATION OVER HYDRAULIC STRUCTURES | 115 |

## LIST OF FIGURES

| FIGURE  | TITLE  | PAGE |
|---------|--|------|
| 2.1     | Free Overfall Flow with Supercritical Shooting Jet   | 6    |
| 2.2 (a) | Hydraulic Jump away from the Overfall  | 9    |
| 2.2 (b) | Hydraulic Jump at the Toe of the Falling Jet   | 10   |
| 2.2 (c) | Submerged Hydraulic Jump   | 10   |
| 2.3     | Free Overfall Flow with Breaking Surface Waves   | 13   |
| 3.1     | General Flume Setup  | 27   |
| 3.2     | Self-Contained Water Circulatory System  | 28   |
| 3.3     | Air Concentration Probe  | 29   |
| 3.4     | Circuit Diagram of Mean Air Concentration Indicator  | 32   |
| 3.5     | Comparison of the Mean Air Concentration Predictions   | 38   |
| 3.6     | Variation of Alpha Value with Time   | 40   |
| 4.1     | Locations of Mean Air Concentration Measurements   | 44   |
| 4.2     | Relationship between Tailwater Depth and Jump Beginning Depth  | 52   |
| 4.3     | Relationship between Tailwater Depth and Jump Beginning Length   | 53   |
| 4.4     | Relationship between Tailwater Depth and Bed Hitting Length  | 54   |
| 4.5 (a) | Mean Air Concentration Profiles at Centreline with Q of 40 L/s and $y_t$ of 0.200 m (Hydraulic Jump)   | 56   |
| 4.5 (b) | Mean Air Concentration Profiles at Centreline with Q of 40 L/s and $y_t$ of 0.231 m                    | 57   |
| 4.5 (c) | Mean Air Concentration Profiles at Centreline with Q of 40 L/s and $y_t$ of 0.312 m                    | 58   |
| 4.5 (d) | Mean Air Concentration Profiles at Centreline with Q of 40 L/s and $y_t$ of 0.407 m                    | 59   |
| 4.5 (e) | Mean Air Concentration Profiles at Centreline with Q of 40 L/s and $y_t$ of 0.505 m                    | 60   |
| 4.6 (a) | Mean Air Concentration Profiles at Wall Section with Q of 40 L/s and $y_t$ of 0.200 m (Hydraulic Jump) | 61   |
| 4.6 (b) | Mean Air Concentration Profiles at Wall Section with Q of 40 L/s and $y_t$ of 0.231 m                  | 62   |

|         |   |    |
|---------|---|----|
| 4.6 (c) | Mean Air Concentration Profiles at Wall Section with Q of 40 L/s and $y_t$ of 0.312 m                         | 63 |
| 4.6 (d) | Mean Air Concentration Profiles at Wall Section with Q of 40 L/s and $y_t$ of 0.407 m                         | 64 |
| 4.6 (e) | Mean Air Concentration Profiles at Wall Section with Q of 40 L/s and $y_t$ of 0.505 m                         | 65 |
| 4.7 (a) | Mean Air Concentration Vertical Profiles at Centreline with Q of 40 L/s and $y_t$ of 0.200 m (Hydraulic Jump) | 66 |
| 4.7 (b) | Mean Air Concentration Vertical Profiles at Centreline with Q of 40 L/s and $y_t$ of 0.231 m                  | 67 |
| 4.7 (c) | Mean Air Concentration Vertical Profiles at Centreline with Q of 40 L/s and $y_t$ of 0.312 m                  | 68 |
| 4.7 (d) | Mean Air Concentration Vertical Profiles at Centreline with Q of 40 L/s and $y_t$ of 0.407 m                  | 69 |
| 4.7 (e) | Mean Air Concentration Vertical Profiles at Centreline with Q of 40 L/s and $y_t$ of 0.505 m                  | 70 |
| 5.1     | Relationship between Tailwater Depth Ratio and Jump Beginning Depth Ratio                                     | 75 |
| 5.2     | Comparison of Tailwater Depth Ratio with Drop Number  | 76 |
| 5.3     | Relationship between Tailwater Depth Ratio and Jump Beginning Length Ratio                                    | 78 |
| 5.4     | Comparison between Bed Hitting Length Ratio with Drop Number  | 80 |
| 5.5     | Relationship between Tailwater Depth Ratio and Bed Hitting Length Ratio                                       | 81 |
| 5.6     | Onset Condition for Flow with Breaking Surface Waves  | 83 |
| 5.7     | Two Air Entrainment Locations for Hydraulic Jump  | 84 |
| 5.8     | Relationship between Maximum Mean Air Concentrations and Drop Number  | 86 |
| 5.9     | Relationship between Maximum Air Entrainment Ratio and Drop Number  | 88 |
| 5.10    | Typical Vertical Profiles of Maximum Mean Air Concentration for Q of 40 L/s                                   | 92 |
| 5.11    | Relationship between Tailwater Depth Ratio and Depth Averaged Maximum Mean Air Concentration                  | 94 |
| 5.12    | Relationship between Tailwater Depth Ratio and Depth Averaged Maximum Mean Air Concentration Ratio            | 95 |

|          |   |     |
|----------|---|-----|
| 5.13     | Relationship between Tailwater Depth Ratio and<br>Maximum Air Entrainment Ratio in Plunge<br>Pool | 97  |
| 5.14     | Relationship between Tailwater Depth Ratio and<br>Absolute Air Entrainment Ratio                  | 99  |
| 5.15 (a) | Dimensionless Longitudinal Profile with Q of 40 L/s<br>and $y_t$ of 0.231 m                       | 100 |
| 5.15 (b) | Dimensionless Longitudinal Profile with Q of 40 L/s<br>and $y_t$ of 0.312 m                       | 101 |
| 5.15 (c) | Dimensionless Longitudinal Profile with Q of 40 L/s<br>and $y_t$ of 0.407 m                       | 102 |
| 5.15 (d) | Dimensionless Longitudinal Profile with Q of 40 L/s<br>and $y_t$ of 0.505 m                       | 103 |

## LIST OF PHOTOGRAPHIC PLATES

| PLATE   | TITLE   | PAGE |
|---------|---|------|
| 3.1     | General Flume Setup   | 28   |
| 3.2 (a) | Air Concentration Probe View 1  | 30   |
| 3.2 (b) | Air Concentration Probe View 2  | 30   |
| 3.2 (c) | Air Concentration Probe View 3  | 31   |
| 3.3     | Time Integrated A.C. Dial Gauge   | 32   |
| 3.4     | Calibration of Known Air Supply (Step 1)                                | 35   |
| 3.5     | Air Rising Through the Calibration Flask (Step 2)                       | 36   |
| 3.6     | Air Concentration Probe in the Calibration Flask<br>(Step 4)            | 37   |
| 4.1 (a) | Photographic Work, $Q=15$ L/s, Time= $1/60$ s with<br>Flash             | 46   |
| 4.1 (b) | Photographic Work, $Q=15$ L/s, Time= $1/60$ s                           | 46   |
| 4.1 (c) | Photographic Work, $Q=15$ L/s, Time= $1/8$ s                            | 47   |
| 4.1 (b) | Photographic Work, $Q=15$ L/s, Time=30 s                                | 47   |
| 4.2 (a) | High Speed Video, $Q=35$ L/s, Supercritical Shooting<br>Jet             | 48   |
| 4.2 (b) | High Speed Video, $Q=35$ L/s, $y_t=0.240$ m                             | 48   |
| 4.2 (c) | High Speed Video, $Q=35$ L/s, $y_t=0.320$ m                             | 49   |
| 4.2 (d) | High Speed Video, $Q=35$ L/s, $y_t=0.425$ m                             | 49   |
| 4.2 (e) | High Speed Video, $Q=35$ L/s, $y_t=0.515$ m                             | 50   |
| 4.2 (f) | High Speed Video, $Q=35$ L/s, $y_t=0.560$ m (breaking<br>surface waves) | 50   |
| 5.1 (a) | Close-up High Speed Video, $Q=35$ L/s, $y_t=0.320$ m                    | 89   |
| 5.1 (b) | Close-up High Speed Video, $Q=35$ L/s, $y_t=0.425$ m                    | 90   |
| 5.1 (c) | Close-up High Speed Video, $Q=35$ L/s, $y_t=0.515$ m                    | 90   |

## LIST OF SYMBOLS

- $A_\beta$  Absolute air entrainment ratio or ratio of maximum air entrainment rate to the critical maximum entrainment rate.
- $C$  Mean air concentration or ratio of volume of air to total volume involved.
- $C_a$  Depth averaged maximum mean air concentration.
- $C_b$  Backpool maximum mean air concentration or maximum mean air concentration found in backpool area.
- $C_c$  Critical maximum mean air concentration or maximum mean air concentration found in the critical hydraulic jump condition of free overfall.
- $C_m$  Maximum mean air concentration.
- $D$  Drop number =  $q^2/gh^3$ .
- $F_r$  Froude number =  $v_1/\sqrt{gy_1}$ .
- $g$  Gravitational acceleration which is taken to be 9.81 m/s<sup>2</sup>.
- $h$  Height of the drop for the free overfall.
- $k$  Air entrainment constant.
- $l_d$  Drop length or the distance from the brink to the location of  $y_1$  at the critical hydraulic jump condition of free overfall.
- $l_j$  Jump beginning length or the distance from the brink to the beginning of hydraulic jump/ the receiving pool water hits the falling jet.
- $l_m$  Maximum mean air concentration length or the distance from the brink to the location of maximum mean air concentration.
- $l_p$  Bed hitting length or the distance between the brink and the location for the centreline of the falling jet to hit the channel bed.

|           |  |
|-----------|--|
| $l_{pc}$  | Bed hitting length for to the critical hydraulic jump condition of free overfall.                          |
| $q$       | Discharge of water per unit width of the crest of overfall.  |
| $q_a$     | Rate of air entrainment per unit width.  |
| $q_{ab}$  | Rate of air entrainment in the backpool area per unit width.   |
| $q_{ac}$  | Rate of air entrainment for the critical hydraulic jump condition of overfall per unit width.              |
| $q_{ap}$  | Rate of air entrainment for the plunge pool area per unit width.   |
| $Q$       | Discharge of Water.  |
| $R_{ED}$  | Measured resistance between the air concentration probe in water alone, i.e. without air entrainment.      |
| $R_h$     | Hydraulic radius.  |
| $R_R$     | Measured resistance of the reference resistor.   |
| $u$       | Velocity distribution.   |
| $v$       | Averaged velocity.   |
| $v_1$     | Averaged velocity just before an ordinary hydraulic jump formed in a channel.                              |
| $v_e$     | Jet entry velocity for the plunge pool condition.  |
| $IV_{EI}$ | Measured potential difference of the air concentration probe scaled so that it varies between 0.0 and 1.0. |
| $x$       | Horizontal distance originated from the brink.   |
| $y$       | Vertical distance originated from the bed of the channel.  |
| $y_1$     | Water depth at the location just before the hydraulic jump/ the receiving pool hits the falling jet.       |

|               |   |
|---------------|---|
| $y_2$         | Sequent depth of water after the hydraulic jump.                              |
| $y_b$         | Depth of water at the backpool area of the overfall.                          |
| $y_c$         | Critical depth of water upstream of the overfall.                             |
| $y_j$         | Depth of water at the toe of the falling jet.                                 |
| $y_t$         | Tailwater depth or depth of water far downstream of the overfall.             |
| $z$           | Air entrainment exponent.   |
| $\alpha$      | Alpha value = $1 + (R_{EO} / R_R)$  |
| $\beta$       | Ratio of air entrainment rate to water discharge rate.                        |
| $\beta_b$     | Ratio of backpool maximum air entrainment rate to water discharge rate.       |
| $\beta_c$     | Ratio of critical maximum air entrainment rate to water discharge rate.       |
| $\beta_p$     | Ratio of maximum air entrainment rate in plunge pool to water discharge rate. |
| $\vartheta$   | Volume of water.  |
| $\vartheta_a$ | Volume of air.  |
| $\vartheta_t$ | Total volume involved = $\vartheta + \vartheta_a$ .                           |
| $\omega$      | Rising speed of air bubbles in water due to buoyancy.                         |

Other symbols used are defined in the text.



## **CHAPTER 1**

### **INTRODUCTION**

#### **1.1 AIR AND WATER**

Air and water are the two most important ingredients for the survival of most living beings. In normal circumstances, air exists in the gas phase while water flows in the liquid phase. The density of air is about one thousand times lighter than water. Due to gravity and the large density difference, air and water do not usually mix together except in a thin interface area where evaporation and condensation take place. However, air and water do mix together in some special circumstances. These special circumstances include high velocity water on the spillway surface, pump intake areas, hydraulic jumps and plunge pools.

Whenever air and water mix, the water surface will become 'white'. This water whiteness is an important indication of air entrainment into the water body. Air entrainment into water can be both detrimental and advantageous. On one hand, air entrainment can cause 'bulking' of the flow depth or even damage pumps. On the other hand, air entrainment can cushion the cavitation damage in high velocity flow (Rutschmann, 1988) or improve water quality (Leutheusser et.al., 1973). In this environmentally conscious society, water quality has become one of the important issues. Air entrainment is one of the most effective ways to improve or restore the water quality of a waterway by encouraging the transfer of oxygen from the atmosphere to the water body.

The original intent of this research was to study the dissolved oxygen transfer or aeration over hydraulic structures. However, the problem was found to be too complicated for the purpose of this research and the topic was subsequently changed. Nevertheless, a summary on aeration over hydraulic structures is included in the appendix of this thesis.

## 1.2 FREE OVERFALL

The free overfall is an interesting channel feature. This particular channel feature can both be attractive and functional at the same time. Naturally occurring waterfalls are prime tourist attractions while simple drop structures are effective energy dissipators. Furthermore, the flow pattern at a free overfall can vary over a wide range depending upon the downstream conditions. With rising tailwater depths, flow at a free overfall changes from a supercritical shooting jet to a hydraulic jump then to a plunge pool and finally a breaking surface waves. Moreover, different air entrainment characteristics are the direct results of different flow conditions of the free overfall. This work attempts, therefore, to associate the air entrainment characteristics with the corresponding flow conditions of the free overfall.

In view of the above mentioned objectives, this thesis will present the results of this research in a systematic way. The existing knowledge on the hydraulics of the free overfall, regarding both the general flow and air entrainment aspects, will be addressed in chapter 2. Chapter 3 will describe the experiment arrangement

while chapter 4 will present the experimental results. The analysis of experimental results will be presented in chapter 5. The conclusions and recommendations for future work will be presented in chapters 6 and 7 respectively. Finally, a list of references is provided at the end of the thesis.

## **CHAPTER 2**

### **HYDRAULICS OF THE FREE OVERFALL**

#### **2.1 INTRODUCTION**

A free overfall is one of the channel features that can be found in both natural and man-made situations. Natural waterfalls are usually founded in bedrock regions while drop structures are usually built in irrigation systems to control the slope of channels. The general flow characteristics of the free overfall have been studied extensively. However, air entrainment at the free overfall has not been studied.

#### **2.2 FLOW CHARACTERISTICS**

A free overfall is a channel discontinuity where water from the upstream channel drops a finite height and hits a receiving channel bed downstream. The location where the water leaves the upstream channel is called the brink and the immediate area around the brink is referred to as the overfall. The downstream receiving channel is usually called the base of the overfall. The tailwater condition is a characteristic of the channel downstream from the base of the overfall.

Traditional interest has been centered on the overfall itself because of its use either as a form of spillway or as a method of flow measurement. Apart from these matters of practical interest, the overfall itself, which can be considered as a sharp-crested weir

of zero height, is also a big challenge to the theoreticians who have attempted to obtain a complete theoretical solution. These problems are interesting and complex enough to warrant individual treatment. However, our interest is focused on the areas other than the overfall itself. Therefore, the hydraulics of the overfall itself will not be presented in this thesis. Readers are referred to the work by Hager (1983) or the summaries provided by Chow (1966) and Henderson (1966) for a critical discussion.

Two major factors affect the flow conditions at the base of a overfall. These factors are the upstream inflow and the downstream tailwater conditions. For each discharge, four different flow regimes can be recognized at the base of the overfall for different tailwater conditions. These flow regimes include supercritical shooting jet, hydraulic jump, plunge pool and breaking surface waves. Most of the previous studies have concentrated on the supercritical shooting jet and hydraulic jump regimes while little attention have paid to the plunge pool and breaking surface waves regimes. The following sections will discuss the current knowledge of the four flow regimes at the base of the overfall.

### 2.2.1 Supercritical Shooting Jet

Figure 2.1 shows the flow at a free overfall with a supercritical shooting jet. As seen from Figure 2.1, the depth of water behind the falling jet is greater than the depth of water downstream. Moore (1943) derived from the momentum principle and obtained the following relationship for the water depth behind the

fall, referred to as the backpool water depth :

$$\left(\frac{y_b}{y_c}\right)^2 = \left(\frac{y_j}{y_c}\right)^2 + 2\left(\frac{y_c}{y_j}\right) - 3 \quad (2.1)$$

where :  $y_b$  is the backpool water depth,  
 $y_c$  is the critical depth upstream of the overfall, and  
 $y_j$  is the water depth at the toe of the falling jet.

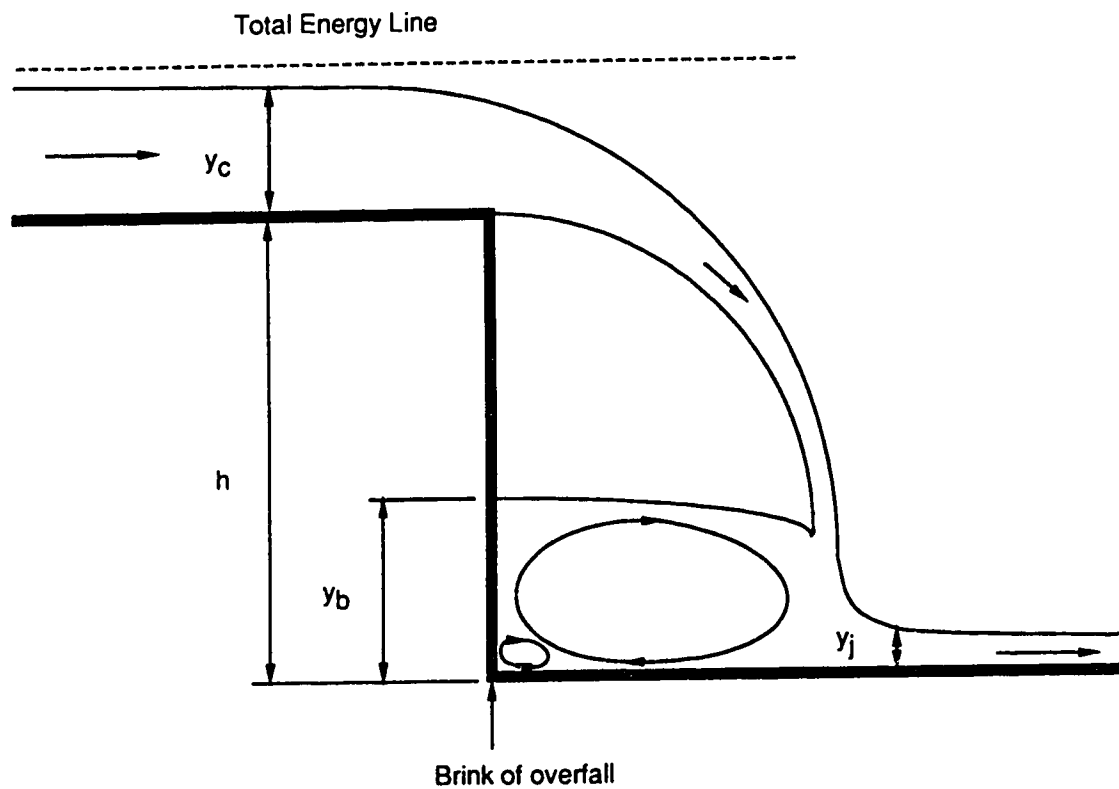


FIGURE 2.1 Free Overfall Flow with Supercritical Shooting Jet

Rand introduced in 1955 the parameter Drop number,  $D$ , which is defined as :

$$D = \frac{q^2}{gh^3} = \left(\frac{y_c}{h}\right)^3 \quad (2.2)$$

where :  $q$  is the water discharge per unit width,  
 $g$  is the gravitational acceleration, and  
 $h$  is the drop height.

Rand argued that all dimensionless flow characteristics should be functions of the Drop number and proposed the following relationship for the backpool water depth :

$$\frac{y_b}{h} = D^{0.22} \quad (2.3)$$

Moore (1943) also found from his experiments that the energy loss at the base of the overfall with a supercritical shooting jet was quite significant. In some instances, the energy loss was found to be in excess of 50% of the original energy. In the discussion of Moore's work, White (1943) derived an equation for this energy loss, which agreed remarkably well with Moore's experimental data, using some simple assumptions and basic equations. However, the assumptions used by White were quite drastic and more realistic assumptions were used by Gill (1979) to obtain another theoretical equation. The resulting theory is in closer agreement with experiment and the empirical equations of Rand than White's theory.

Since this research is not concerned with the area of energy loss, readers are referred to the quoted references for more details.

### 2.2.2 Hydraulic Jump

The upstream influence on free overfall gives rise to the supercritical shooting jet. On the other hand, rising downstream tailwater depth will try to impose a subcritical flow at the base of the overfall. The result is a conflict between the upstream supercritical and downstream subcritical flows. The transition occurs in the form of a hydraulic jump.

The sequent or conjugate depths relationship of an ordinary hydraulic jump formed in a level rectangular channel is well-known and the relationship is usually given as follows :

$$\frac{y_2}{y_1} = \frac{1}{2} (\sqrt{1 + 8F_r^2} - 1) \quad (2.4)$$

where :  $y_1$  is the water depth just before the hydraulic jump,  
 $y_2$  is the subcritical sequent water depth after the jump,  
 and  
 $F_r$  is the upstream Froude number and is written as :

$$F_r = \frac{v_1}{\sqrt{gy_1}} \quad (2.5)$$

where :  $v_1$  is the average velocity just upstream of the jump.



Three different kinds of hydraulic jumps are found at the base of an overfall. The first kind forms at some distance away from the falling jet. The second kind forms at the toe of the falling jet. The third kind forms before the toe of the falling jet which is usually called a submerged hydraulic jump. Interestingly, a submerged hydraulic jump is also part of the plunge pool regime. Figures 2.2 (a) to (c) show these three different kinds of hydraulic jumps forming at the base of the overfall. The critical condition has been found to be the hydraulic jump forming at the toe of the falling jet.

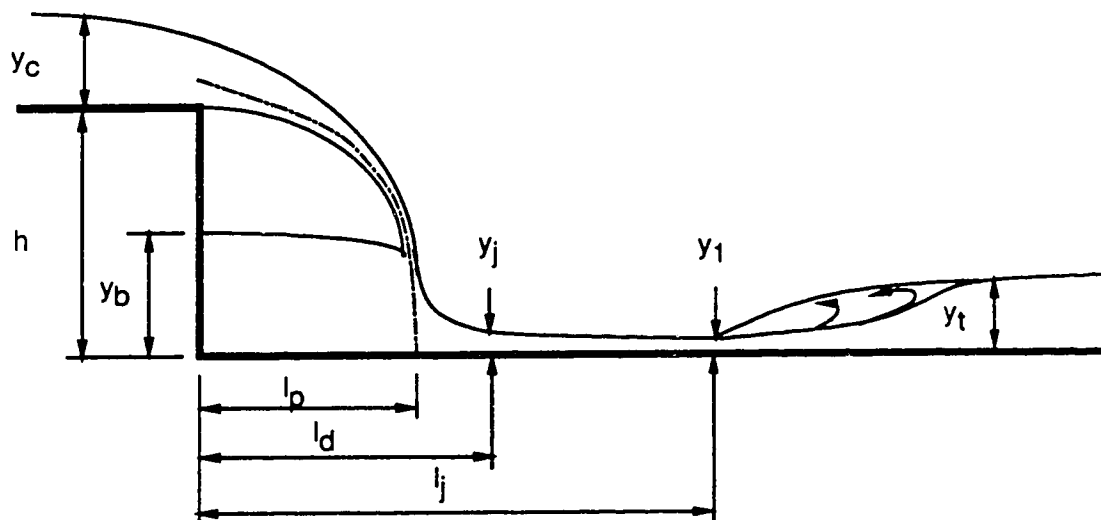


FIGURE 2.2 (a) Hydraulic Jump away from the Overfall

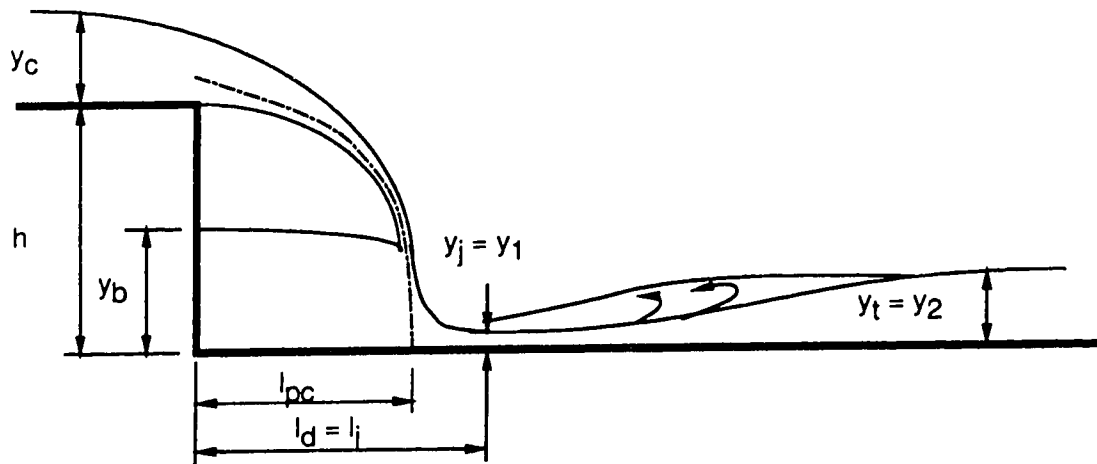


FIGURE 2.2 (b) Hydraulic Jump at the Toe of the Falling Jet

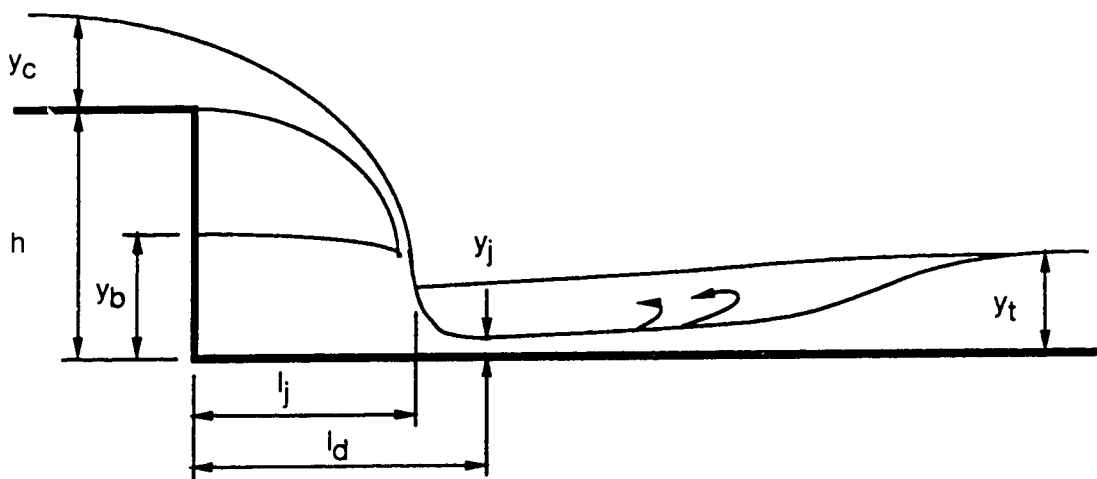


FIGURE 2.2 (c) Submerged Hydraulic Jump

Moore (1943) did some experiments on the critical hydraulic jump condition of the free overfall. However, the main purpose of Moore's work was to find the extra energy loss due to the hydraulic jump. Rand (1955) recognized the importance of the location of the hydraulic jump. At the critical hydraulic jump condition of free overfall, the drop length equals to the jump beginning length while the sequent tailwater depth equals to the corresponding tailwater depth as shown in Figure 2.2 (b). Having defined the exact location of critical hydraulic jump, Rand then showed that all dimensionless characteristic lengths are functions of the Drop number. Some of these relationships are as follows :

$$\frac{y_1}{h} = 0.54 D^{0.425} \quad (2.6)$$

$$\frac{y_2}{h} = 1.66 D^{0.27} \quad (2.7)$$

$$\frac{l_d}{h} = 4.30 D^{0.27} \quad (2.8)$$

$$\frac{l_{pc}}{h} = 1.98 \sqrt{D^{1/3} + 0.357 D^{2/3}} \quad (2.9)$$

where :  $l_d$  is the drop length, and  
 $l_{pc}$  is the bed hitting length at the critical condition.

### 2.2.3 Plunge Pool

As mentioned in the last section, hydraulic jump forming at

the toe of the falling jet is the critical condition. Any subsequent rise in the tailwater depth will result in a submerged hydraulic jump condition. This submerged hydraulic jump condition is the beginning of the plunge pool regime. A plunge pool regime is defined as a water jet impinging on a water body. This plunge pool regime for a free overfall can be maintained until the formation of breaking surface waves.

Research on plunge pool regime on free overfalls has been very limited. Moore (1943) investigated the effect of submergence only until the hydraulic jump was completely submerged. Nevertheless, Moore noted that increasing submergence caused the high velocity jet to persist for a greater distance downstream. Apart from this, there appears to be little research into the flow characteristics of this regime. More research is thus required to improve our current knowledge on this regime of free overfall.

#### 2.2.4 Breaking Surface Waves

As the tailwater depth continues to increase, the plunging jet is subjected to increasing submergence. At some point of this rise in the tailwater depth, the flow phenomenon changes abruptly to a series of breaking surface waves. The flow from upstream appears to 'ride' on top of the water at the base of the overfall as illustrated on Figure 2.3. The flow near the channel bed appears to be undisturbed by the violent waves on top. Sene et.al. (1989) found that this 'wavy' regime is remarkably independent of the entry flow condition.

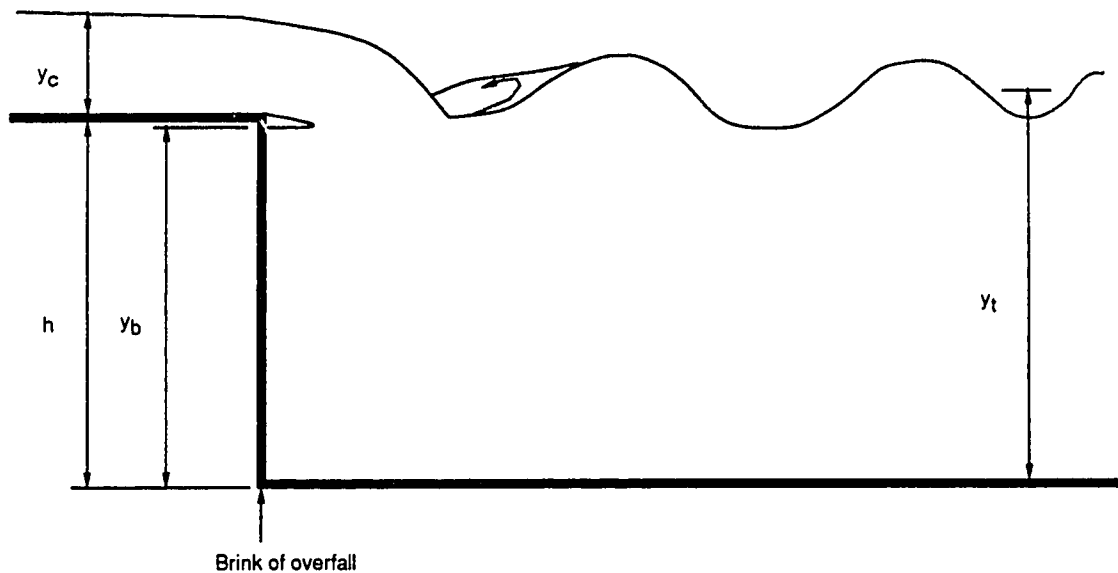


FIGURE 2.3 Free Overfall Flow with Breaking Surface Waves

The breaking surface waves are an interesting phenomenon and may also be applied in the protection scheme for channel bed as well. However, research in flow with breaking surface waves of free overfall is very limited. The basic criteria for the formation of breaking surface waves on overfall flow has not even been established as yet.

### 2.3 AIR ENTRAINMENT CHARACTERISTICS

Air and water usually do not mix together due to gravity and density differences except at the air-water interface area. However,

air and water do mix together quite evidently with the 'white' water appearance in some special circumstances. One of these special circumstances occurs at the base of a free overfall.

Air is usually entrained into the water in the form of air bubbles at the air-water interface. Once entrained into the flow, air bubbles are distributed across the flow stream by the process of turbulent momentum transfer. This distribution process is generally influenced by the buoyant nature of the air bubbles. The entrained bubbles will thus not only be distributed but also rise and pass out of the flow as well. This air removal mechanism is called detrainment. In addition to being distributed across the flow, air bubbles are also transported with the flow.

The amount of air in water is usually expressed either as a mean air concentration or as a ratio of air flow rate to the water flow rate called  $\beta$ . The mean air concentration,  $C$ , and the air entrainment ratio,  $\beta$ , are defined respectively as follows :

$$C = \frac{\vartheta_a}{\vartheta_a + \vartheta} = \frac{\vartheta_a}{\vartheta_t} \quad (2.10)$$

$$\beta = \frac{q_a}{q} \quad (2.11)$$

where :  $\vartheta_a$  is the volume of air,  
 $\vartheta$  is the volume of water,  
 $\vartheta_t$  is the total volume of air and water, and  
 $q_a$  is the air entrainment rate per unit width.

The research on air entrainment characteristics at the base of free overfall is not only difficult by itself but also complicated by the different flow regimes of overfall as well. Apparently, an organized effort to examine the general air entrainment characteristics of free overfall has not been made. Many researches were done for a specific regime only. Furthermore, a vast subject area has been related to the air entrainment characteristics. However, the mechanics of air entrainment, the prediction of quantities of entrained air and the air distribution characteristics are thought to be more pertinent to the purpose of this research. As a result, the following sections will present only the current knowledge on these specific air entrainment characteristics for each flow regime. Readers who are interested in other area of air entrainment characteristics are referred to some of the references provided (Rao and Kobus, 1973; Casteleyn et.al., 1977; Elsayy and McKeogh, 1977; Ervine and Himmo, 1984, Kobus, 1984; Pan and Shao, 1984).

### 2.3.1 Supercritical Shooting Jet

Free overfall having a supercritical shooting jet condition at the base can generally be divided into two main regions. The first region is the backpool area while the other region is the supercritical jet. The air entrainment research on the respective regions will be summarized accordingly.

Air entrainment in the backpool area is distinctively visible in the laboratory setup. Air seems to be entrained at the base of the

falling jet by the intense circulatory motion created when the falling jet hits the floor of the channel. Kobus (1984) identified jet striking a rigid surface as one of the local mechanisms for self-aeration. However, details of this air entrainment process are not known.

Air entrainment in the supercritical jet has, on the other hand, been studied quite extensively (Salih, 1980). While the particular air entrainment characteristics in the overfall mode have not been studied, they are similar to the widely studied problem of air entrainment in open channels such as spillways or chutes (Pinto and Neidert, 1982). In these situations, air is thought to be entrained by the multitude of randomly distributed vortices as suggested by Wood (1985). The quantity of air entrained is usually expressed in the following form :

$$\beta = k F_r^2 = k \frac{v^2}{gR_h} \quad (2.12)$$

where :  $k$  is the air entrainment constant,  
 $v$  is the average velocity of flow, and  
 $R_h$  is the hydraulic radius.

The air entrainment constant lies between 0.0035 and 0.0104.

Air distribution in a supercritical jet is difficult to analyze because of the high speed of the flow. Nevertheless, some theoretical derivation of air concentration has been provided in the excellent summary of Falvey and Ervine (1988). In addition to the



theoretical prediction, many investigators have made remarkable measurements both in experimental flumes and field studies as well (Straub and Anderson, 1958; Falvey, 1980; Wood, 1985).

In summary, a lot of research has been done on air entrainment in spillways or chutes. However, the supercritical jet of a free overfall usually has not only a small flow depth and low Froude number but also a short downstream persistence distance as well in most practical cases. The air entrainment contribution from the supercritical jet is thus considered to be minimal as compared to the backpool entrainment.

Finally, air can also entrained through the falling jet as well. This mode of air entrainment is usually called free jet entrainment. Haindl (1984) attributed this entrainment mechanism to the disintegration of the water jet in the ambient air. However, the air entrainment contribution from the free falling jet is again considered to be minimal because of the finite distance provided for the free falling jet.

### 2.3.2 Hydraulic Jump

The main air entrainment regions for the hydraulic jump in free overfall can also be divided into the backpool area and the jump area. The entrainment characteristics in the backpool area were discussed in the last section and thus the air entrainment characteristics in the jump area will be the only concern in this section. Again, most researches derived their contribution from ordinary open channel hydraulic jump and not exactly the hydraulic

jump situation in a free overfall. Nevertheless, the research results should be applicable, at least approximately, in any hydraulic jump situation.

Two air entrainment modes can be identified in a hydraulic jump. The first entrainment mode is the direct result of organized vorticity formed at the toe of the hydraulic jump as suggested by Wood (1985). A strong shear layer is formed when the upstream high velocity jet penetrates the downstream lower velocity water. The vortices in the shear layer are strong enough to entrain air into the vortex cores which are perpendicular to the flow direction. The second entrainment mode is similar to the mechanics of free surface air entrainment as suggested by Falvey and Ervine (1988). Air is entrained when the turbulent fluctuations caused by the breaking wave of the jump overcome the surface tension of water.

Prediction of the quantities of air entrained in a hydraulic jump has received most of the research attention. Many researchers have tried to relate the air entrainment ratio with the flow parameters. The most common flow parameter used in hydraulic jump situation is the upstream Froude number. One form of expression proposed by many investigators (Kalinske and Robertson, 1943; Rajaratnam, 1967; Thomas, 1982) is the following :

$$\beta = k (F_r - 1)^z \quad (2.13)$$

where :  $z$  is the air entrainment exponent.

The air entrainment constant ranges from 0.0066 to 0.03 while the

air entrainment exponent ranges from 1.0 to 1.4. Renner (1975) proposed another form of relationship using experimental results of a plane water jet with surface roller :

$$\beta = k F_r^2 \quad (2.14)$$

The air entrainment constant is about 0.005 and the air entrainment exponent is 2. In addition, scale effects (Thomas, 1982), and effects of turbulence and viscosity (Kobus, 1984) on air entrainment have been recognized as well. However, their influences are usually minimal. In general, the quantities of air entrained in a hydraulic jump is mainly a function of the upstream Froude number.

Finally, the air concentration distribution in a hydraulic jump was examined quite thoroughly by Rajaratnam (1967). It was found that the mean air concentration at any section increases from zero to a maximum within some short finite distance and decreases from the maximum to zero again in a considerably longer distance than the original ascending one. Further, the maximal mean concentration is related to the upstream Froude number in the following form :

$$C_m = F_r^{1.35} \quad (2.15)$$

where :  $C_m$  is the maximum mean air concentration.

### 2.3.3 Plunge Pool

Air entrainment characteristics for the plunge pool condition

have received increasingly more attention in recent decades. However, most researches of this nature employed a vertical shooting jet, either round or rectangular in cross-section, into a large stagnant water body. The plunging jet in a free overfall, on the other hand, usually falls at an angle to the downstream receiving pool. Nevertheless, the air entrainment characteristics of plunge pool has been relatively well studied.

Air is entrained into the plunge pool by different mechanisms. Haindl (1984) suggested that one of these mechanisms is the suction effect of flowing water. The space under an overflow jet is subject to negative pressures and air entrainment is encountered wherever negative pressures occur in the flow. The major entrainment mechanism is, however, thought to be the formation of organized vorticity when a strong shear layer again develops with the jet plunging into the water body (Wood, 1985). The vortices are strong enough to entrain air in the vortex cores that are perpendicular to the flow of the jet. This entrainment process is enhanced by the development of turbulence on the surface of the falling jet before hitting the water surface and by the formation of a foam layer on the water surface downstream from the jet. Another theory has the major entrainment mechanism as the formation of the air pocket (Falvey and Ervine, 1988). Air is entrained when the receiving water cannot follow the undulation on the free jet surface and thus an air pocket is formed. This entrainment mechanism is thought to be valid for mean flow velocities less than 10 m/s. For jet velocities greater than about 10 m/s, a continuous air layer exists between the free jet surface and the receiving water.

Many researchers have tried to correlate the air entrainment rates in the plunge pool to the existing flow parameters. The most popular flow parameter used is the upstream Froude number. The relationship proposed by Renner (1975) for hydraulic jump condition has been adopted to the plunge pool condition with a different entrainment constant. Furthermore, some investigators have argued about the importance of the entry velocity for the falling jet to entrain air into the water body. The following relationship was thus proposed :

$$\beta = k F_r^2 \left(1 - \frac{0.8}{v_e}\right)^3 \quad (2.16)$$

where :  $v_e$  is the jet entry velocity.

The minimum jet entry velocity to entrain air is usually taken to be 0.8 m/s as in Equation 2.16 based on some dimensional arguments (Wood, 1985). This minimum condition for the occurrence of air entrainment is sometimes called the inception limit (Kobus, 1984). The exponent for the jet entry velocity term was also found to vary from 1.5 to 3 for high and low velocity plunging jet conditions respectively (Sene, 1988). Many other authors, however, simply proposed completely different relationships using the parameters of the jet entry velocity, the angle of the jet entry, the geometric dimensions of the plunging jet and the effective fall height for the plunging jet (Ervine and Elsayy, 1975; Van De Sande and Smith, 1973; Van De Sande and Smith, 1976; Amed et.al., 1984; Bin , 1984).

The turbulence intensity in the plunge pool was also considered to be a major factor for the air entrainment ratio (Ervine and Falvey, 1987), but the analysis of the turbulence function has been very limited. In general, the prediction on air entrainment ratio for plunge pool condition is unsatisfactory. Moreover, the fact that the important influences from the receiving pool have been almost completely overlooked needs further clarification.

Finally, the studies on entrainment distribution for plunge pool have been few. Air concentration profiles were measured (McKeogh and Elsayy, 1980) and air diffusion characteristics in water were studied (Ervine and Falvey, 1987). However, a circular jet on a large stagnant water body was used in both studies. A theoretical study on the transport and detrainment of air bubbles in a guided plunging flow was also made (Sene et.al., 1989). The resulting air concentration profile compares well with the experimental measurements and is quite similar to the profiles described in the hydraulic jump condition. However, our understanding of the entrainment distribution for plunge pool regime is far from complete.

#### 2.3.4 Breaking Surface Waves

Our knowledge on the breaking surface waves regime of free overfall is quite limited in the flow aspect and even worse in the entrainment aspect. Kobus (1984) mentioned the breaking wave as one of the local self-air entrainment techniques but gave few details. Sene et.al. (1989) made a more detailed report on the 'wavy'

or surface waves regime but concentrated on the flow characteristics. The reason for the lack of entrainment study on the breaking surface waves regime is possibly because of the limited amount of air being entrained into the flow.

## 2.4 CONCLUSIONS

The hydraulics of the free overfall is both complex and difficult to analyze. For the purpose of this thesis, it has been divided into two main groups. The first group deals with the flow characteristics while the other group deals with the air entrainment characteristics.

Flow characteristics of the free overfall have been known to vary with tailwater conditions. A supercritical jet, hydraulic jump, plunge pool or breaking waves can be found at the base of the overfall depending upon the tailwater situation. A significant depth of water is always present behind the shooting jet. Researchers have also identified that a critical condition exists when the hydraulic jump takes place at the toe of the falling water. Rand (1955) further found out that all flow characteristics can be expressed in terms of the Drop number. The flow characteristics of the other two regimes of free overfall are not well understood. The plunge pool condition has only been determined to have a greater jet persistence distance downstream while the formation of the breaking surface waves was also only recently found to be upstream independent.

Air entrainment characteristics of free overfall are also expected to change with the flow regimes as well. However,

systematic experiments have not been made. As a result, only relevant researches to the present study have been summarized. The supercritical shooting jet has been studied quite extensively as in chutes and yet the length of the jet is too short in the overfall situation to be considered a major air contributor. The backpool air entrainment, on the other hand, is quite significant and yet has not well understood. The air entrainment in the hydraulic jump regime is well researched and found to be a function of the upstream Froude number. The air entrainment researches in the plunge pool regime have been concentrated on the plunging conditions and have little regard for the influences from the receiving pool. Finally, insignificant amount of air is thought to be entrained into the flow in the breaking surface waves regime.

The flow and air entrainment characteristics of the free overfall are too difficult to generalize. Furthermore, the inter-relationship between the two characteristics has not been studied yet. More research is thus necessary to clear up some of the difficulties in predicting and relating both the flow and air entrainment characteristics together.



## **CHAPTER 3**

### **EXPERIMENTAL ARRANGEMENT**

#### **3.1 INTRODUCTION**

The purpose of this research is first to identify some of the missing links in predicting the flow characteristics of free overfall, especially for the plunge pool regime. The other purpose of this research is to identify the air entrainment characteristics with the corresponding flow regime. The emphasis will again be placed on the plunge pool condition. Many methods have been established over the years to investigate the air entrainment characteristics. This research has chosen to measure the air concentration of the related flow regimes in order to derive the air entrainment characteristics.

The experimental arrangement of this research can thus be divided into two major components. The first component is the general setup for experimental equipment while the second component is the measurement technique.

#### **3.2 EXPERIMENTAL EQUIPMENT**

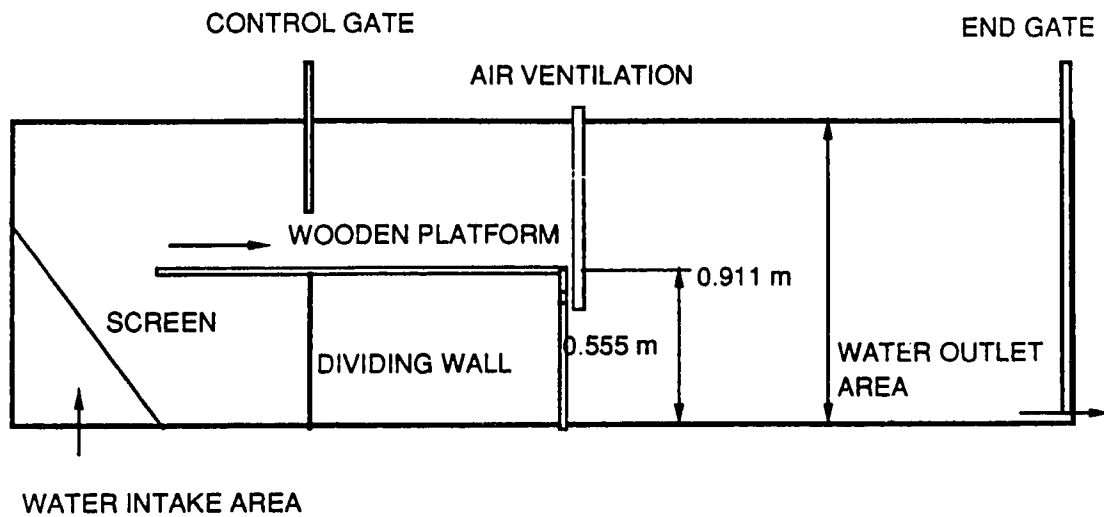
The experimental equipment included a flume for free overfall flow and an indicator for air concentration. The general setup for the flume will first be described in details. An air concentration probe was chosen for measuring mean air concentration and will also be discussed as well.

### 3.2.1 Flume Setup

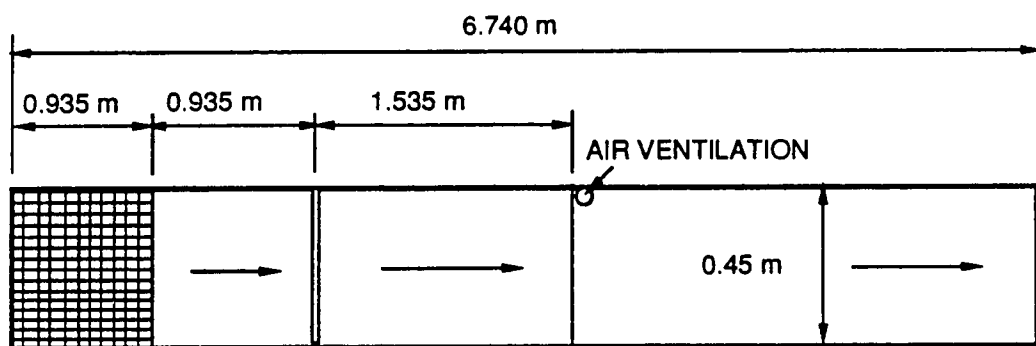
A horizontal, rectangular flume, 6.74 m long, 0.45 m wide and 0.911 m deep was selected in the Blench Hydraulics Laboratory of the University of Alberta. The general setup of the flume and the self contained circulatory water system are shown in Figures 3.1 and 3.2 respectively. Plate 3.1 also shows the general setup of the flume.

The flume had Plexiglass side panels, except in the water inlet area where everything was made of steel, with galvanized steel bed. An adjustable gate was located at the end of the flume to control the depth of the tailwater. A wooden platform was built extending into the water inlet area and had a drop height of 0.558 m. A fixed drop height was chosen for this study.

Water for the system was stored in a galvanized steel sump with an overflow gate. Water was pumped into the flume inlet area through a 0.16 m diameter circular pipe. A magnetic flow meter with a digital readout was located in the outlet area of the sump with a control valve located near the inlet area of the flume in the above mentioned pipe. To avoid the air entrainment into the pump intake especially at high discharges, it was found necessary to keep the sump in an overflowing state. As a result, an overflow gate was located at the side wall of the sump opposite the intake location.



**ELEVATION OF FLUME**



**PLAN OF FLUME**

**FIGURE 3.1 General Flume Setup**

### 3.2.2 Air Concentration Probe

Many techniques are available for measuring air concentration in water (Babb and Aus, 1981). In this study, a simple air concentration probe developed by Lamb and Killen (1950) was chosen. The air concentration probe can be easily built and is believed to provide reasonably accurate results.

The probe itself was made of two 10 mm by 25 mm long galvanized steel plates supported by a plastic rod as shown in Figure 3.3. The steel plates were insulated all around except for a 10 mm by 10 mm area on the inside. This area is thus the indicative area for measuring the mean air concentration. Plates 3.2 (a) to (c) show the different views of the air concentration probe.

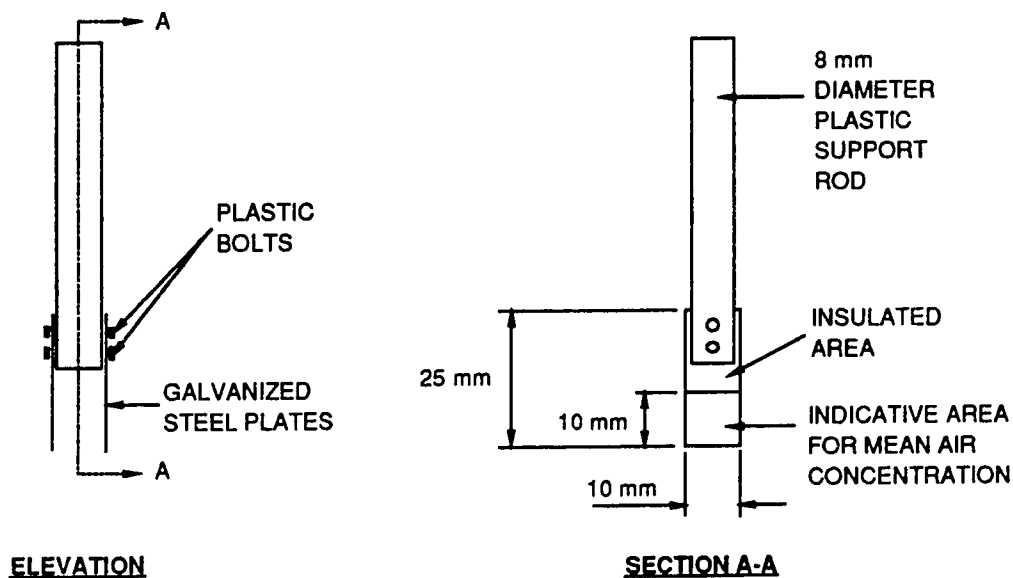


**FIGURE 3.3 Air Concentration Probe**

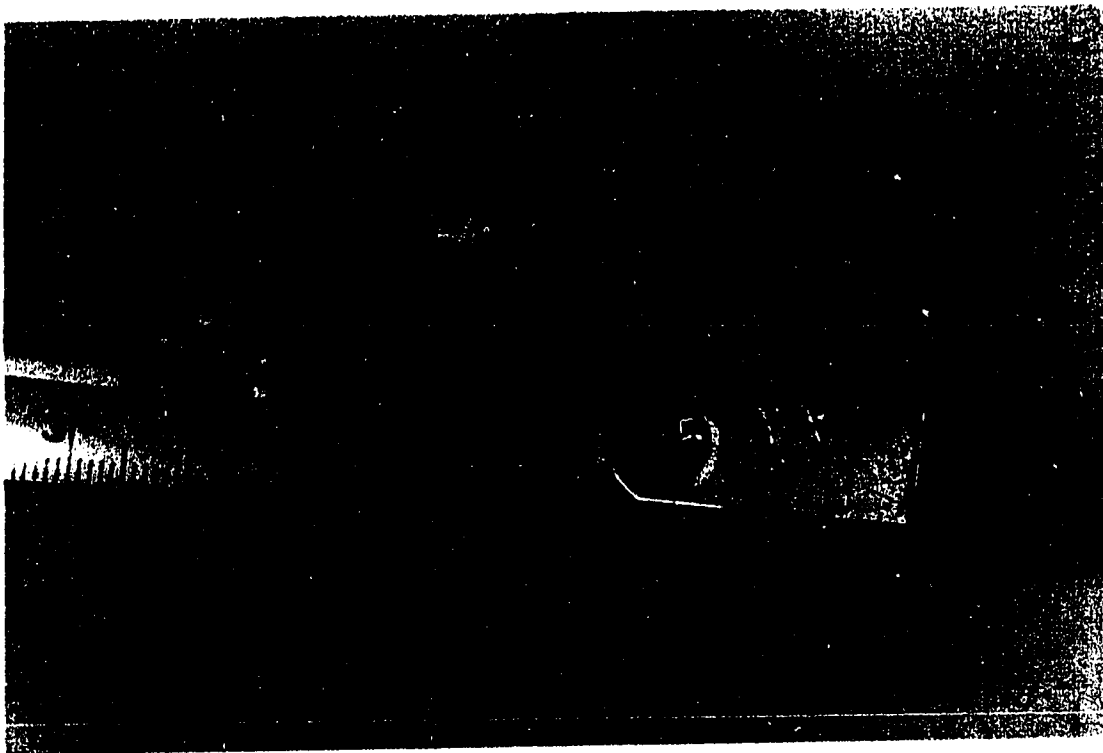


PLATE 3.2 (a) Air Concentration Probe View 1



PLATE 3.2 (b) Air Concentration Probe View 2

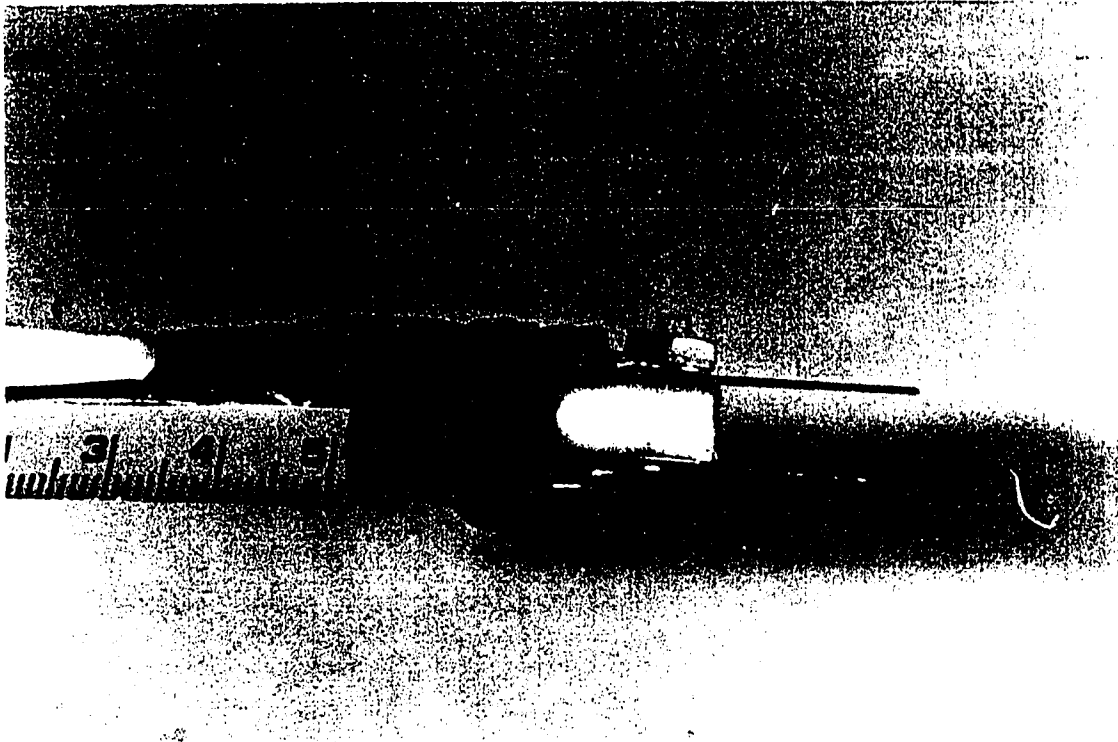


PLATE 3.2 (c) Air Concentration Probe View 3

Figure 3.4 shows the circuit diagram of the probe. A variable reference resistor was placed in series with the probe. The supply voltage was fed through a constant wave generator and the potential difference between the probe was measured by a time integrated alternate current (A.C.) dial gauge. The time integrated A.C. dial gauge is shown in Plate 3.3.

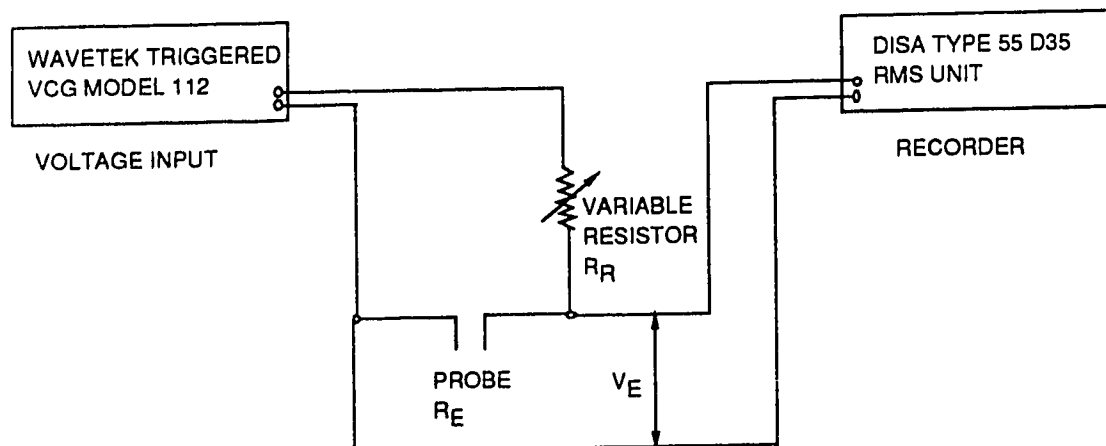


FIGURE 3.4 Circuit Diagram of Mean Air Concentration Indicator

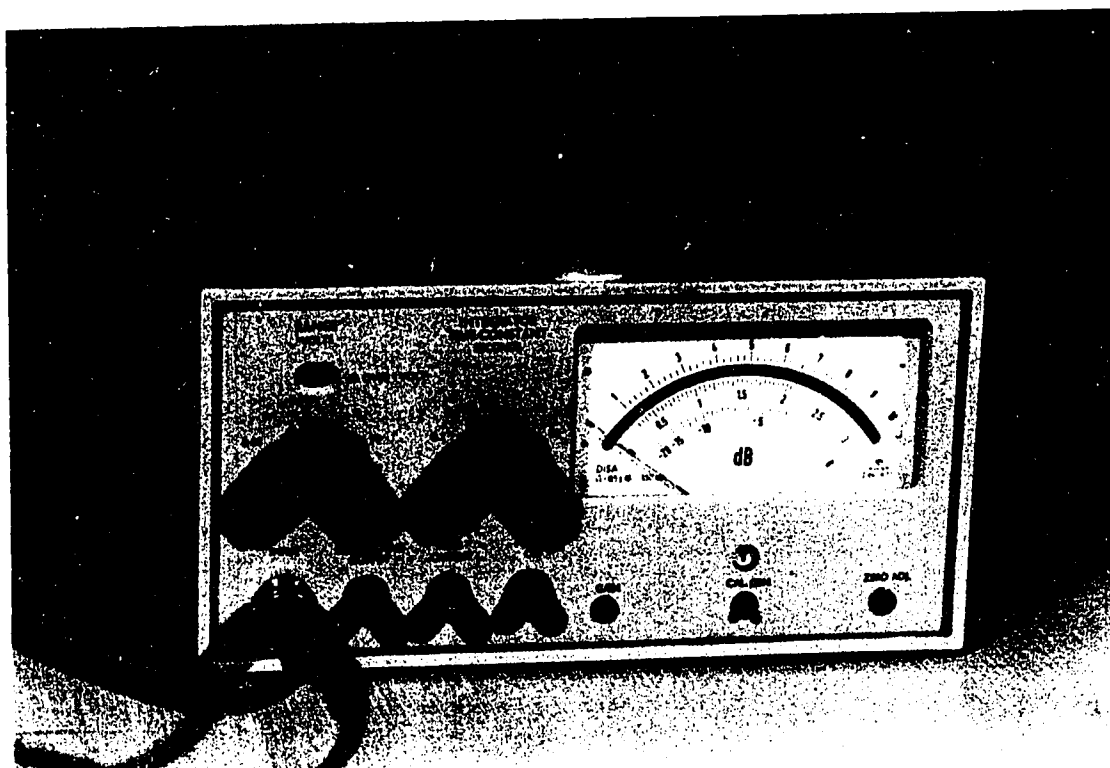


PLATE 3.3 Time Integrated A.C. Dial Gauge

### 3.3 MEASUREMENT TECHNIQUE

Two types of measurements are required for this experiment. The first type is the general flow measurements while the second type is the air concentration. General measurements involve flow quantity and flow characteristics. Air concentration is measured by properly calibrating the air concentration probe. The following sections will describe these two types of measurement techniques in detail.

#### 3.3.1 General Measurements

Discharge was measured by means of a magnetic flow meter. The flow meter was connected to a direct current (D.C.) voltage output and calibrated to give  $0.005 \text{ m}^3/\text{s}$  or  $5 \text{ L/s}$  for each unit of output voltage. The maximum discharge for the pump without air entrainment was found to be  $0.040 \text{ m}^3/\text{s}$  or  $40 \text{ L/s}$ .

Flow depth was measured using a point gauge, which was accurate to  $0.0003 \text{ m}$ , located on top of the flume. A scale which was accurate to  $0.003 \text{ m}$  was also located on top of the flume to indicate the location of the measuring station. Another measuring scale used on the side of the flume was accurate to  $0.001 \text{ m}$ .

#### 3.3.2 Probe Calibration

The air concentration probe operates under the general principle that electrical resistance changes with the presence of air



bubbles in water. Lamb and Killen first developed the probe in 1950 and obtained excellent agreement with a mechanical sampler. Cain and Wood (1981) further confirmed the validity of the probe and derived the following relationship for the mean air concentration :

$$C = \frac{2 \alpha |V_E|}{3 (\alpha - 1) + (3 - \alpha) |V_E|} \quad (3.1)$$

with :

$$\alpha = 1 + \frac{R_{EO}}{R_R} \quad (3.2)$$

where :  $R_{EO}$  is the resistance of probe in water alone,  
 $R_R$  is the resistance of the reference resistor, and  
 $|V_E|$  is the scaled value of measured potential difference.

The measured potential differences  $|V_E|$  are scaled so that they vary between 0.0 and 1.0.

Despite the demonstrated reliability of the air concentration probe, a calibration procedure was nonetheless undertaken not only to check the validity of the probe but also to examine the operation limit for the probe as well. The calibration procedures for the air concentration probe are as follows :

- 1.) A known air supply was first calibrated against the gauge pressure by means of the time for it to displace a known volume of water as demonstrated in Plate 3.4. A known air discharge was then obtained.
- 2.) The air supply was then passed through known volume of water in a calibrated flask as shown in Plate 3.5. The elapsed time for the air

bubbles to rise through the water column was found, accurate to 0.01 seconds.

3.) A mean air concentration was calculated from the known air discharge from step 1 and the time for the air bubbles to rise through the water column as found from step 2. The obtained value was called a known mean air concentration.



PLATE 3.4 Calibration of Known Air Supply (Step 1)



PLATE 3.5 Air Rising Through the Calibration Flask (Step 2)

- 4.) The air concentration probe was then placed inside the flask at this condition to obtain a reading as seen in Plate 3.6.
- 5.) Another mean air concentration which was called a calculated concentration could thus be found from the reading using equation 3.1.

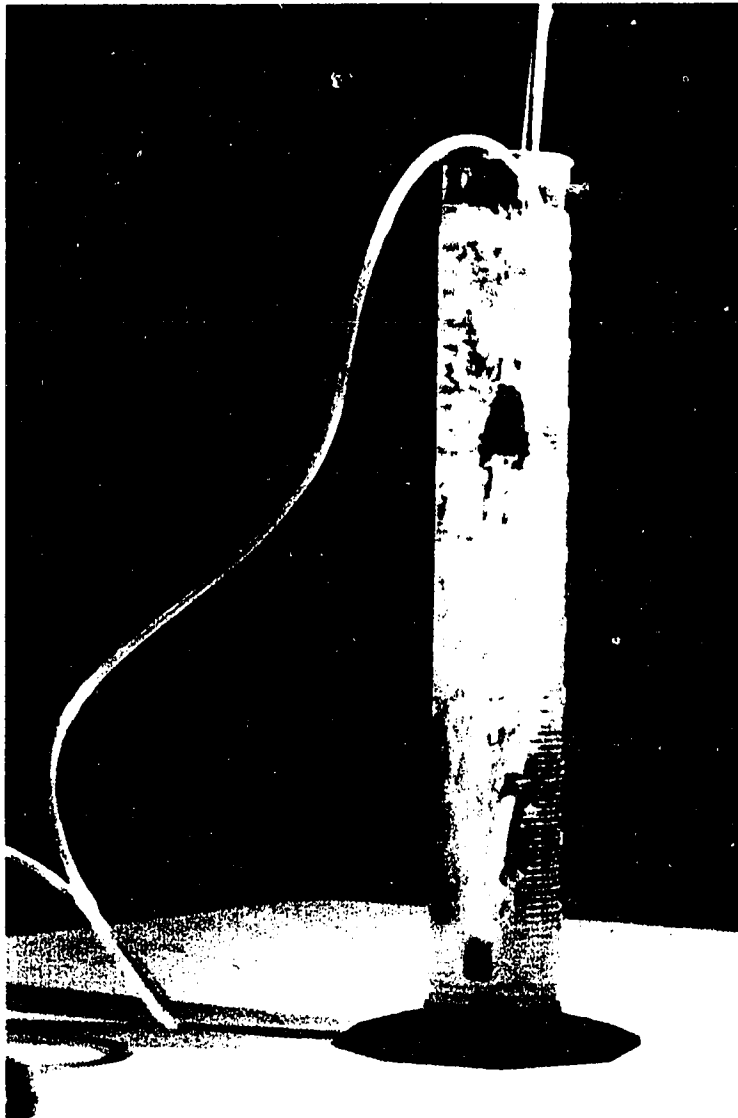


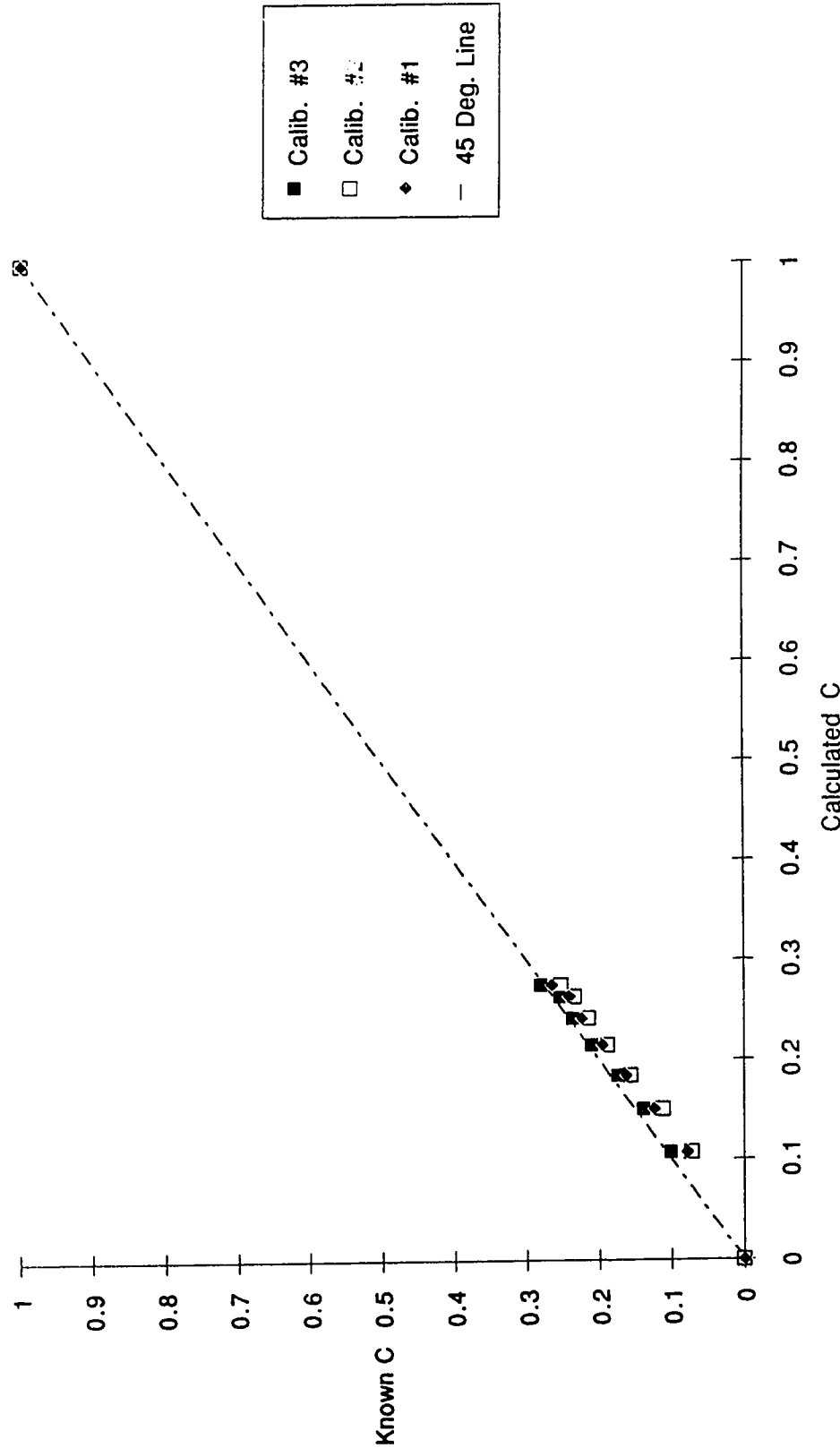
PLATE 3.6 Air Concentration Probe in the Calibration Flask (Step 4)

6.) The calculated concentration was finally checked against the known concentration for accuracy of the probe.

7.) Steps 1 to 6 were repeated for different air supply rates and thus different mean air concentrations.

The final results for the calibration of the air concentration probe are shown in Figure 3.5. The air concentration measurements were

FIGURE 3.5 Comparison of the Mean Air Concentration Predictions



accurate to 0.01. It was during this calibration procedure that the reading of resistances, and thus the value of  $\alpha$ , was found to change with time when all other conditions remained constant. Resistance of the probe in particular increased quite significantly during the early stage of power-on period which is referred to the 'warm-up' period. This warm-up period lasted about two hours. Figure 3.6 shows this change in the value of  $\alpha$  with time. The probe was reliable to provide good results if proper warm-up period was given.

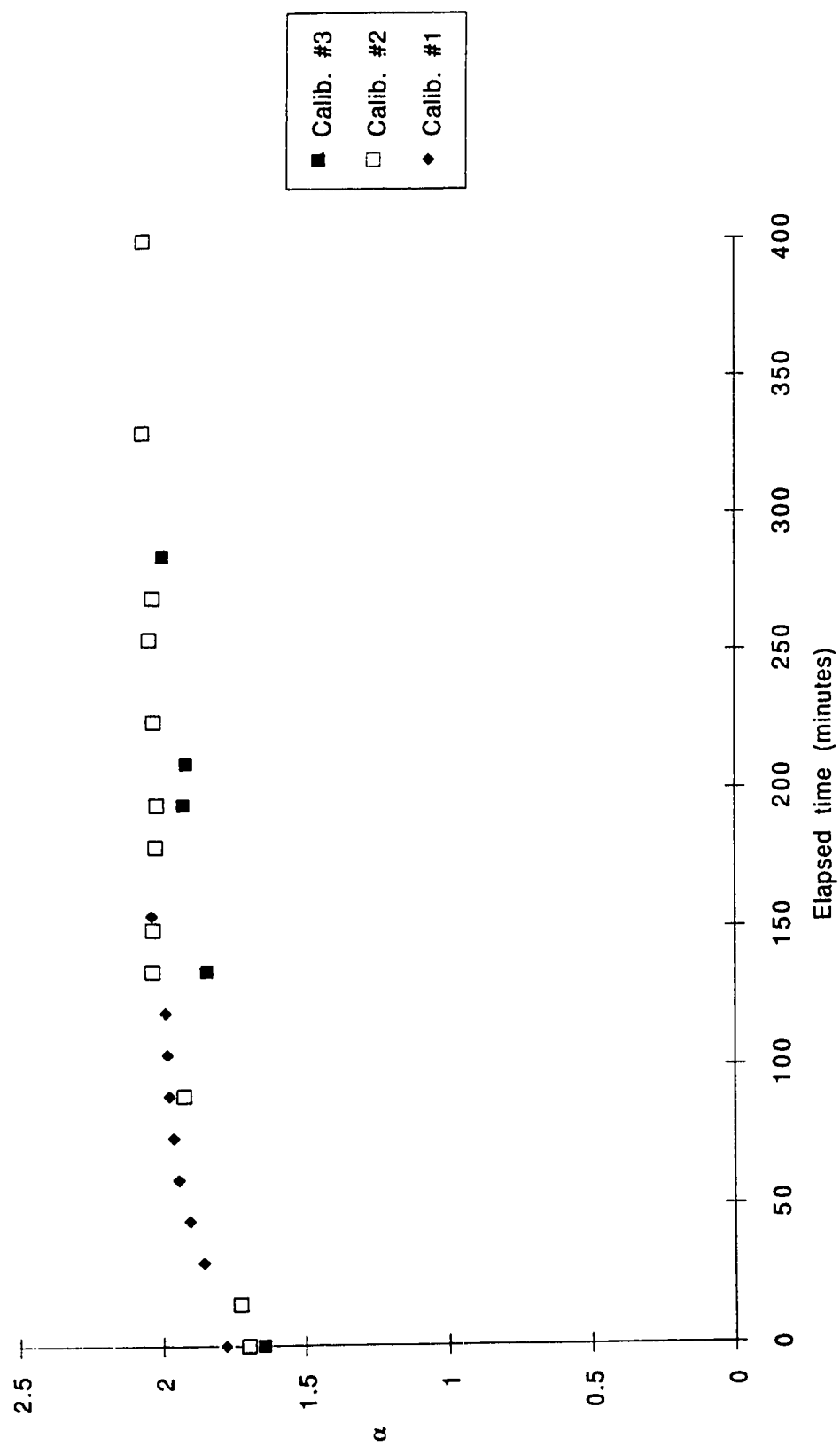
Furthermore, it was also determined that an input frequency of 50 kHz and a maximum resistance on the reference resistance would provide the most expanded range in the A.C. gauge. More consistent results were also obtained from the A.C. gauge by using a 30 second time integrated reading. Finally, the air concentration probe required a minimum of 25 mm submergence into the water in order to avoid the disturbance from the water surface.

### 3.4 CONCLUSIONS

The experimental flume was set up so that the flow characteristics of free overfall could be measured. These flow characteristics were being measured by means of magnetic flow meter, point gauge and scales.

More time and effort were spent on developing a reliable air concentration indicator. Finally, an easy-to-build electrical resistance probe was chosen. The calibration on this probe was laborious but provided remarkably good results. There was some concern, however, on the drifting nature of the probe.

FIGURE 3.6 Variation of Alpha Value with Time



## **CHAPTER 4**

### **EXPERIMENTS AND EXPERIMENTAL RESULTS**

#### **4.1 INTRODUCTION**

The objectives of the experiments were to measure the flow characteristics along with the air concentration profiles at different tailwater conditions. This dual experimental objectives made the experiment itself difficult to organize. An effective way to run the experiment was further complicated by the long 'warm-up' period and drifting nature of the air concentration probe. As a result, an in-depth description of the experimental work along with the experimental results is provided in the following sections.

#### **4.2 EXPERIMENTAL WORK**

The height of drop for this experiment was fixed at a constant value because the change in Drop number was considered to be more important than the change in the height of the drop itself. The change in the Drop number can also be achieved by the change in discharges alone. The experimental work was thus begun by the selection of the discharges. Four discharges were selected and were 15 L/s, 25 L/s, 35 L/s and 40 L/s.

Two types of measurements were made. These two types of measurements included the general flow characteristics and the air concentration profiles. The flow characteristics were especially measured on the plunge pool and breaking surface waves regimes.



The air concentration profiles involved mostly the plunging flow condition. Furthermore, photographs and high speed video were taken as well.

#### 4.2.1 Flow Characteristics

Flow characteristics were measured for five to seven tailwater conditions for each discharge. These tailwater conditions were chosen so that all the regimes in the free overfall could be examined for each discharge. More measurements were taken from the plunge pool regime. The measured flow parameters included the tailwater depth, the jump beginning depth and length, and finally the bed hitting length. All measurements were taken along the centreline of the flume when possible.

The most important flow parameter is the tailwater depth. The depth of water at 2.44 m downstream from the brink of the overfall was determined to be the controlling tailwater depth. This location was chosen because it was observed to be far enough from the base of the overfall and yet was not affected by the flume outlet condition.

The corresponding length and depth at the beginning of the hydraulic jump or the receiving water were measured and were thereafter called the jump beginning length and depth. These measurements were obviously applicable only to the hydraulic jump or plunge pool conditions only.

The length at which the centreline of the free falling jet would hit the flume bed was also taken and was thereafter called the bed

hitting length. However, this measurement could not be obtained directly from the centreline of the flume. An indirect method was then adopted by the indication of air bubbles on the Plexiglass side wall. The bed hitting length on the side wall was determined to be the location where the air bubbles changed from being carried into backpool to being carried forward downstream. The bed hitting length was thus obtained by properly adjusting the measurement at the side wall to the centreline of the flume.

Finally, the water surface profiles were only taken when the air concentration profiles were taken. The scheme for the air concentration measurements will be described in details in the following section.

#### 4.2.2 Air Concentration Measurements

In order to avoid the drifting nature of the air concentration probe, a minimum of two hours of 'warm-up' period was allowed before the probe was used for measurements. This 'warm-up' period was determined to be sufficient for the air concentration probe to reach reasonable stability and provide consistent results.

Five different tailwater conditions were selected specifically for the air concentration measurements from the one used for the measurements of the flow characteristics for each discharge. One of the tailwater conditions corresponded to a free hydraulic jump formed downstream, but not necessarily at the toe of the falling jet. The other tailwater conditions were in the plunge pool regime.

Two major sections of measurements were then taken for each

tailwater condition in order to find out the effect of wall shear on air entrainment. The first section of measurement was along the centreline of the flume while the second section of measurement was close to the side wall away from the air intake area. Figure 4.1 shows the plan view of the two sections.

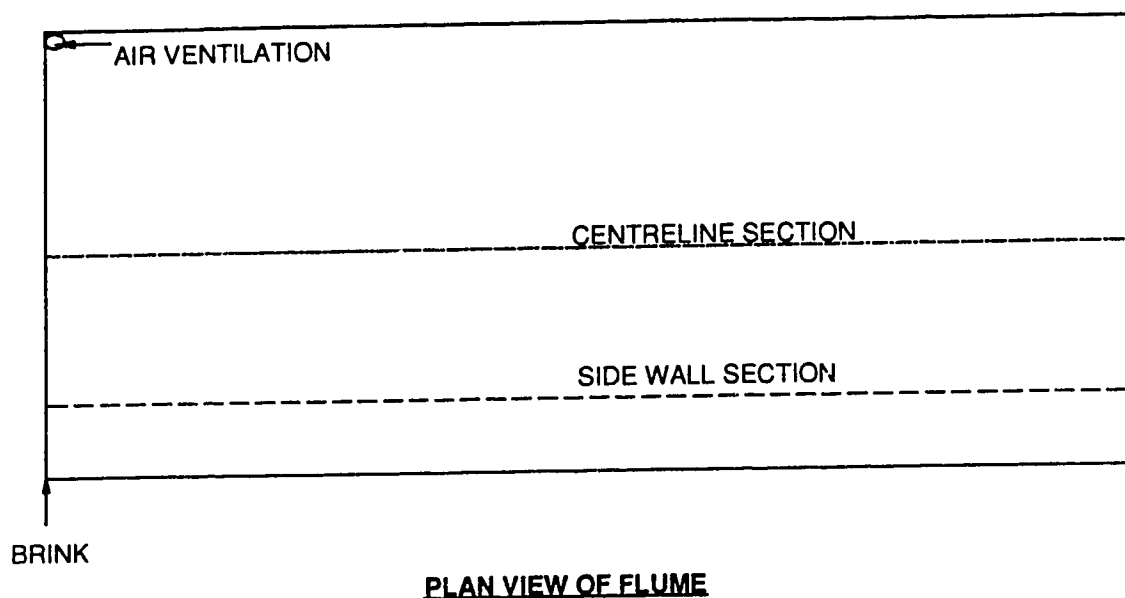


FIGURE 4.1 Locations of Mean Air Concentration Measurements

For each section, air concentration profiles were taken longitudinally at a constant depth in order to minimize the drifting nature of the air concentration probe. These constant depth longitudinal profiles started from the brink of the overfall to the

end of air entrainment as determined visually by the appearance of the air bubbles. The reading taken at the tailwater location was regarded as the 'no air' or initial reading at that particular depth. The longitudinal profiles were taken at some intervals until they reached the water surface. A minimum of three longitudinal profiles were taken in each section. Vertical air concentration profiles were also derived from these longitudinal profiles as well.

#### 4.3 EXPERIMENTAL RESULTS

Typical results from the photographic work for the discharge of 15 L/s are shown on Plates 4.1 (a) to (d). The four pictures were all taken for the same tailwater condition with different camera exposure times. With longer exposure times, the extent of air entrainment effect can be easily seen. Moreover, typical pictures from high speed video are also shown on Plates 4.2 (a) to (f) for the different flow situations taking place at the base of the overfall at the discharge of 35 L/s. These flow situations range from the supercritical shooting jet to the breaking surface waves regimes. Air is apparently being entrained into the flow by the formation of eddies especially in plunge pool situations as mentioned by Wood (1985).

Apart from the general observations from the photographic and high speed video work, the experimental results could also be divided into the flow characteristics and air concentration profiles due to the objectives mentioned for this experiment. Summary of the experimental results are presented in the following sections.

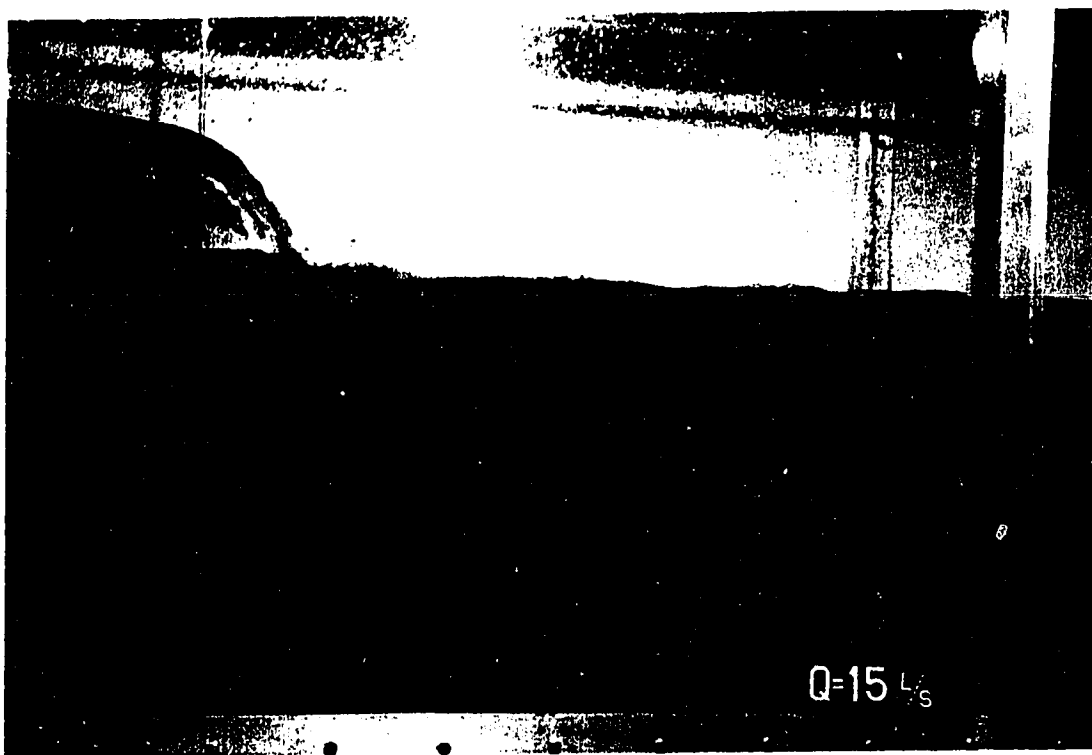


PLATE 4.1 (a) Photographic Work.  $Q=15$  L/s. Time= $1/60$  s with Flash



PLATE 4.1 (b) Photographic Work.  $Q=15$  L/s. Time= $1/60$  s

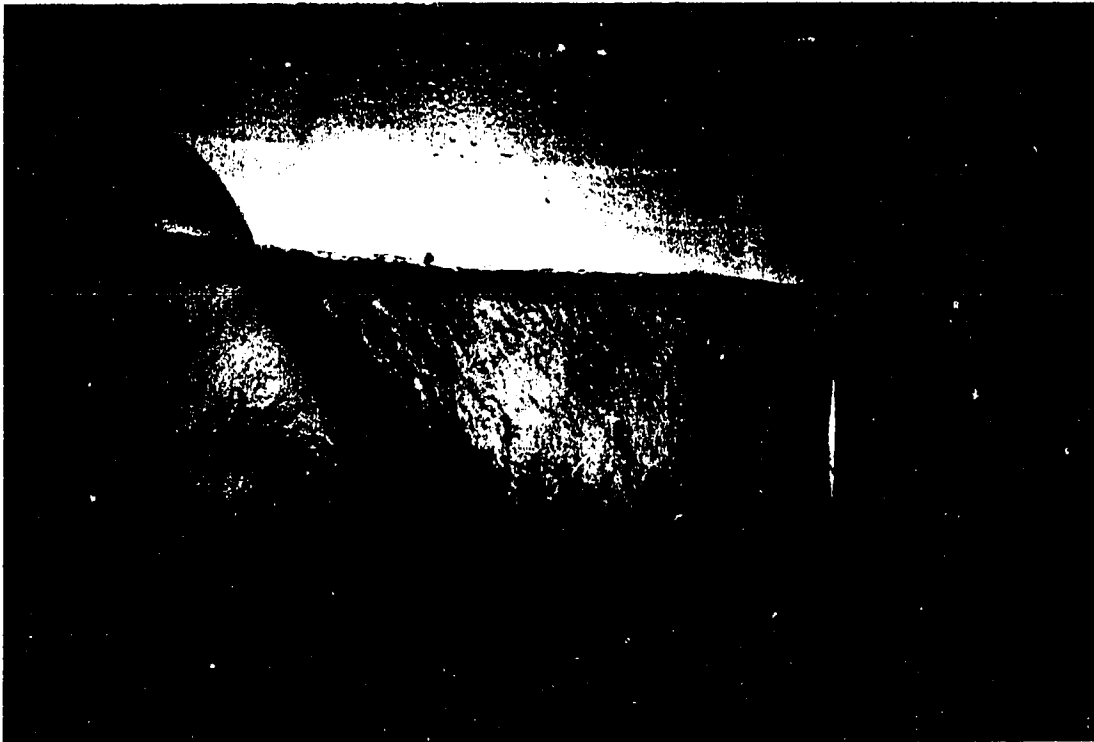


PLATE 4.1 (c) Photographic Work.  $Q=15$  L/s. Time= $1/8$  s



PLATE 4.1 (d) Photographic Work.  $Q=15$  L/s. Time=30 s



PLATE 4.2 (a) High Speed Video.  $Q=35$  L/s. Supercritical Shooting Jet

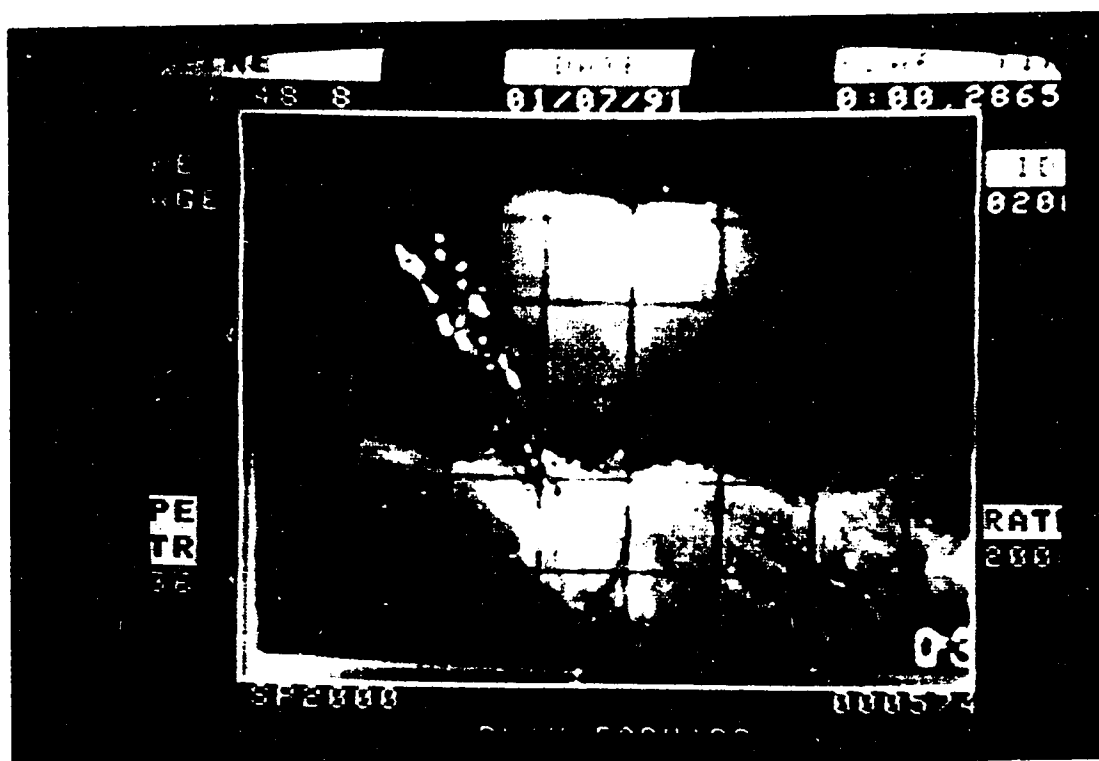


PLATE 4.2 (b) High Speed Video.  $Q=35$  L/s.  $y_t=0.240$  m

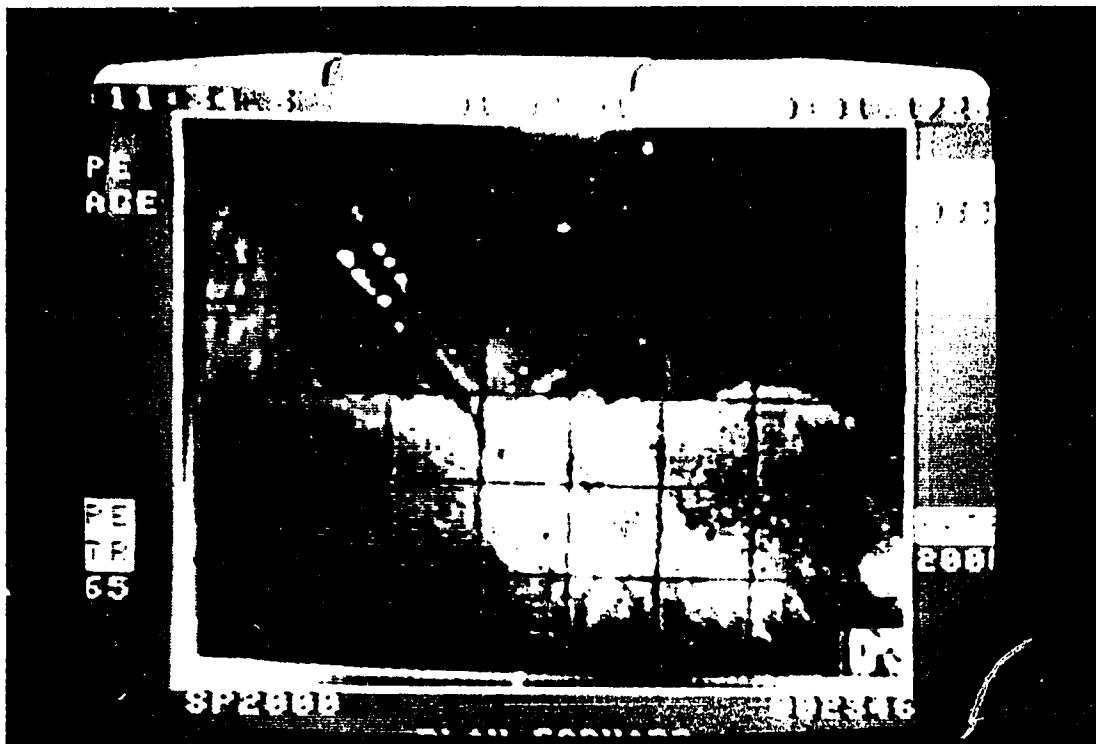


PLATE 4.2 (c) High Speed Video .  $Q=35$  L/s.  $y_t=0.320$  m

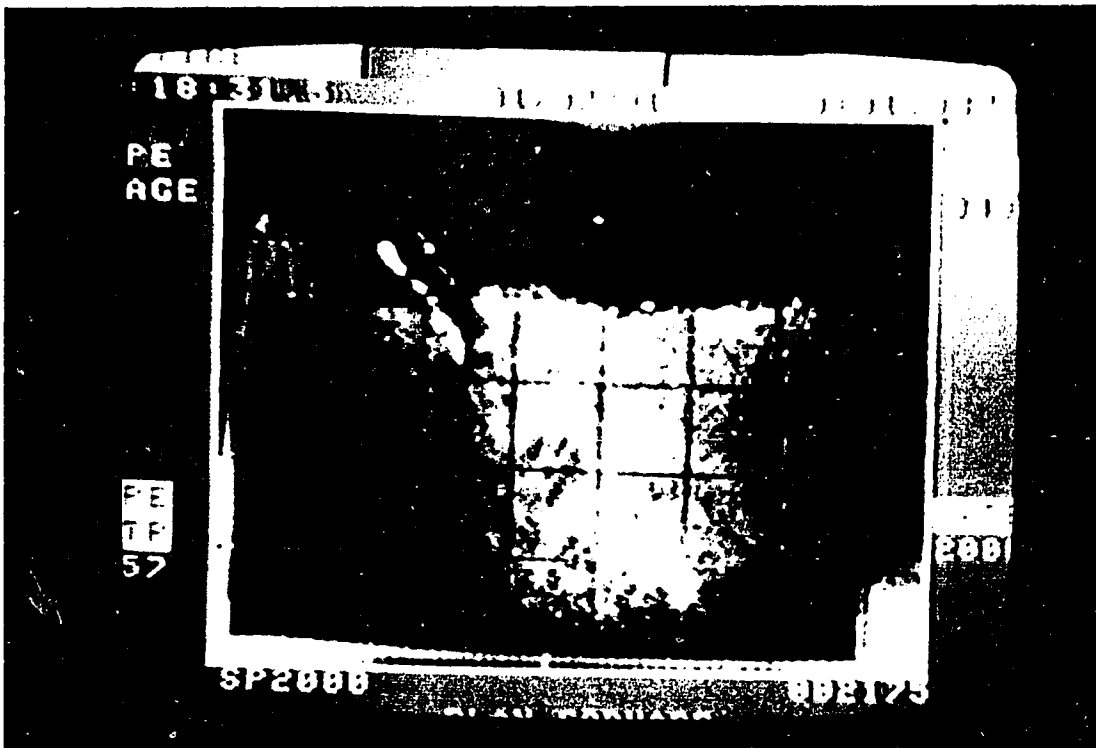


PLATE 4.2 (d) High Speed Video.  $Q=35$  L/s .  $y_t=0.425$  m



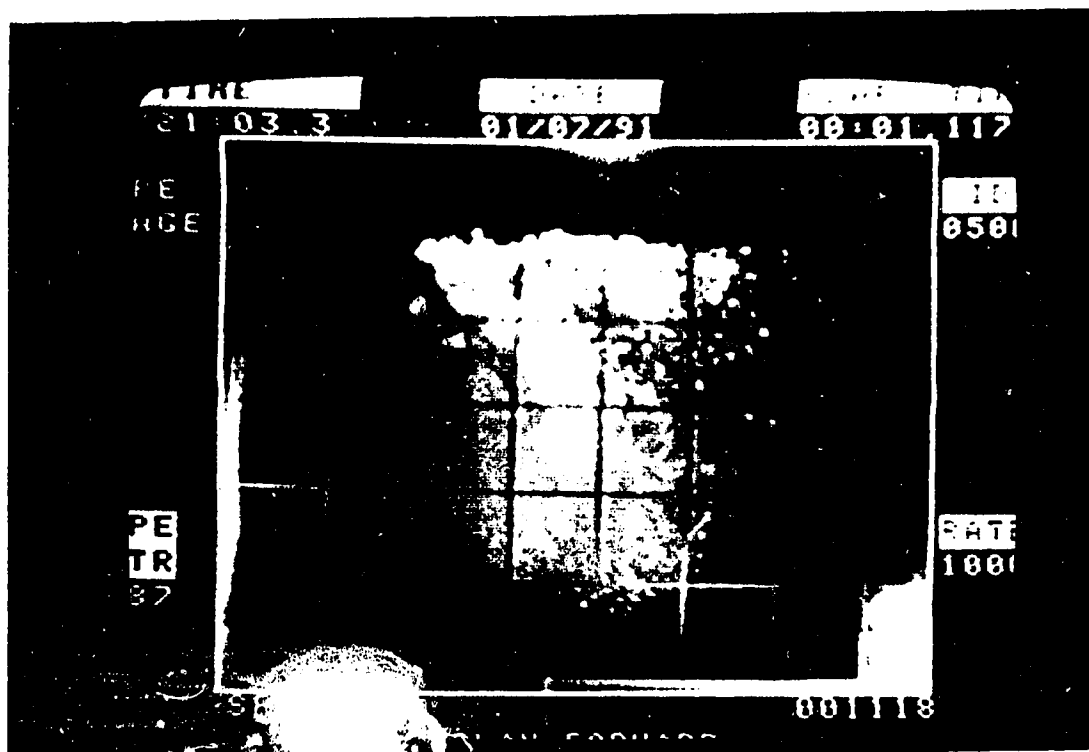


PLATE 4.2 (e) High Speed Video.  $Q=35$  L/s.  $y_t=0.515$  m

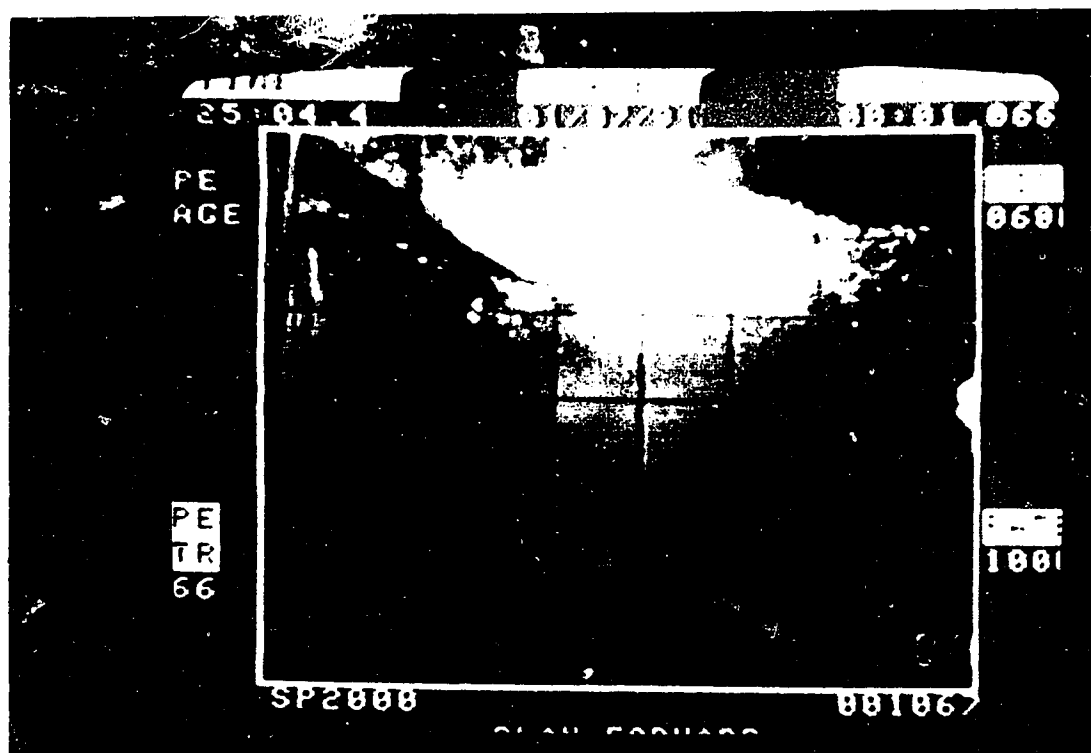


PLATE 4.2 (f) High Speed Video.  $Q=35$  L/s.  $y_t=0.560$  m (breaking surface waves)

#### 4.3.1 Flow Characteristics

Four flow parameters have been specially measured. These flow parameters include the tailwater depth, the jump beginning depth and length, and finally the bed hitting length. With the apparent importance of the tailwater conditions, all other flow parameters are thus plotted against corresponding tailwater depth.

Figure 4.2 shows the relationship between the tailwater depth and the jump beginning depth. As seen from Figure 4.2, the jump beginning depth increases rapidly with the increase in tailwater depth. Figure 4.3 shows the relationship between the tailwater depth and the jump beginning length. The jump beginning length is seen to decrease with increasing tailwater depth. There are, of course, no jump beginning depth and length for the supercritical shooting jet regime.

Figure 4.4 shows the relationship between the tailwater depth and the bed hitting length. The bed hitting length stays at an almost a constant value for the shooting jet, hydraulic jump and early part of plunge pool regimes. During the latter part of the plunge pool situation, the bed hitting length increases quite rapidly. Finally, the plunging jet never hits the bed of the flume at the breaking surface waves regime. This particular condition is sometimes called the 'lift-off' of the falling jet.

#### 4.3.2 Air Concentration Results

Typical longitudinal air concentration profiles are shown in

**FIGURE 4.2 Relationship between Tailwater Depth and Jump beginning Depth**

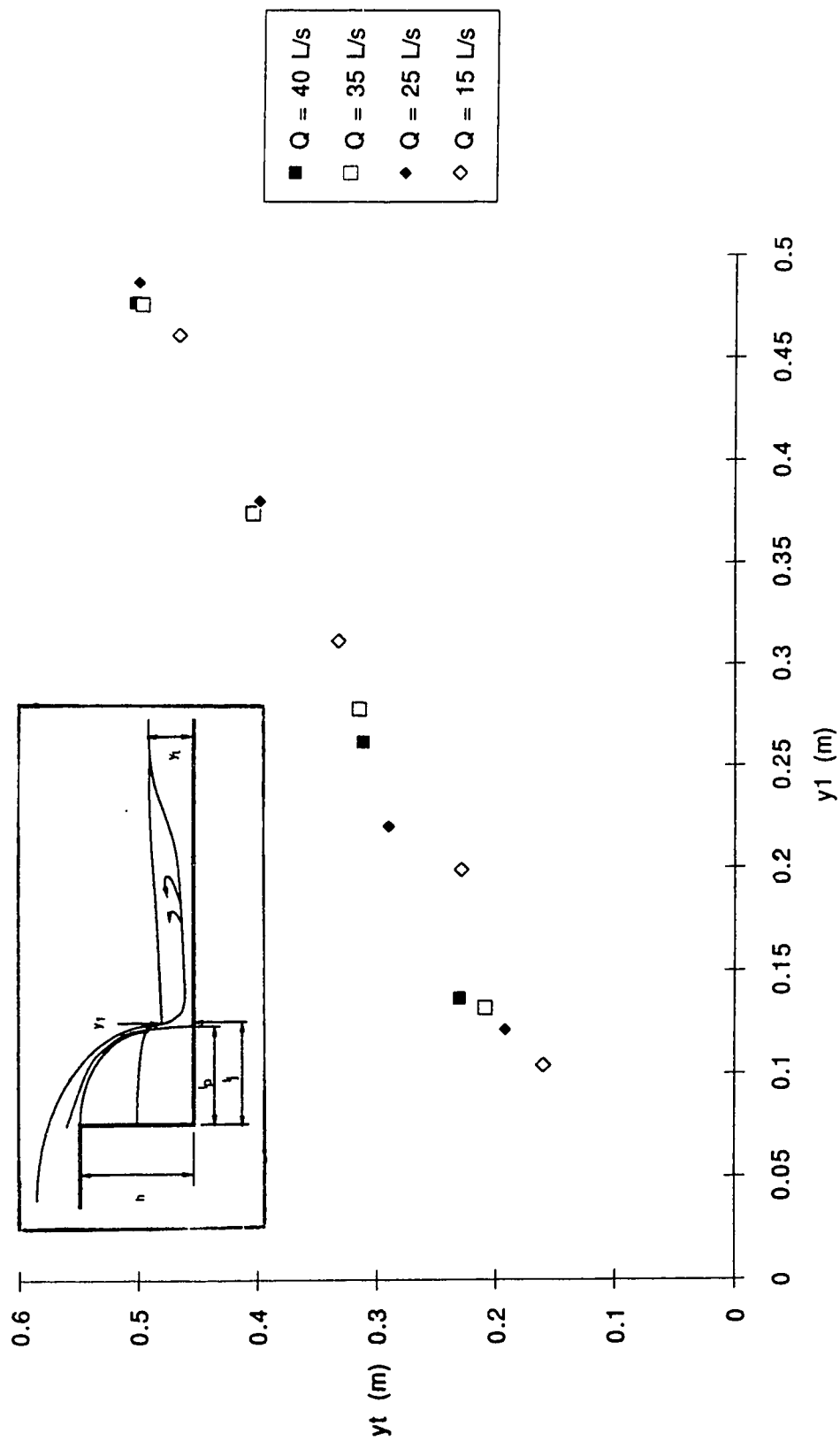


FIGURE 4.3 Relationship between Tailwater Depth and Jump Beginning Length

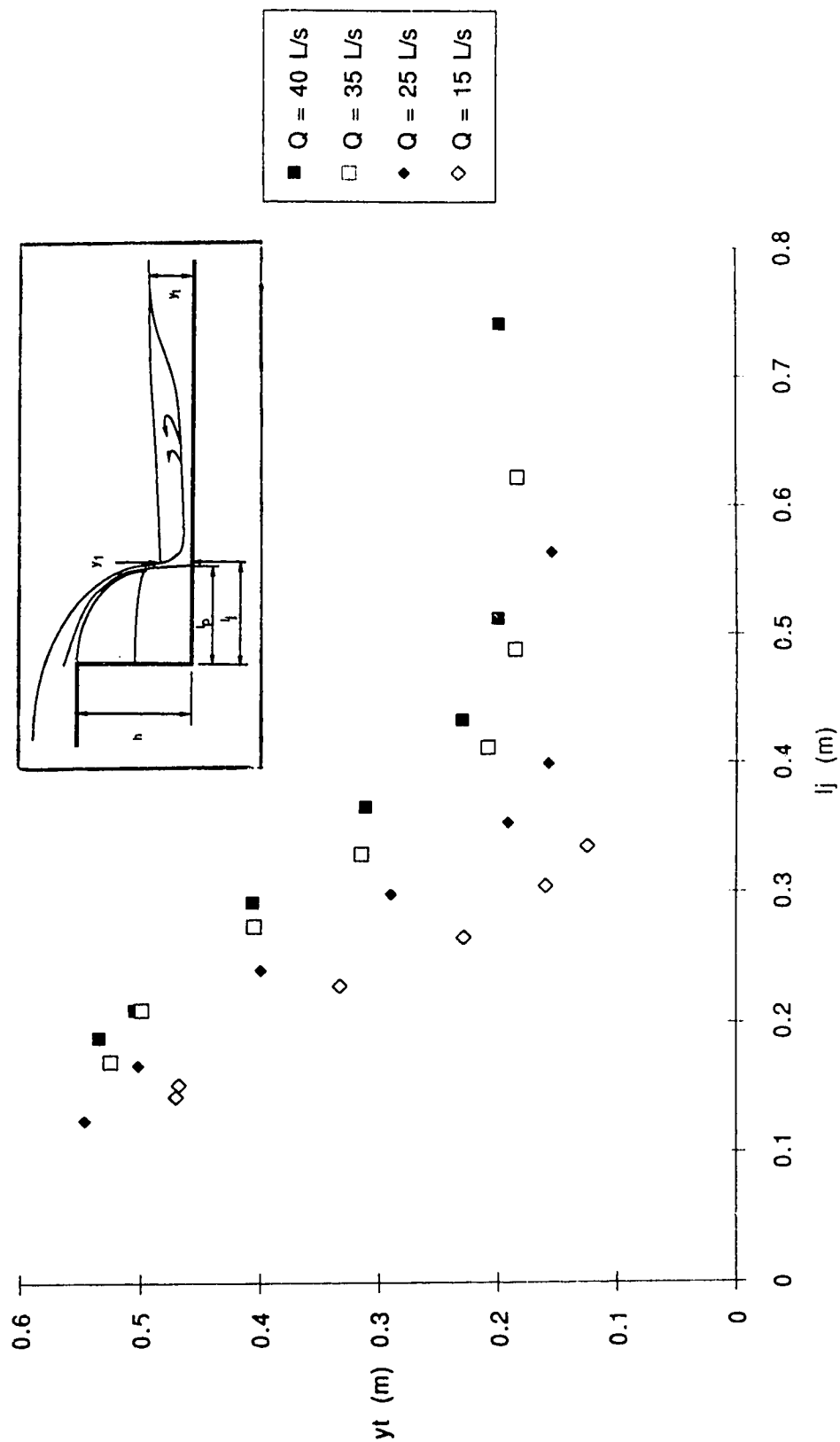
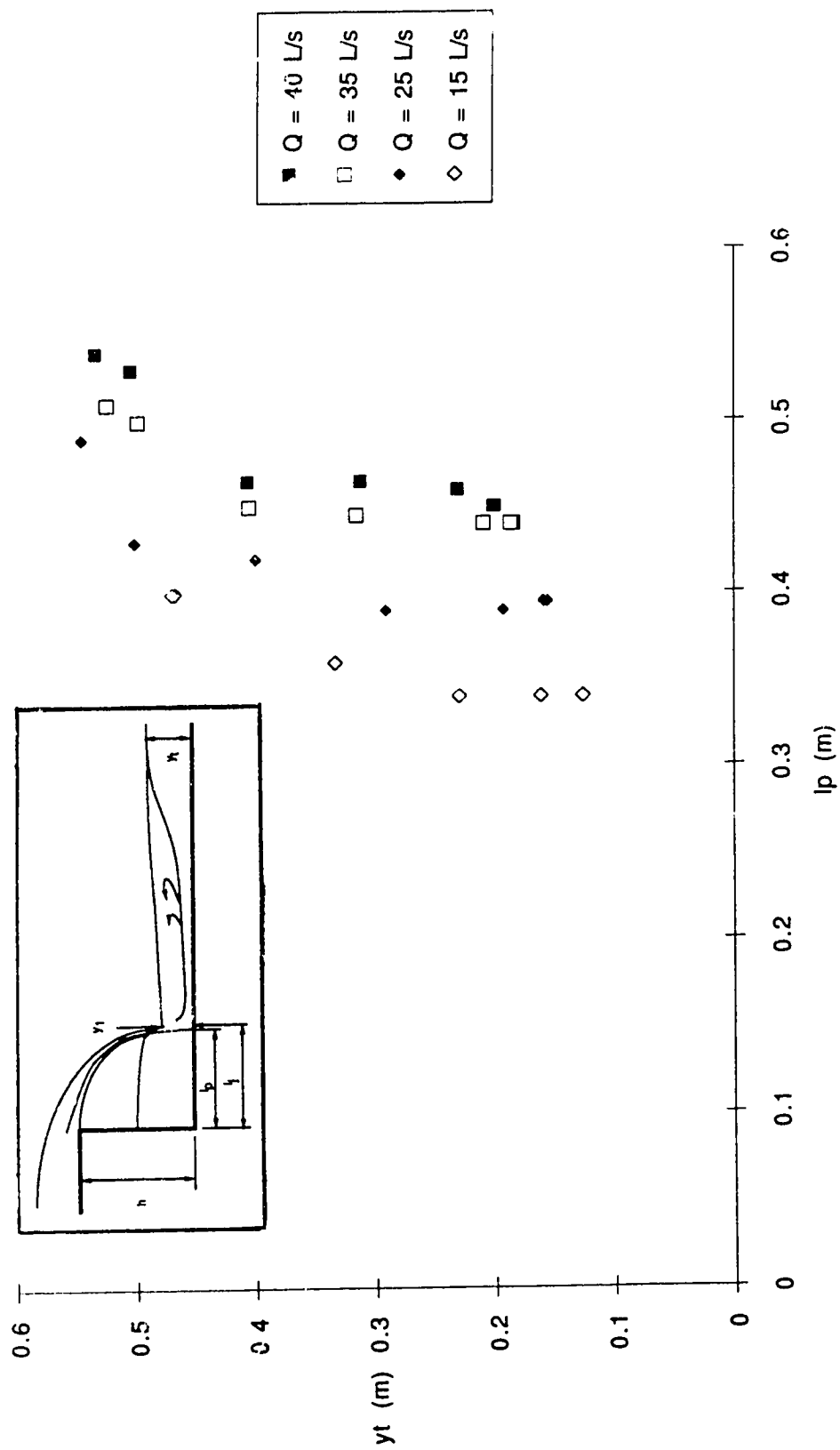


FIGURE 4.4 Relationship between Tailwater Depth and Bed Hitting Length



Figures 4.5 and 4.6, (a) to (e) respectively, for the different tailwater conditions at a constant discharge of 40 L/s. Figures 4.5 typify the air concentration profiles obtained in centreline section while Figures 4.6 show the typical profiles in the wall section. From these figures, the air concentration profiles between the centreline and wall section were almost identical. The effect of wall shear on air entrainment is, therefore, probably negligible for this discharge condition. At lower discharges, the effect of wall shear on air entrainment is noticeable but minimal.

Typical vertical air concentration profiles are also shown in Figures 4.7 (a) to (e) for the different tailwater conditions at a constant discharge of 40 L/s. The vertical air concentration profiles are derived from the centreline longitudinal profiles. The vertical profiles show that air concentration increases rapidly from bed and stays at this particular value for some depth until close to the water surface. This trend is especially evident for the higher tailwater conditions.

Mean air concentration appears in general to increase with increasing depth, increasing discharges or Drop number, and finally decreasing tailwater conditions.

#### 4.4 CONCLUSIONS

Air concentration profiles were taken on four different discharges at five different tailwater conditions for two sections each. Additional flow characteristics were measured on additional tailwater conditions for each discharge as well. Moreover,

FIGURE 4.5 (a) Mean Air Concentration Profiles at Centreline with Q of 40 L/s and  $y_t$  of 0.200 m (Hydraulic Jump)

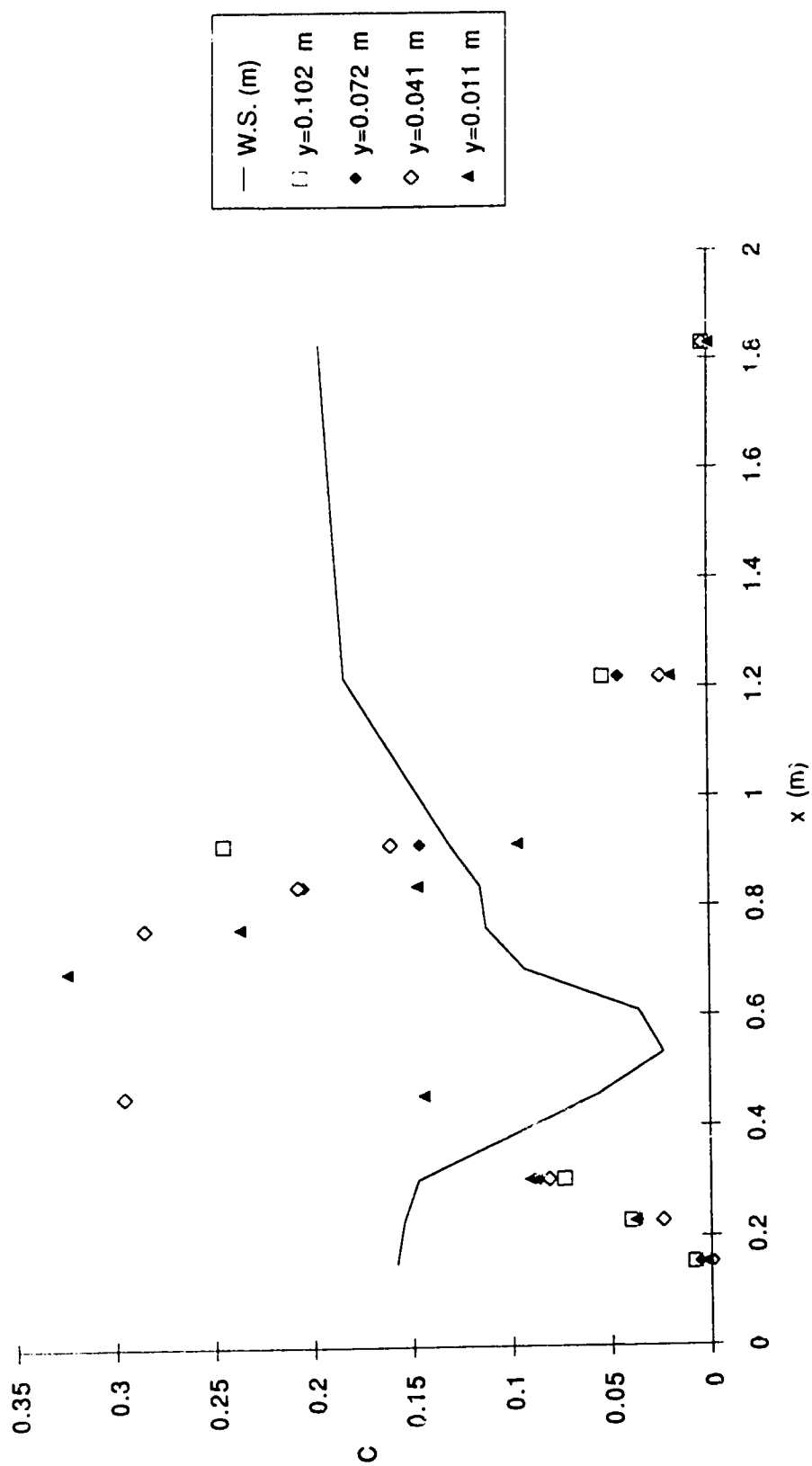


FIGURE 4.5 (b) Mean Air Concentration Profiles at Centreline with Q of 40 L/s and  $y_t$  of 0.231 m

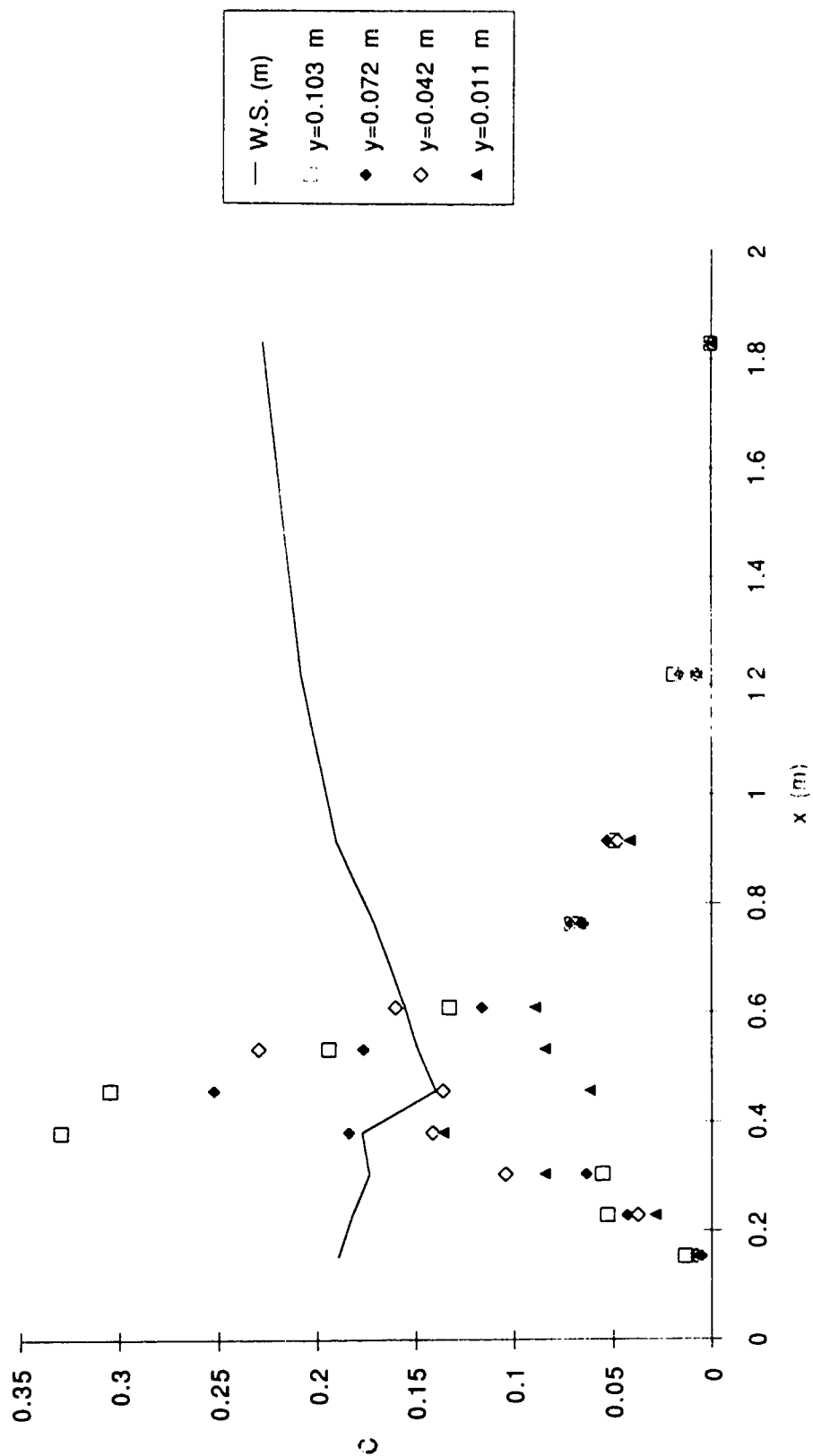




FIGURE 4.5 (c) Mean Air Concentration Profiles at Centreline with Q of 40 L/s and  
yt of 0.312 m

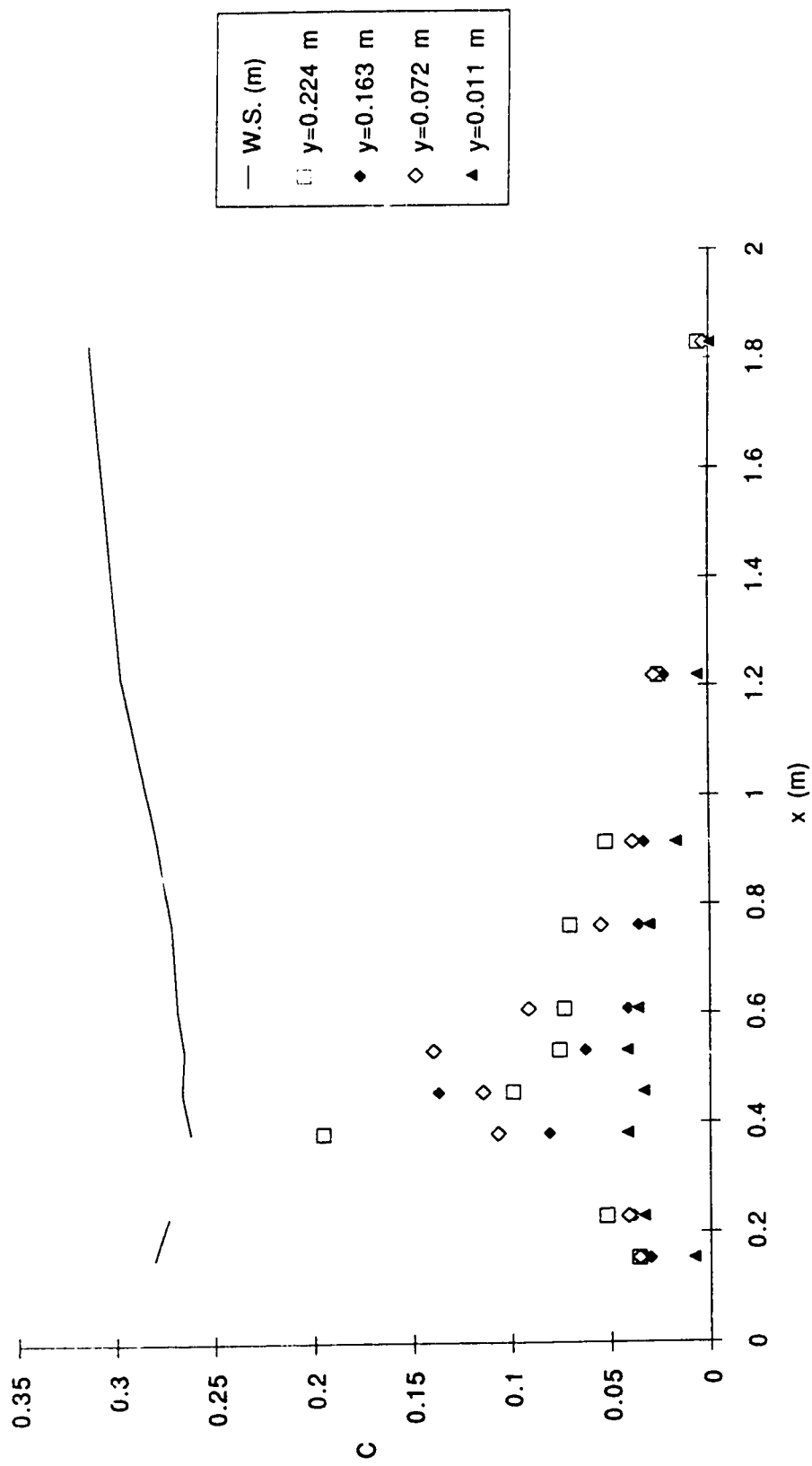


FIGURE 4.5 (d) Mean Air Concentration Profiles at Centreline with Q of 40 L/s and  
yt of 0.407 m

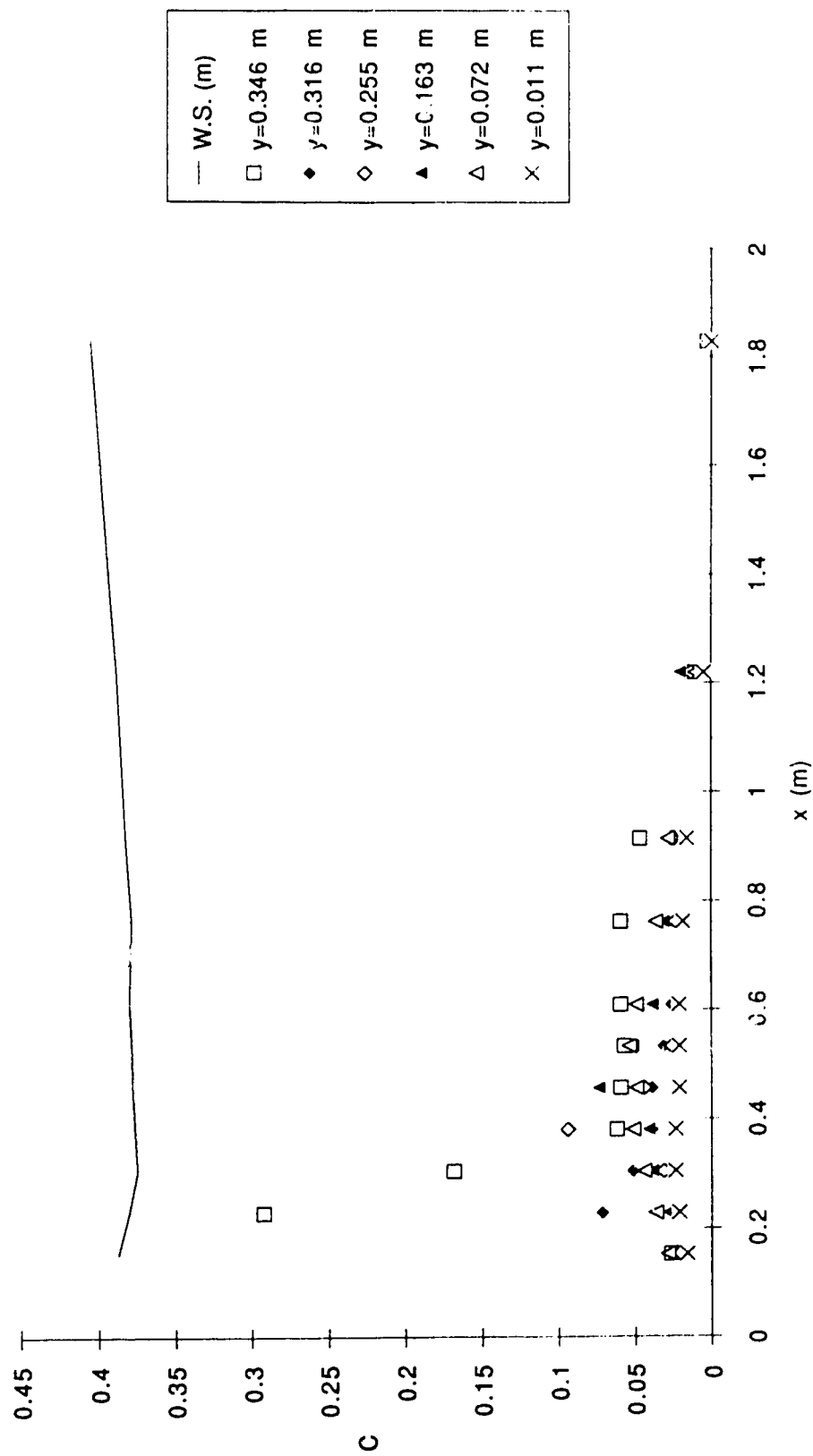


FIGURE 4.5 (e) Mean Air Concentration Profiles at Centreline with Q of 40 L/s and  
yt of 0.505 m

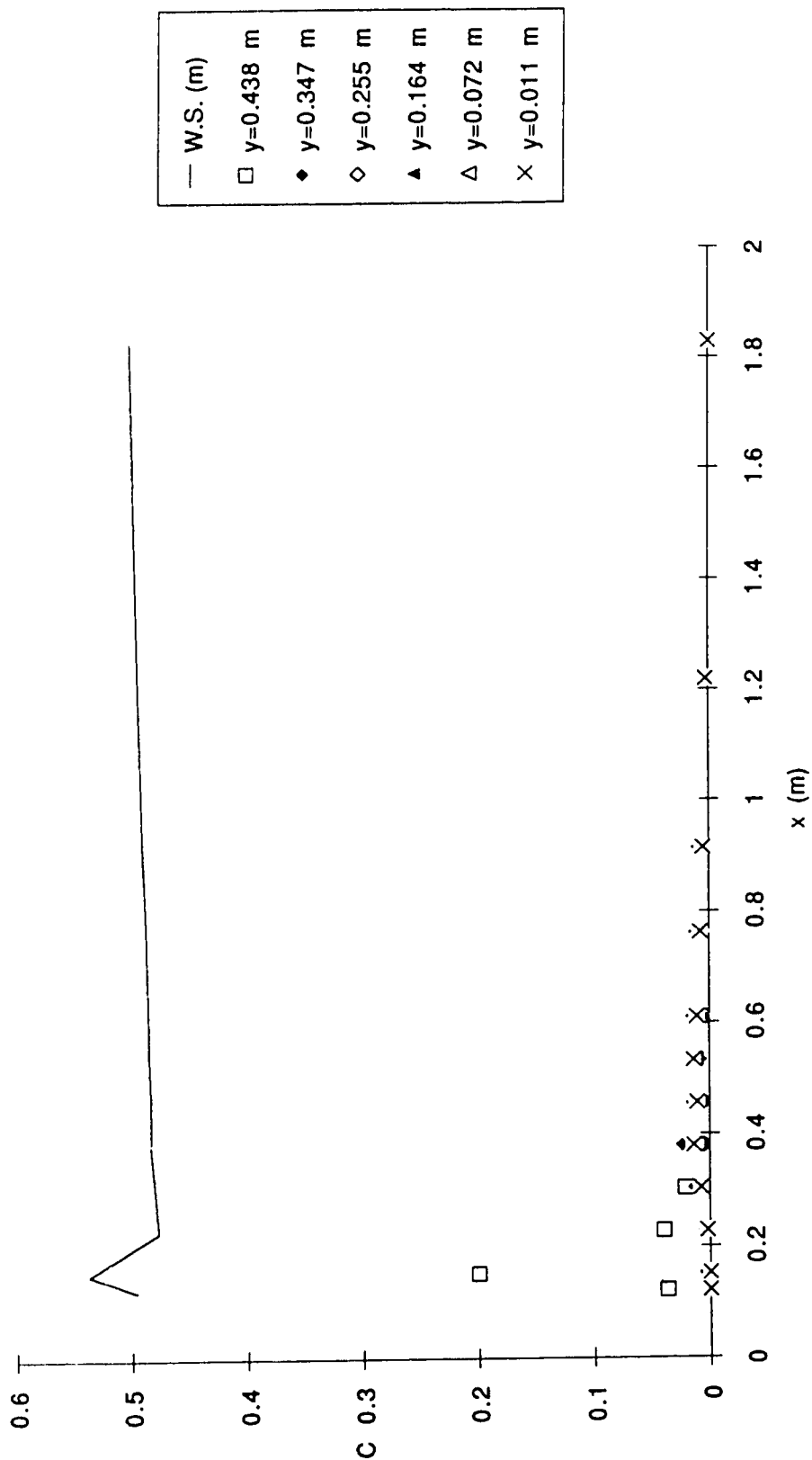


FIGURE 4.6 (a) Mean Air Concentration Profiles at Wall Section with Q of 40 L/s and yt of 0.200 m (Hydraulic Jump)

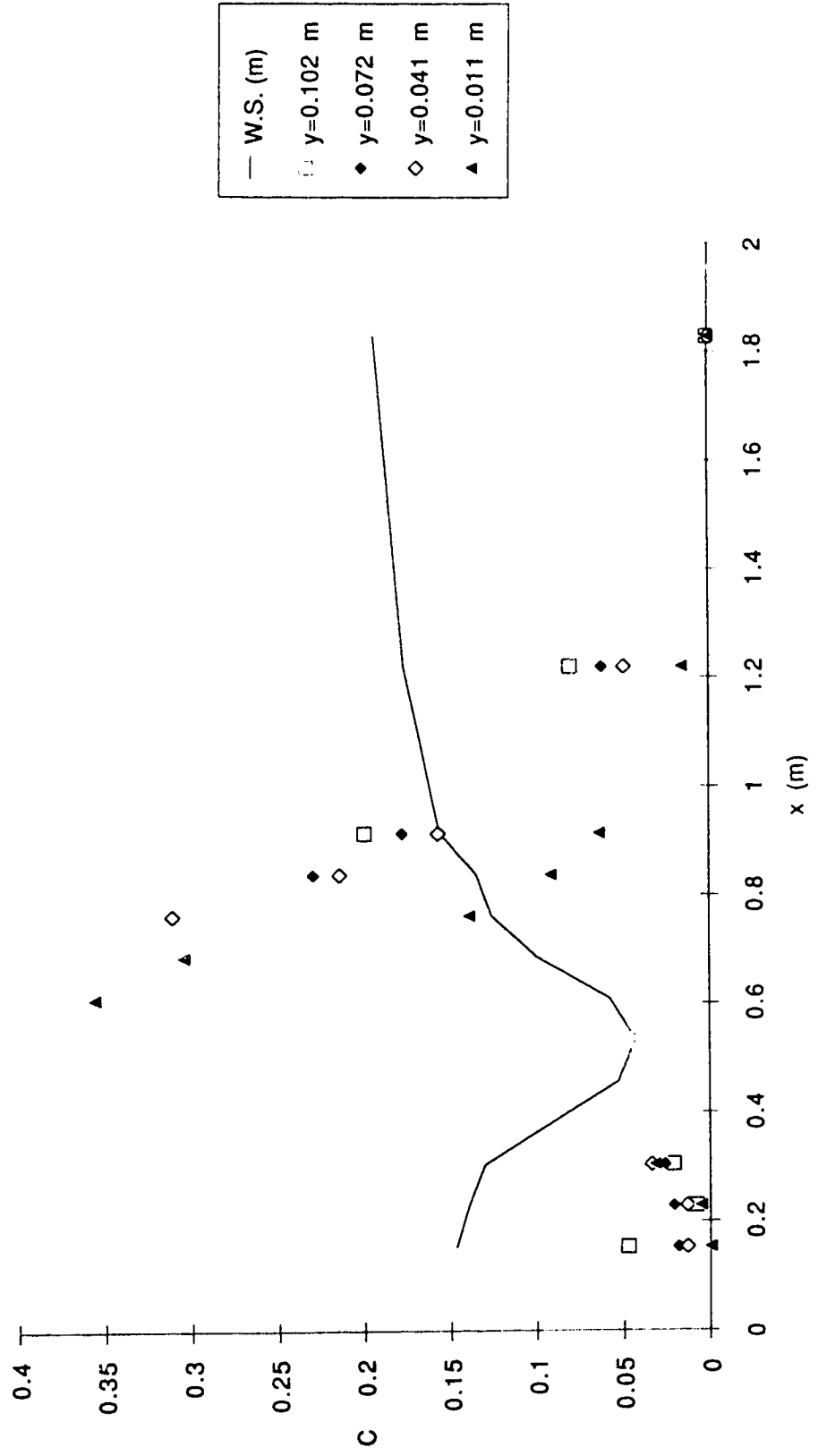


FIGURE 4.6 (b) Mean Air Concentration Profiles at Wall Section with Q of 40 L/s and  $y_t$  of 0.231 m

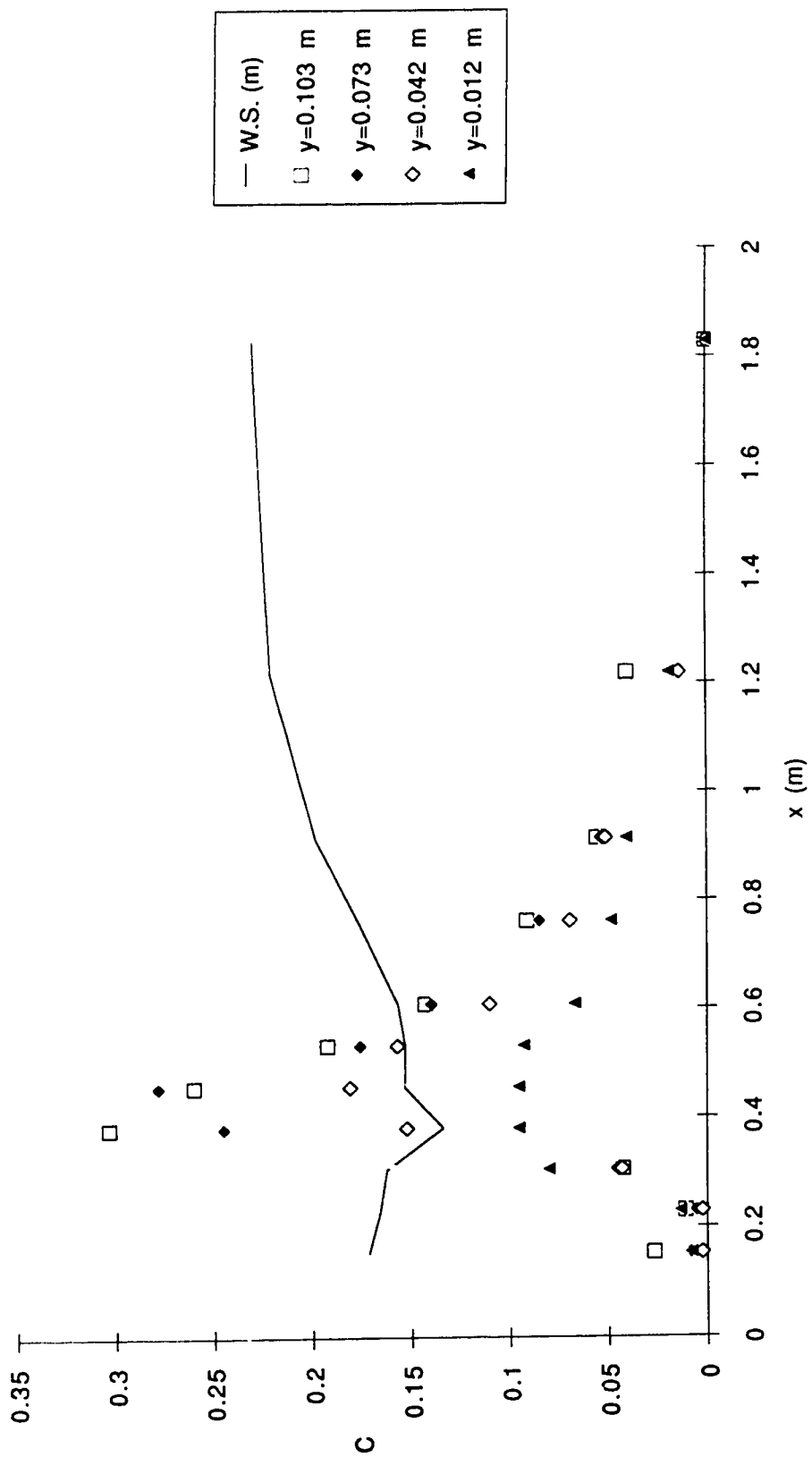


FIGURE 4.6 (c) Mean Air Concentration Profiles at Wall Section with Q of 40 L/s and  $y_t$  of 0.312 m

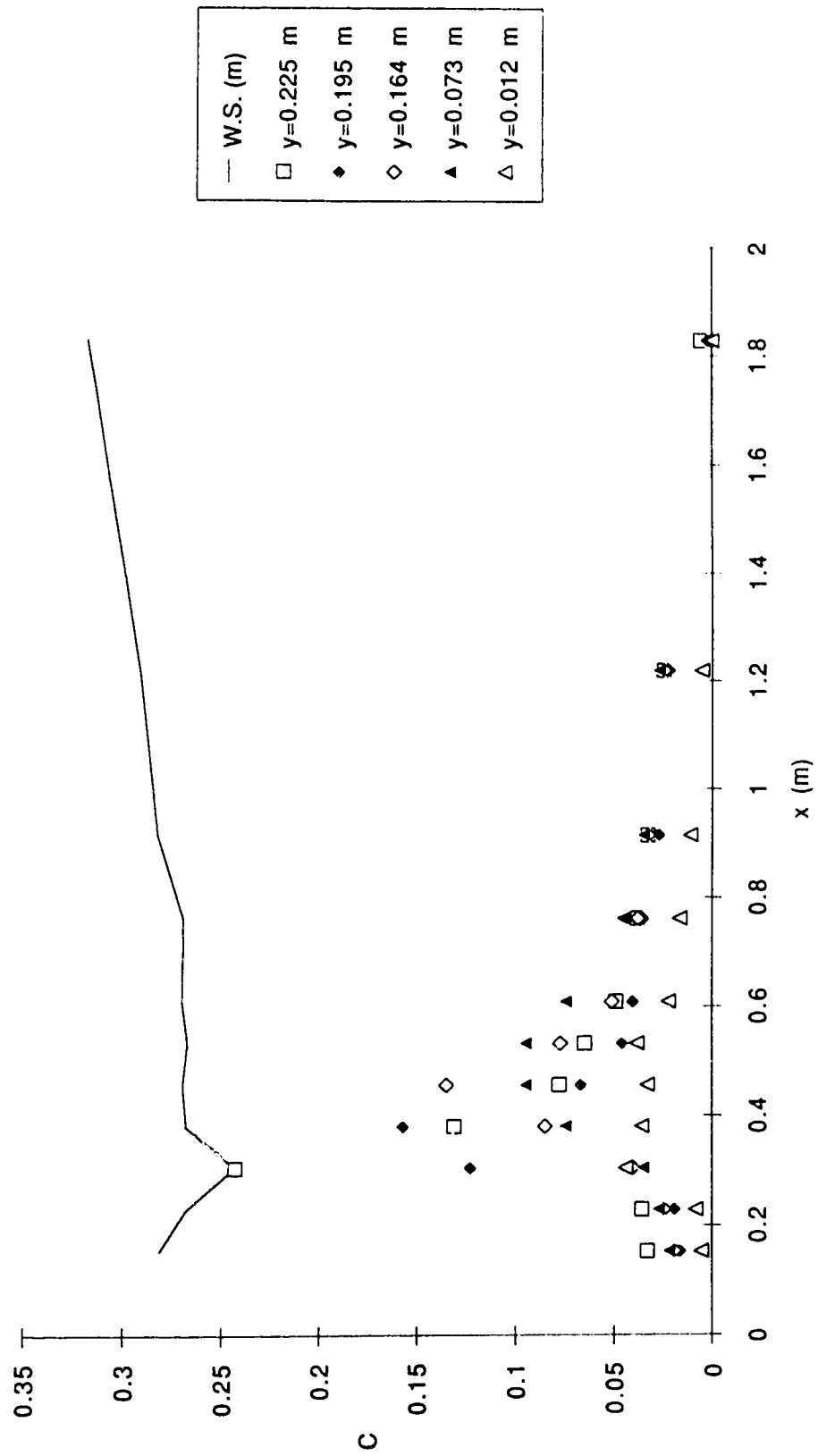




FIGURE 4.6 (e) Mean Air Concentration Profiles at Wall Section with:  $Q$  of 40 L/s  
and  $y_t$  of 0.505 m

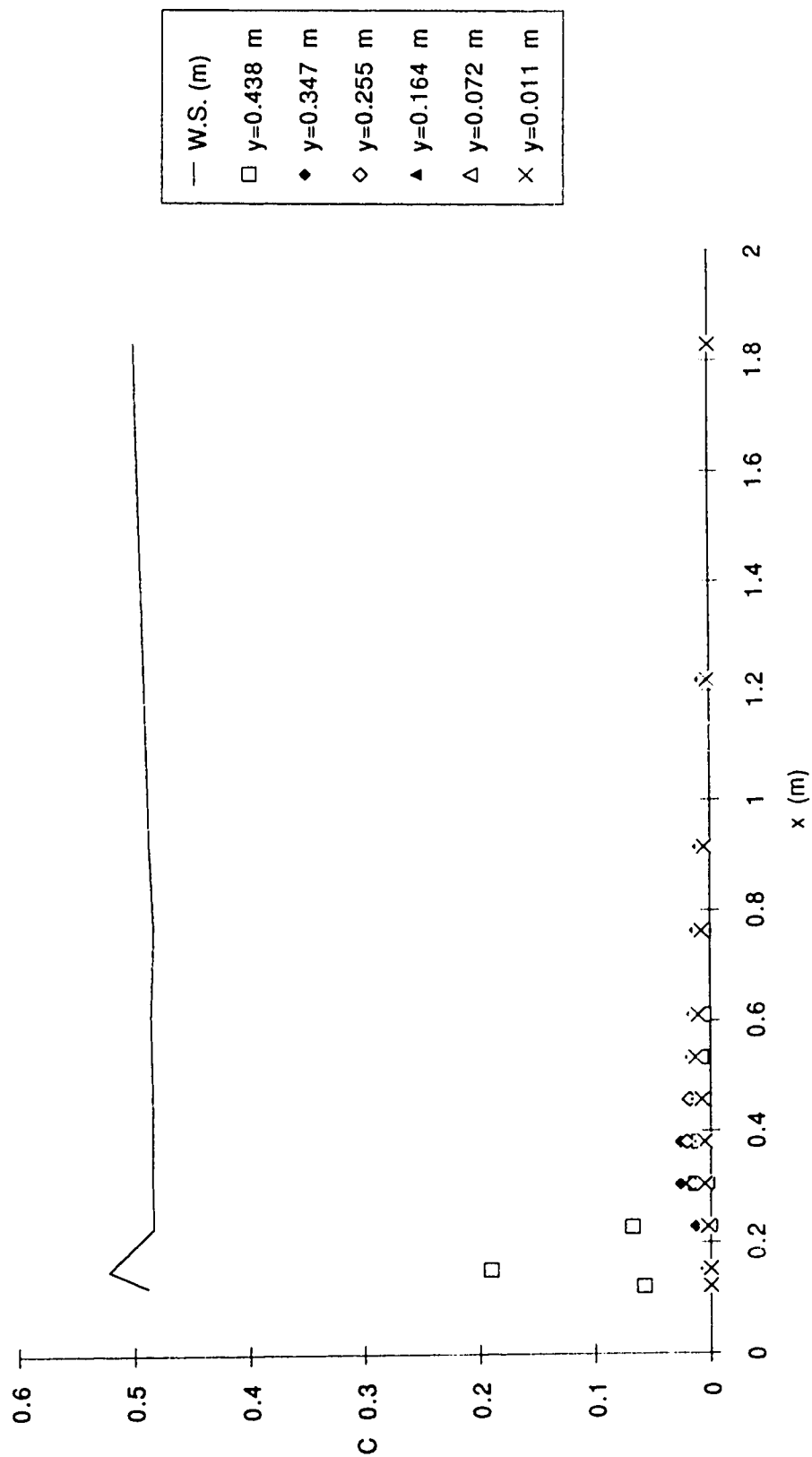




FIGURE 4.7 (a) Mean Air Concentration Vertical Profiles at Centreline with Q of 40 L/s and  $y_t$  of 0.200 m (Hydraulic Jump)

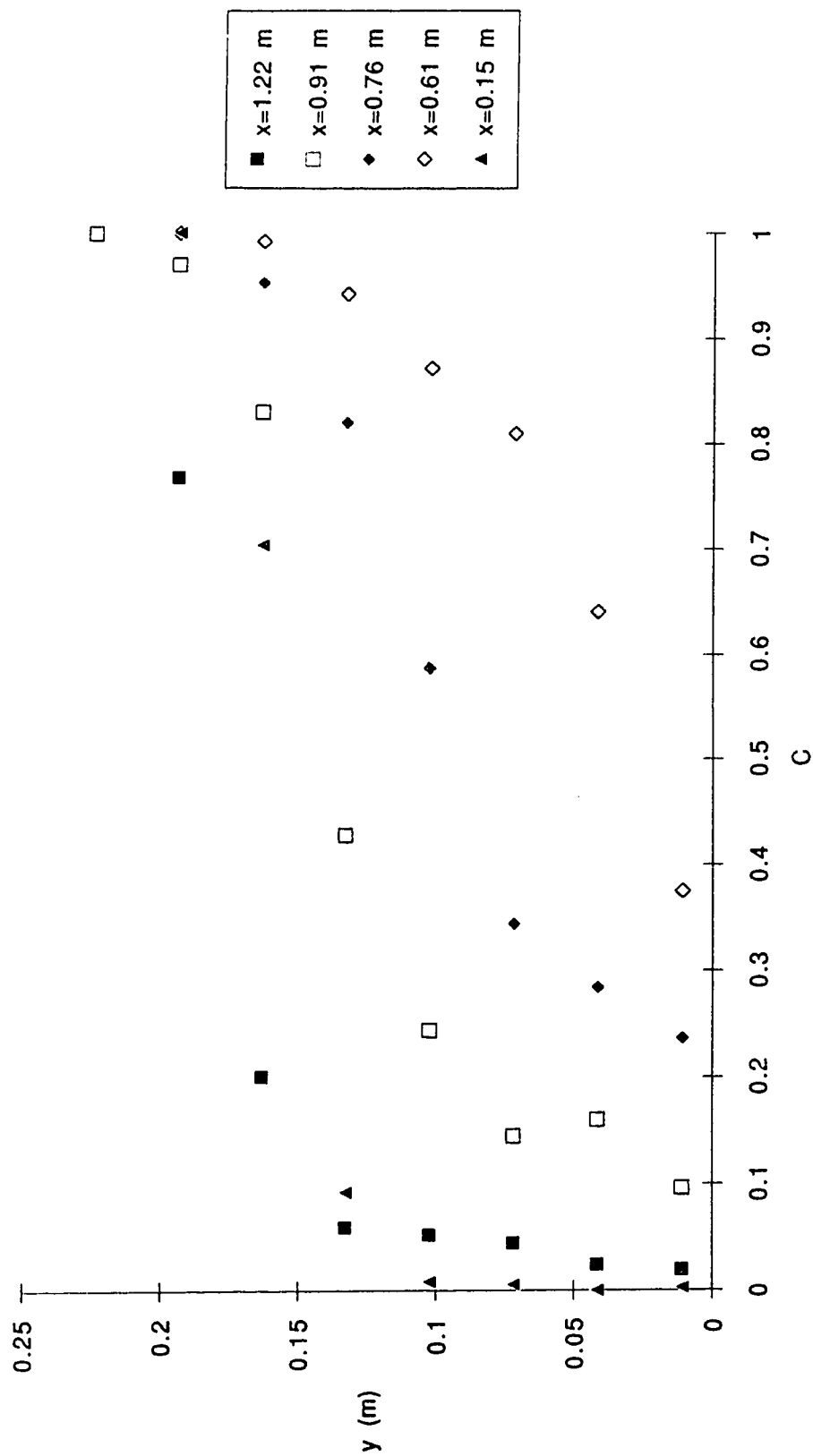


FIGURE 4.7 (b) Mean Air Concentration Vertical Profiles at Centreline with Q of 40 L/s and  $y_t$  of 0.231 m

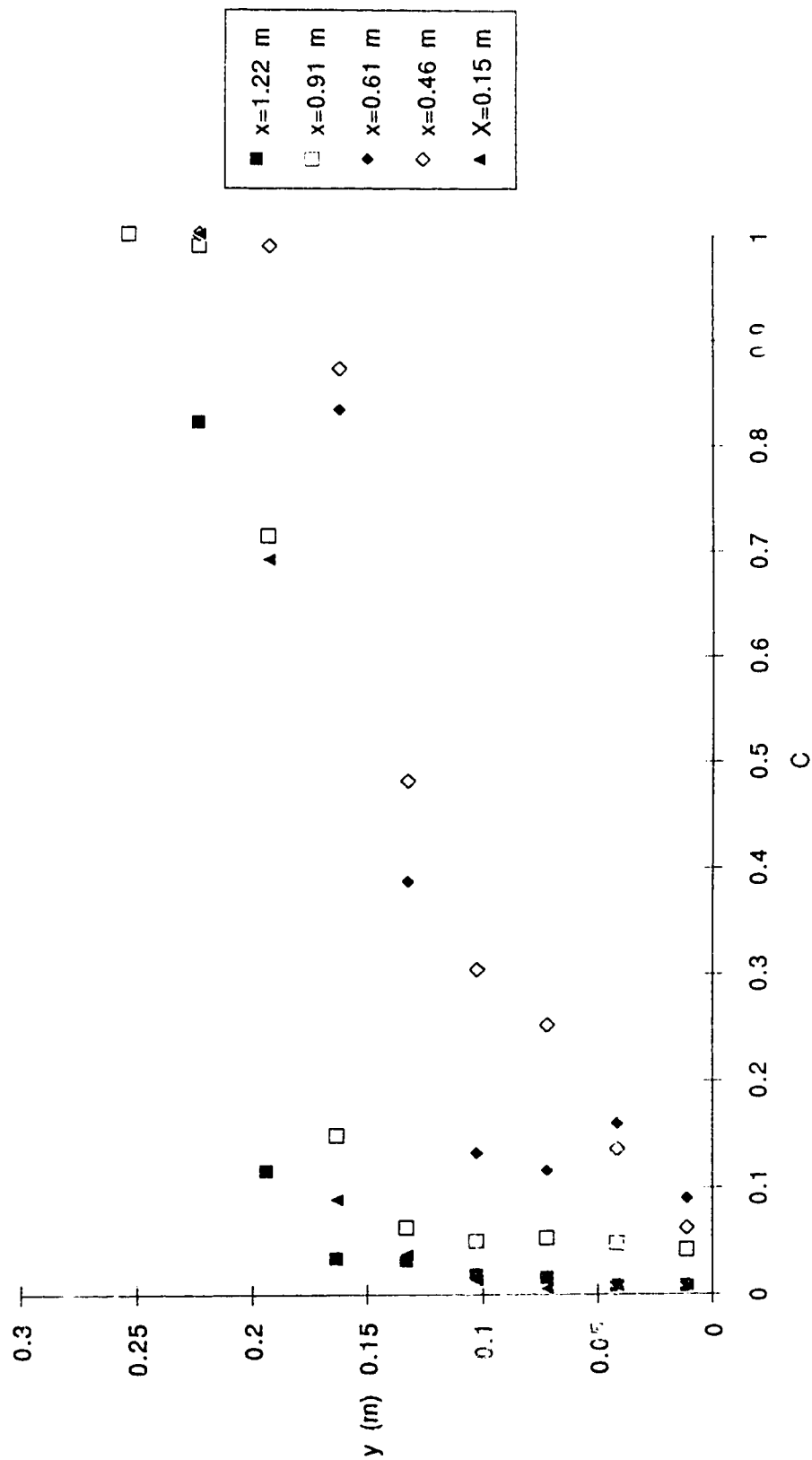


FIGURE 4.7 (c) Mean Air Concentration Vertical Profiles at Centreline with Q of 40 L/s and  $y_t$  of 0.312 m

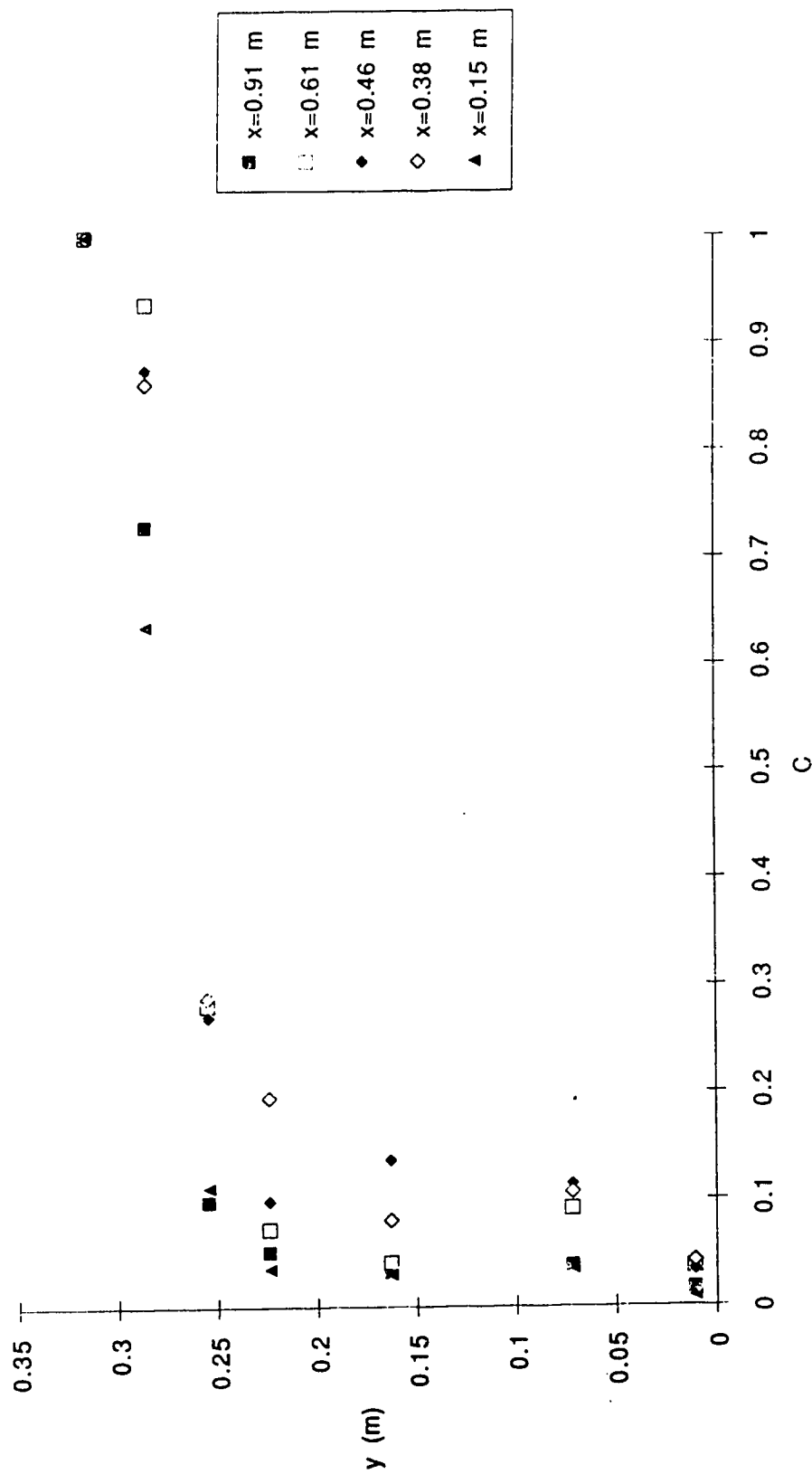


FIGURE 4.7 (d) Mean Air Concentration Vertical Profiles at Centreline with Q of 40 L/s and  $y_t$  of 0.407 m

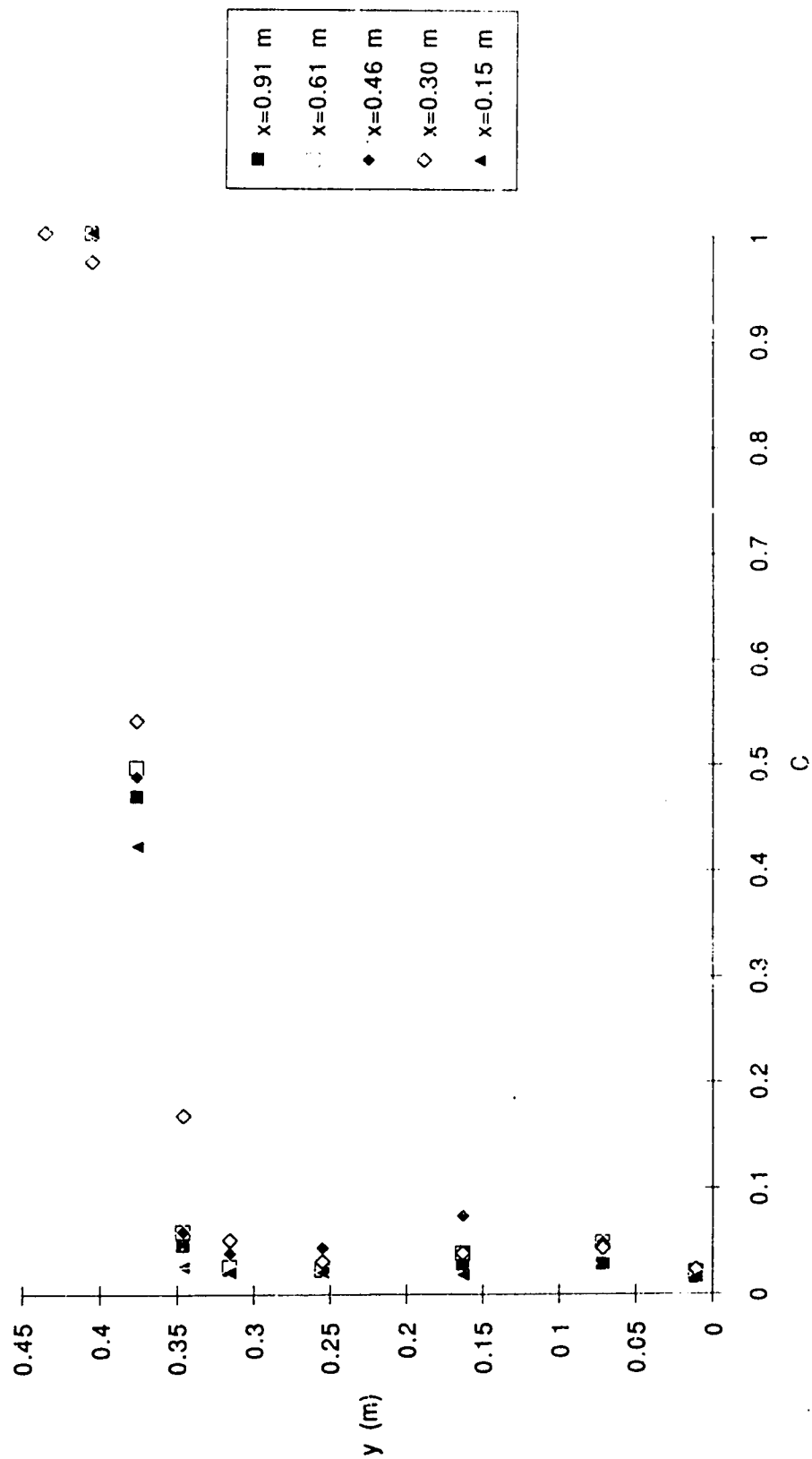
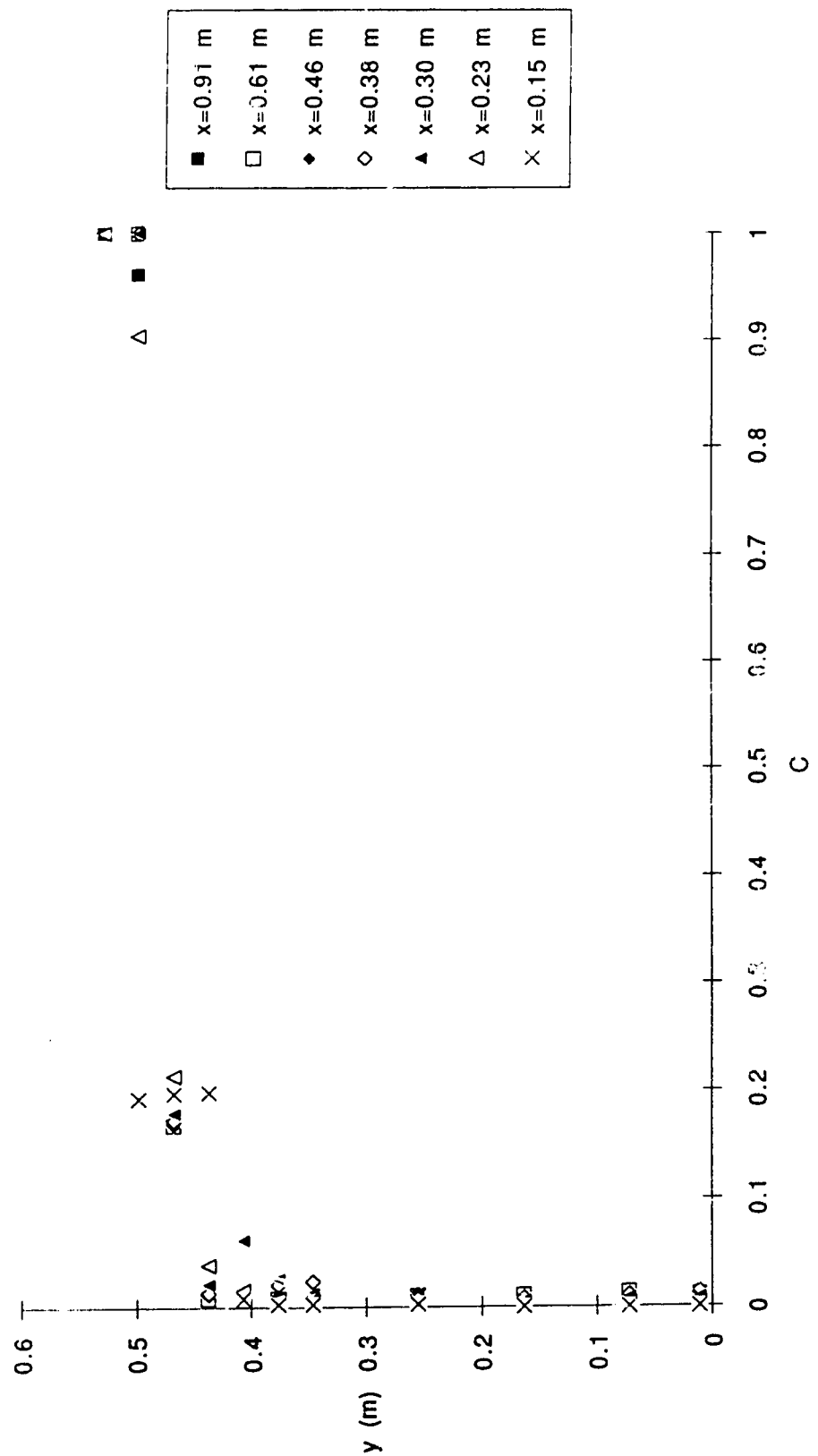


FIGURE 4.7 (e) Mean Air Concentration Vertical Profiles at Centreline with Q of 40 L/s and  $y_t$  of 0.505 m



photographic and high speed video pictures were also taken to examine the general situations.

Photographic and high speed video work showed that air is mainly entrained into the plunge pool by the formation of eddies. Flow measurements showed that the jump beginning depth and length, and the bed hitting length have a unique relationship with the corresponding tailwater depth. Furthermore, exhaustive air concentration profiles have revealed some interesting longitudinal and vertical profiles. The effect of wall shear on measured air concentrations has also been proved to be minimal.

Moreover, air entrainment characteristics appear to relate to the corresponding flow conditions of the free overfall. These experimental results will be analyzed in the next chapter in order to find the relationships for the air entrainment characteristics with the specific flow conditions of free overfall.

## CHAPTER 5

### ANALYSIS OF EXPERIMENTAL RESULTS

#### 5.1 INTRODUCTION

The goal of these experiments was to find generalized relationships between the flow conditions and air entrainment characteristics of free overfalls. The existing knowledge on the flow conditions is far more complete than that on the air entrainment characteristics of free overfall. The analysis, therefore, would start from the flow conditions of free overfalls by following Rand's (1955) method and using the Drop number. Applying similar analytical method, the air entrainment results were also analyzed in order to find the general relationships.

#### 5.2 FLOW ANALYSIS

The flow conditions for both the supercritical shooting jet and the hydraulic jump regimes have been studied well. Furthermore, the hydraulic jump forming at the toe of the falling jet has been determined by Rand (1955) to be the 'critical' condition of free overfall. Many flow characteristics have shown to be functions of the Drop number at this critical condition. As a result, flow conditions can be predicted quite confidently for these two regimes when the inflow, i.e. Drop number, conditions are known.

On the other hand, the flow conditions for both the plunge pool and the breaking surface waves regimes have not been studied well.

Many flow characteristics cannot be estimated for these two regimes even if the inflow conditions are given. Therefore, the flow analysis will only be done for these two flow regimes. The analysis will, if possible, start from the critical condition and elaborate into the other flow conditions of the overfall. The experimental data are compared to the relationships proposed by Rand (1955) wherever possible.

### 5.2.1 Plunge Pool

Our knowledge on the flow characteristics for the plunge pool regime of free overfalls has been amazingly little considering its popularity in practical situations. Despite the importance of Drop number, which represents the inflow conditions of the overfall, many flow characteristics cannot be derived from the Drop number alone for the plunge pool conditions. Another parameter is thus required and this parameter is the tailwater depth which represents the receiving pool conditions of the overfall. A dimensionless ratio is also more useful because general relationships can be derived for all conditions. The ratio between the tailwater depth and the drop height is then used and called the tailwater depth ratio.

Three flow characteristics are specifically measured to describe the plunge pool regime. These flow characteristics are the jump beginning depth and length, and bed hitting length. The following sections will describe in detail the analysis on these flow characteristics.



#### 5.2.1.1 Jump beginning depth

The jump beginning depth is the depth of the receiving pool water at the location where the falling jet hits the receiving pool and indicates the level of submergence for the plunge pool condition. To obtain a general relationship, all terms have to be made dimensionless. The jump beginning depth can also be made dimensionless by the drop height much in the same way as the tailwater depth ratio. The resulting relationship is shown on Figure 5.1.

For supercritical shooting jet regime, no jump is formed and thus the jump beginning depth do not exist. At the critical condition of hydraulic jump, the jump beginning depth and the tailwater depth will follow the relationship described by the conjugate depths equation, i.e. Equation 2.4. As the tailwater depth continues to increase, the hydraulic jump is thus submerged and the plunge pool regime begins. At the plunge pool regime, the tailwater depth ratio and the jump beginning depth ratio will follow the trend as shown in Figure 5.1. As the level of submergence increases, the jump beginning depth increases rapidly as well and almost equals to the tailwater depth at the highest level of submergence. Therefore, an asymptote exists at the high tailwater depth ratio where the relationship will follow the  $45^\circ$  line as shown in Figure 5.1. Finally, the tailwater depth ratio as determined from the hydraulic jump conditions correspond well with the relationship proposed by Rand (1955) as shown in Figure 5.2.

FIGURE 5.1 Relationship between Tailwater Depth Ratio and Jump Beginning Depth Ratio

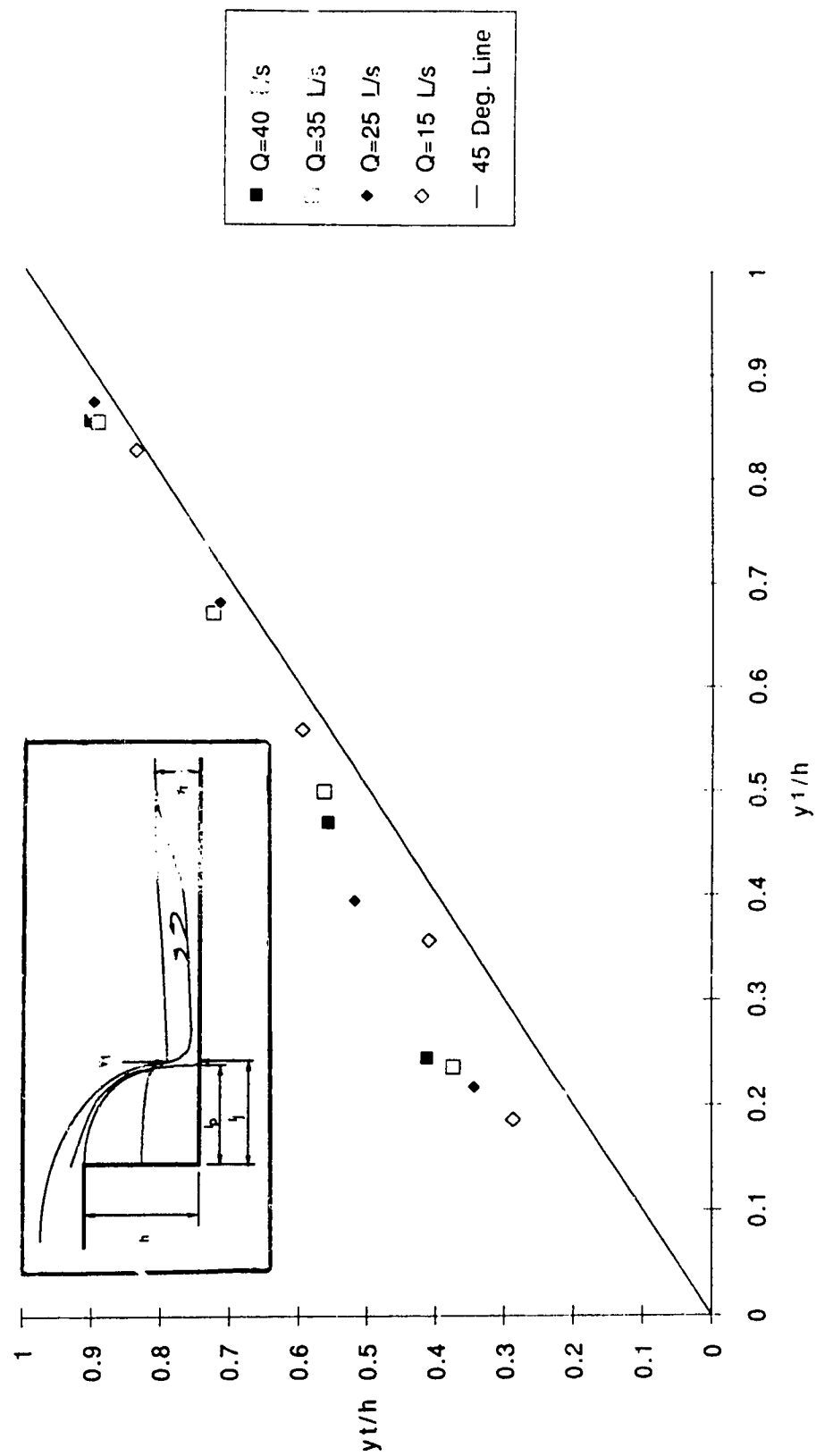
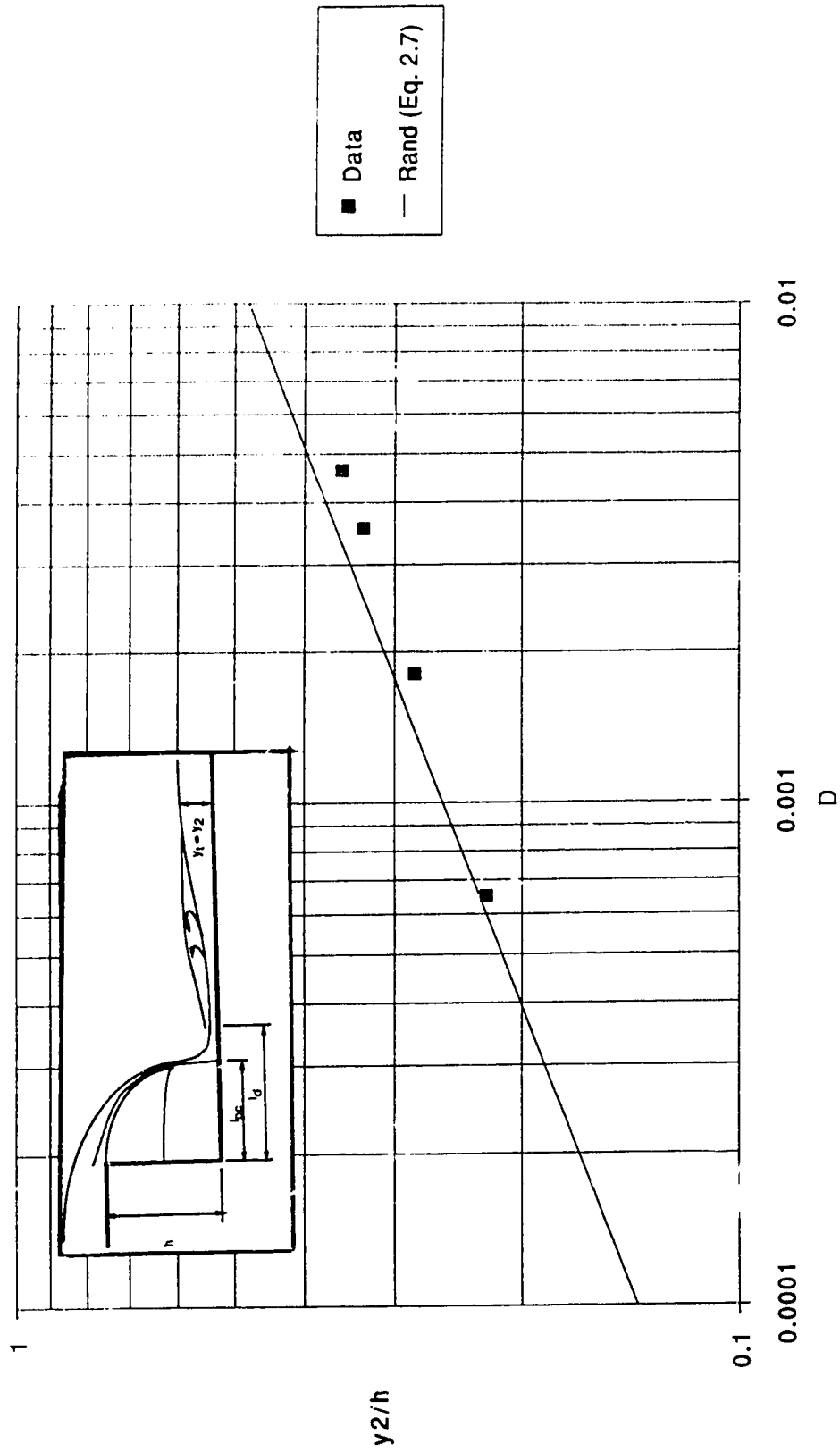


FIGURE 5.2 Comparison of Tailwater Depth Ratio with Drop Number



### 5.2.1.2 Jump beginning length

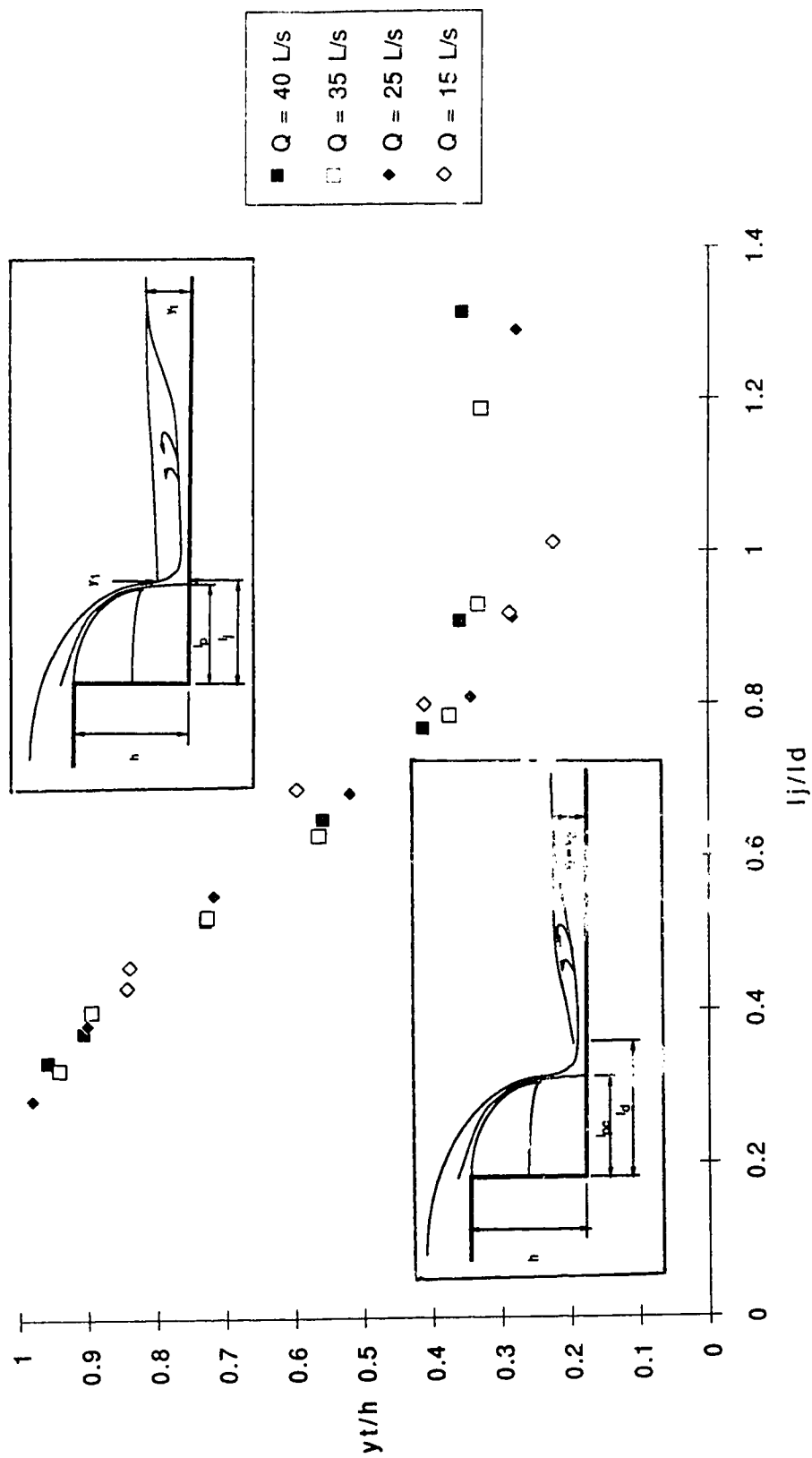
The jump beginning length is the distance from the brink to the location where the falling jet hits the receiving pool of the overfall. Making the jump beginning length dimensionless is not as straightforward as the corresponding depth situation. Drop height is not a suitable scale as in the depth situations because length and depth are in different directions. Rand (1955) proposed that the jump beginning length and the drop length are identical at the critical condition of free overfall. Therefore, the corresponding drop lengths as found from Rand's equation, i.e. Equation 2.8, are used to make all the jump beginning lengths dimensionless. The resulting jump beginning length ratio is plotted against the tailwater depth ratio as shown in Figure 5.3.

As noted earlier, no jump beginning length is found in the supercritical shooting jet condition. At the critical hydraulic jump condition, the jump beginning length ratio is one at the corresponding tailwater depth ratio. As the tailwater continues to increase, the jump beginning length ratio will follow the trend as shown in Figure 5.3. A unique relationship is distinctively seen for all discharges from the tailwater depth ratio of higher than 0.3. This tailwater depth ratio of 0.3 corresponds to the condition of complete submergence of the hydraulic jump.

### 5.2.1.3 Bed hitting length

The bed hitting length is the distance from the brink to the

FIGURE 5.3 Relationship between Tailwater Depth Ratio and Jump Beginning Length Ratio



location where the falling jet hits the channel bed and is an indication on the relative strength of the falling jet. First of all, the bed hitting lengths have been made dimensionless by the drop height and compared with Rand's equation for bed hitting length, i.e. Equation 2.9, as shown in Figure 5.4. Figure 5.4 proves that the bed hitting length data at the free jump condition compare well with Rand's equation. As a result, the bed hitting length for the critical condition as predicted by Rand's equation is used to make all the bed hitting lengths dimensionless and thereafter called the bed hitting length ratios. The resulting relationship between the tailwater depth ratio and the bed hitting length ratio is shown in Figure 5.5.

At the conditions of supercritical shooting jet, hydraulic jump and early part of plunge pool, the bed hitting length remains relatively constant. The relative strength of the falling jet is thus the same for low tailwater depth ratio. As the tailwater depth ratio continues to rise, the bed hitting length ratio will increase in the trend as shown in Figure 5.5 and indicates that the relative strength of the falling jet decreases by the increase in the level of submergence. Finally, the bed hitting length will cease to exist as the falling jet does not hit the flume bed but ride on top of the water in the receiving pool. This situation indicates that the falling jet does not have enough strength to penetrate into the water body of the receiving pool. This phenomenon also corresponds to the beginning of the breaking surface waves regime which will be discussed in the next section.

FIGURE 5.4 Comparison between bed hitting length ratio with Drop Number

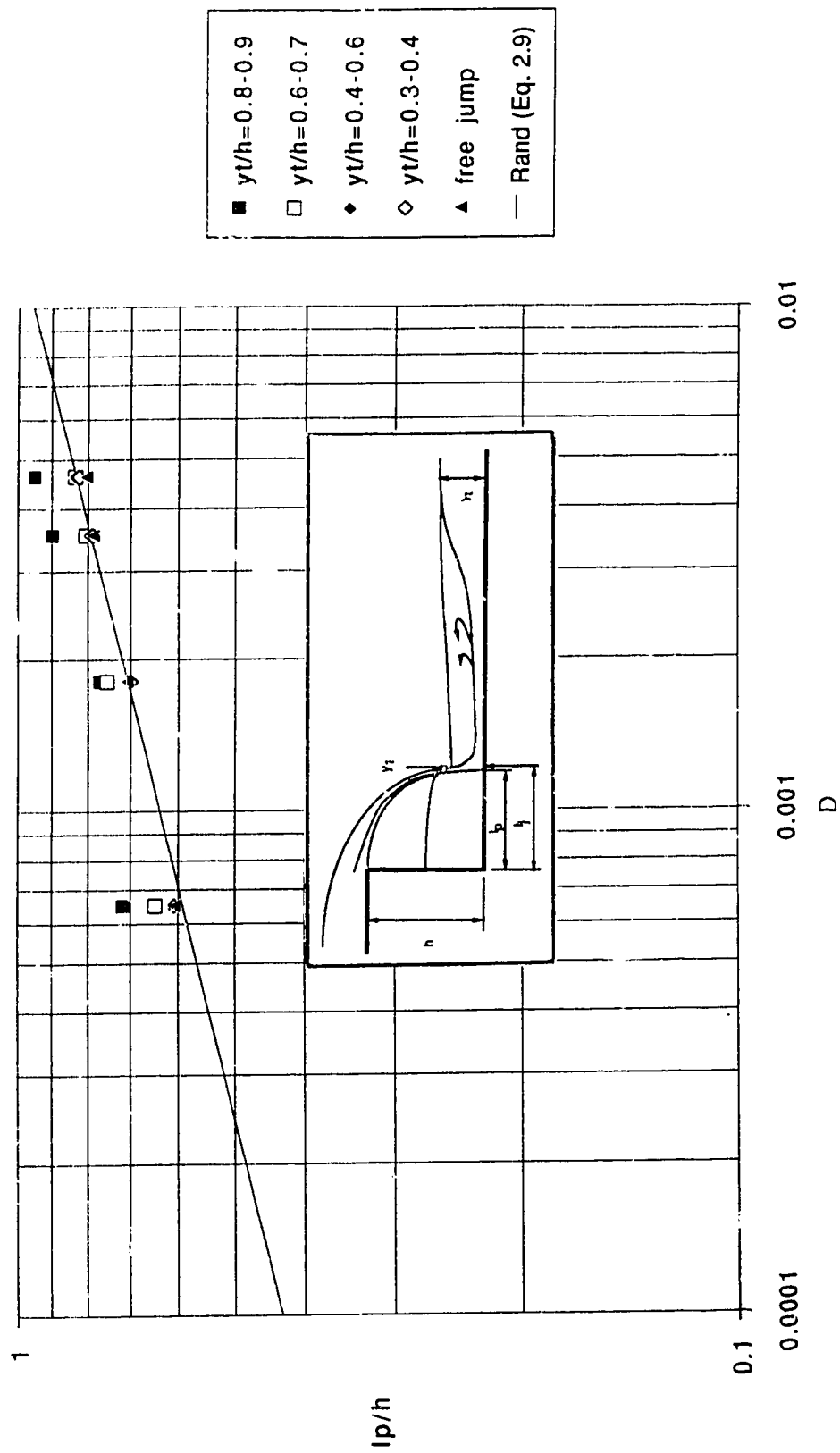
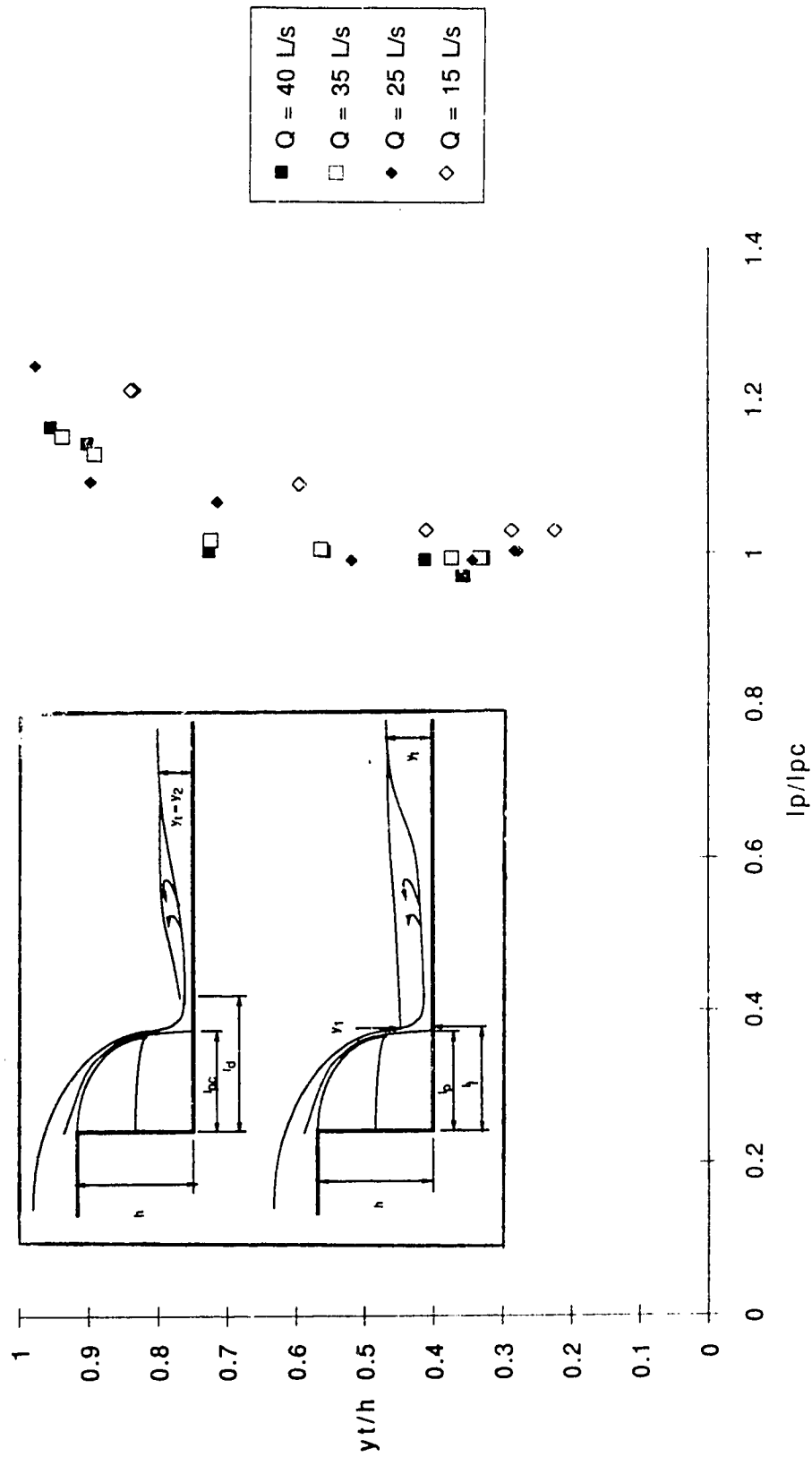


**FIGURE 5.5 Relationship between Tailwater Depth Ratio and Bed Hitting Length Ratio**





### 5.2.2 Breaking Surface Waves

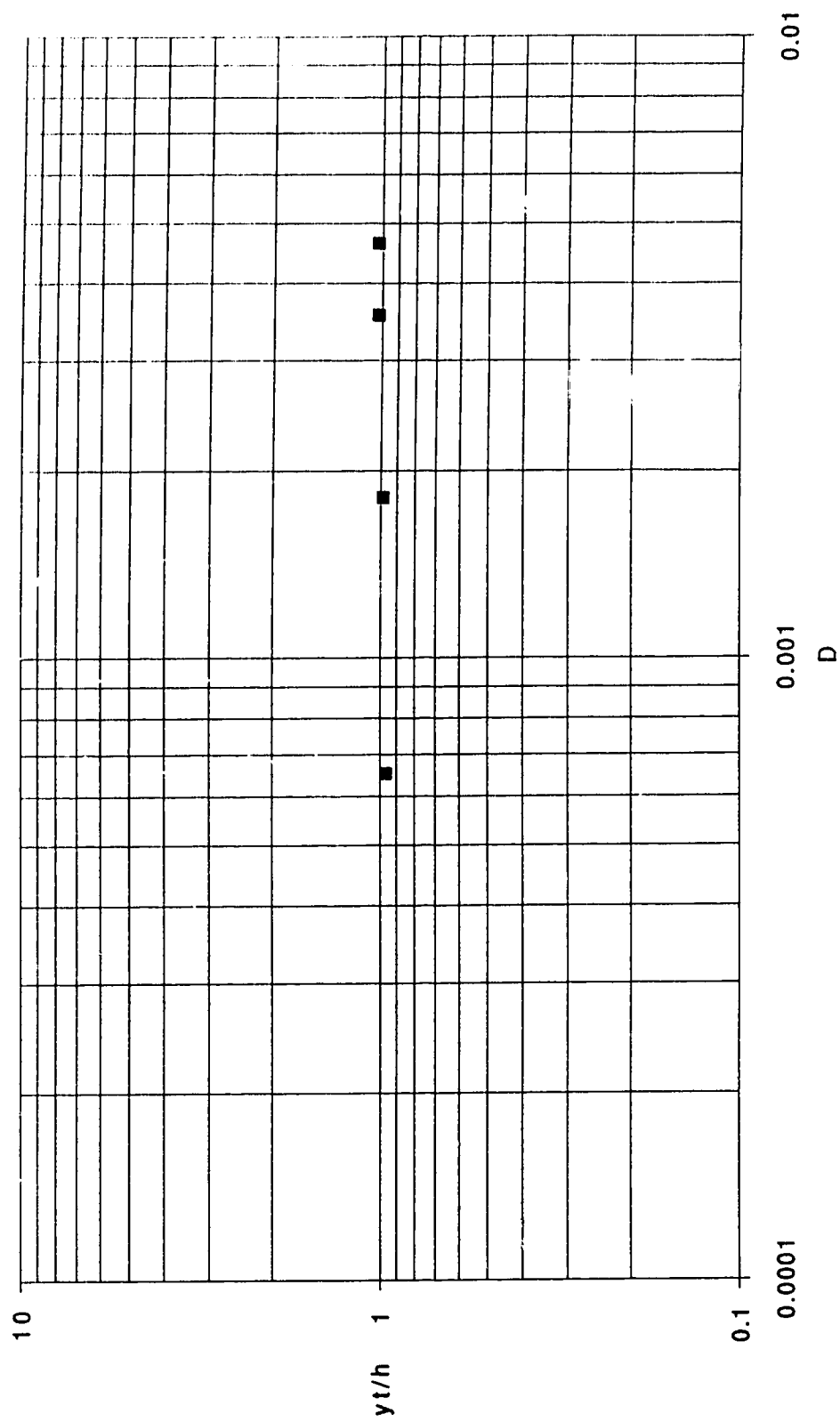
The flow characteristics of the breaking surface waves regime of free overfalls is difficult to quantify. The basic criteria for the formation of the breaking surface waves will be the only concern for this thesis. As mentioned in the last section, the formation of flow with breaking surface waves corresponds to the situation where the bed hitting length suddenly becomes infinity. As shown in Figure 5.5, the bed hitting length disappears at the condition where the tailwater depth ratio reaches one. Careful observations have also shown that the onset, or beginning, of flow with breaking surface waves begins when the tailwater depth reaches approximately the drop height. Figure 5.6 shows the tailwater depth ratio with the Drop number for the onset of breaking surface waves regime.

As seen from Figure 5.6, the tailwater depth ratio remains constant at the onset of breaking surface waves regime for the different Drop number or inflow conditions and thus indicates that the onset of breaking surface waves is influenced mainly by the tailwater conditions rather than the inflow conditions. This conclusion confirms the observations by Sene, Thomas and Goldring (1989) that the formation of the flow with breaking surface waves is independent of the entry or inflow conditions.

### 5.3 AIR ENTRAINMENT ANALYSIS

In the supercritical shooting jet regime, only the backpool entrainment mechanism is considered to be a significant air

FIGURE 5.6 Onset Condition for Flow with Breaking Surface Waves



contributor. The backpool air entrainment is also found in the critical hydraulic jump condition of free overfall. In the breaking surface waves regime, limited amount of air is entrained into the flow and will not be discussed further. Consequently, the air entrainment analysis is only performed on the hydraulic jump and plunge pool regimes. As a matter of practical interest, the Reynolds numbers for the experiments were in the range of 33,000 to 88,000 and thus the viscous effect on air entrainment was minimal.

### 5.3.1 Hydraulic Jump

Figure 5.7 shows two distinct locations where air entrainment is prominent in the critical hydraulic jump condition, and these locations are in the backpool area and the hydraulic jump area. Air entrainment analysis is thus performed to the backpool and the hydraulic jump or called critical areas of the hydraulic jump regime.

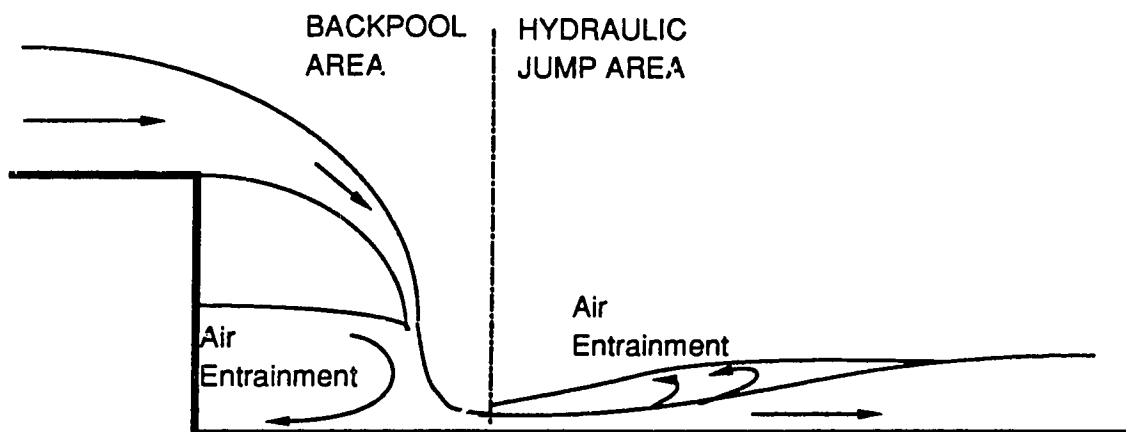


FIGURE 5.7 Two Air Entrainment Locations for Hydraulic Jump

As seen in the flow analysis, the data correspond well with Rand's equations for the critical hydraulic jump condition although the hydraulic jumps for this experiment did not form at the exact critical location of the overfall. Therefore, the air entrainment characteristics should also correspond well to the critical condition.

Rand (1955) showed that the dimensionless flow characteristics are functions of the Drop number at the critical hydraulic jump condition. Similar relationships are then sought for the air entrainment characteristics at the critical condition as well. Two different air entrainment characteristics are specifically investigated and they are the maximum mean air concentrations and the air entrainment rates.

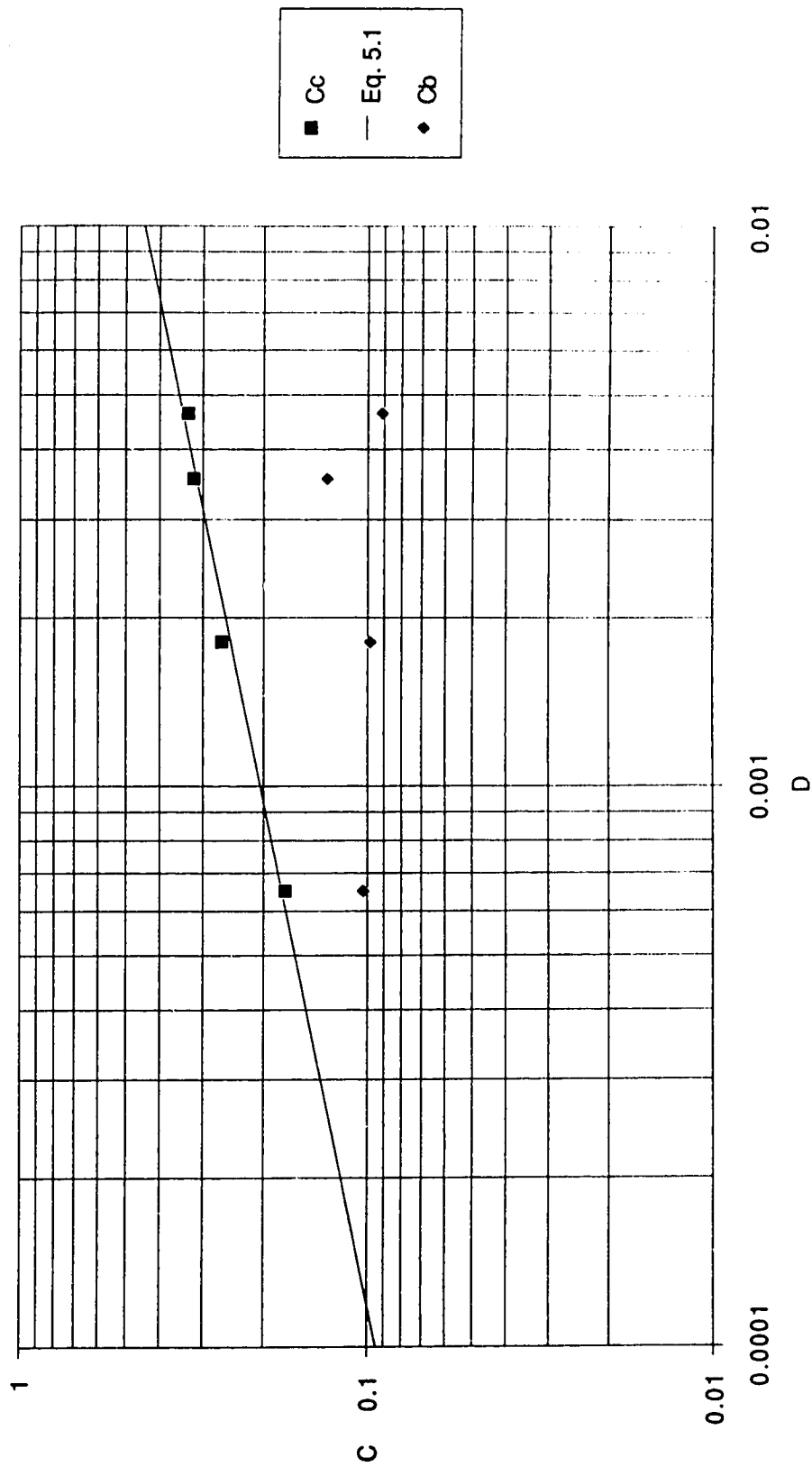
#### 5.3.1.1 Maximum mean air concentrations

Figure 5.8 shows the variation of the two maximum mean air concentrations with the Drop number. As seen in Figure 5.8, the maximum mean air concentration in the backpool area is constant at about 0.10 for the different Drop number. The upstream influence on the backpool maximum mean air concentration is thus minimal. On the other hand, the critical maximum mean air concentration,  $C_c$ , has the following relationship with the Drop number :

$$C_c = 2.087 D^{0.336} \quad (5.1)$$

The coefficient of correlation,  $r^2$ , for the above relationship is

**FIGURE 5.8 Relationship between Maximum Mean Air Concentrations and Drop Number**



0.980.

### 5.3.1.2 Air entrainment rates

Air entrainment rate is defined as the rate at which the volume of air is being entrained into the flow. Although the air entrainment rate has not been measured directly, it could be derived from the mean air concentrations by the following relationship :

$$q_a = \int_0^y u C dy \quad (5.2)$$

where :  $u$  is the velocity of the flow.

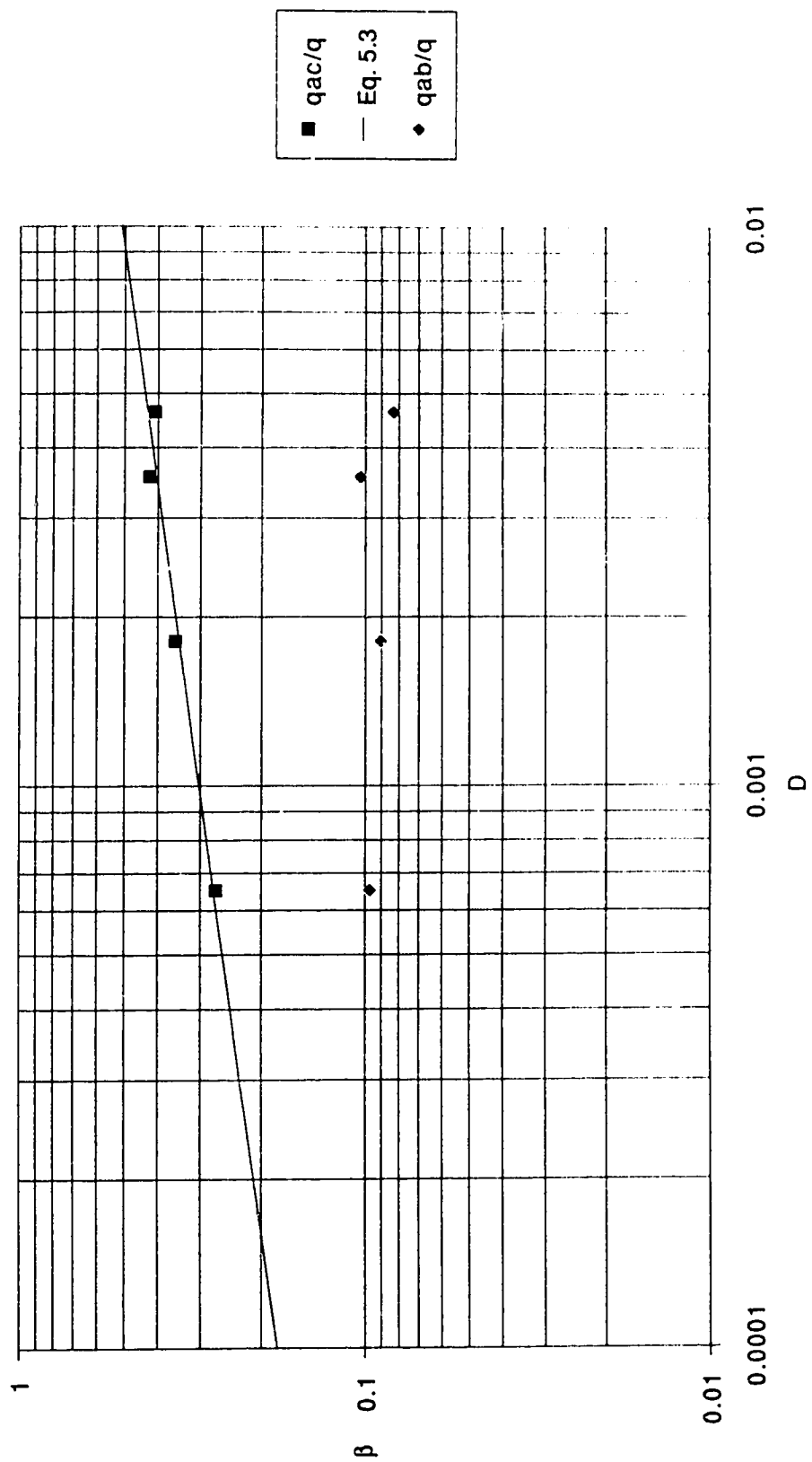
Figure 5.9 shows the variation of the two air entrainment ratios with the Drop number. Similar to the findings in the maximum mean air concentration, the backpool air entrainment ratio is found to be upstream independent and has an almost constant value of 0.10, while the critical air entrainment ratio,  $\beta_c$ , has the following relationship with the Drop number :

$$\beta_c = \frac{q_{ac}}{q} = 1.444 D^{0.226} \quad (5.3)$$

where :  $q_{ac}$  is the critical air entrainment rate.

The coefficient of correlation,  $r^2$ , of the above relationship is 0.955.

**FIGURE 5.9 Relationship between Maximum Air Entrainment Ratio and Drop Number**



### 5.3.2 Plunge Pool

The main concentration of this research has been on the air entrainment characteristics for the plunge pool regime of overfall. As mentioned in chapter 4, high speed video studies have shown that air is entrained into the plunge pool by the formation of eddies at the plunge point of the falling jet. Plates 5.1 (a) to (c) show the close-up of the air entrained eddies at different tailwater conditions for the constant discharge of 35 L/s. As seen from the plates, the amount of entrained air decreases with the increase in the tailwater depth.



PLATE 5.1 (a) Close-up High Speed Video.  $Q=35$  L/s.  $y_t=0.320$  m



In spite of the observations from the high speed video, the analysis on the air entrainment characteristics is still very difficult. Therefore, a procedure similar to the flow analysis is applied to the air entrainment analysis. The air entrainment characteristics for the critical hydraulic jump condition are once again used as a basis for comparison. The resulting ratios of air entrainment characteristics are then related to the corresponding tailwater depth ratio in order to find the general relationships.

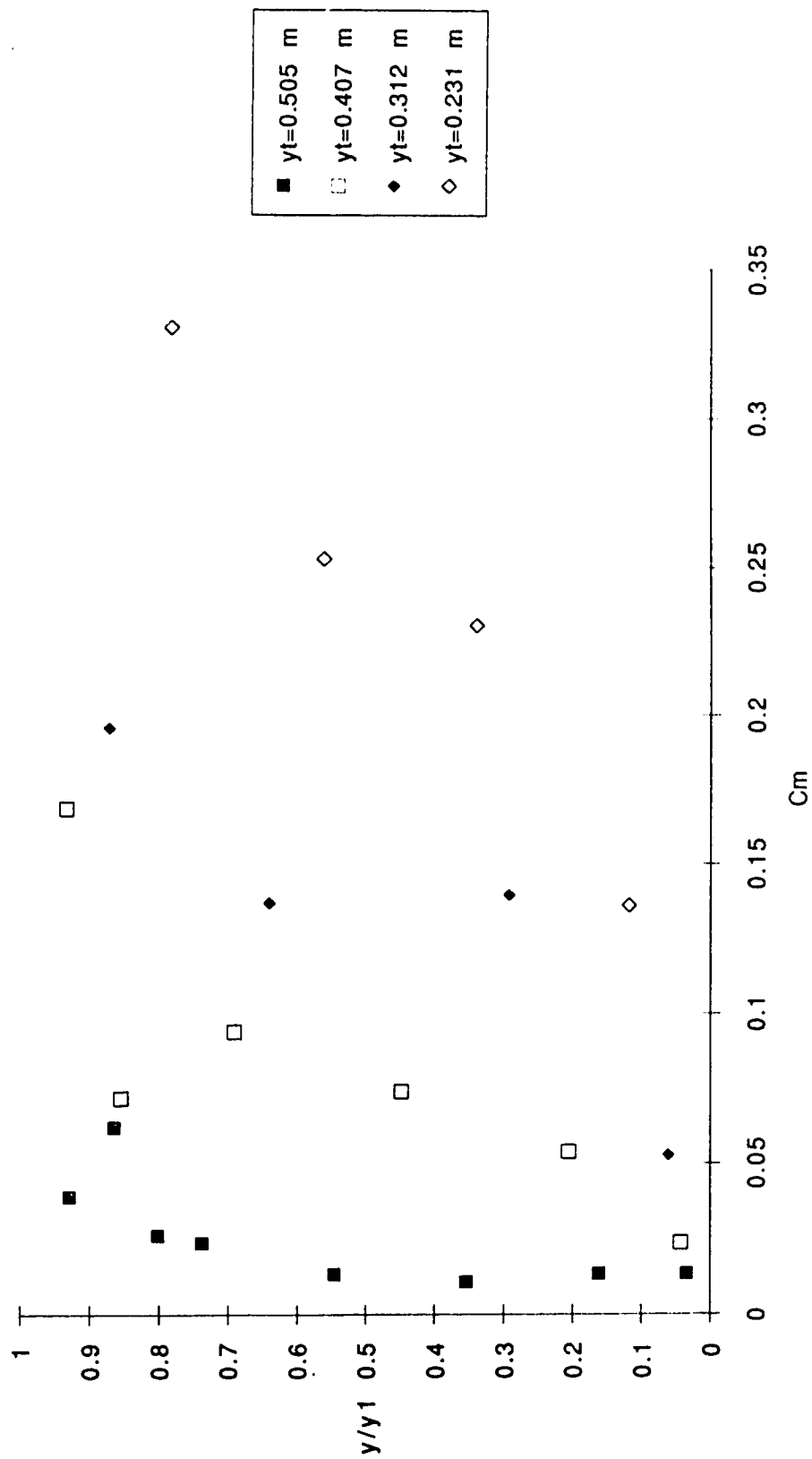
Three types of entrainment characteristics are specifically investigated. These three types include the maximum mean air concentrations, the air entrainment rates and finally the mean air concentration profiles.

#### 5.3.2.1 Maximum mean air concentrations

The maximum mean air concentration can be located for the plunge pool conditions of free overfall. However, this maximum mean air concentration has been found to be an ineffective parameter to describe the plunge pool situations probably because of the limitation of the air concentration probe and the fluctuating nature of the air entrained eddies as mentioned earlier. Another parameter is thus proposed for the plunge pool situations and is called the depth averaged maximum mean air concentration.

Figure 5.10 shows typical vertical profiles of maximum mean air concentrations found in the plunge pool area. A depth averaged maximum mean air concentration,  $C_a$ , can thus be determined for each discharge for each tailwater condition with the following

**FIGURE 5.10 Typical Vertical Profiles of Maximum Mean Air Concentration for Q of 40 L/s**



relationship :

$$C_a = \frac{1}{y_1} \int_0^{y''} C_m dy \quad (5.4)$$

where :  $dy$  is the vertical distance increment.

The jump beginning depth has been chosen as the depth of integration because it corresponds to the locations of maximum mean air concentration. Figure 5.11 shows the relationship between the depth averaged maximum mean air concentration and the tailwater depth ratio. A ratio of air concentrations can then be obtained by comparing the critical maximum with the depth averaged conditions and its general relationship with the tailwater depth ratio is shown in Figure 5.12. A remarkably uniform trend, especially at higher tailwater depth ratio, is found in Figure 5.12.

#### 5.3.2.2 Air entrainment rates

In the plunge pool conditions, there is a stagnant or even reverse flow on top of the underflow jet. Therefore, Equation 5.2 is not valid for the plunge pool regimes due to the lack of a well defined vertical velocity field. However, using the longitudinal mean air concentration profiles and the rising speed of the entrained air bubbles, the air entrainment rate for the plunge pool conditions could be approximated by :

**FIGURE 5.11 Relationship between Tailwater Depth Ratio and Depth Averaged Maximum Mean Air Concentration**

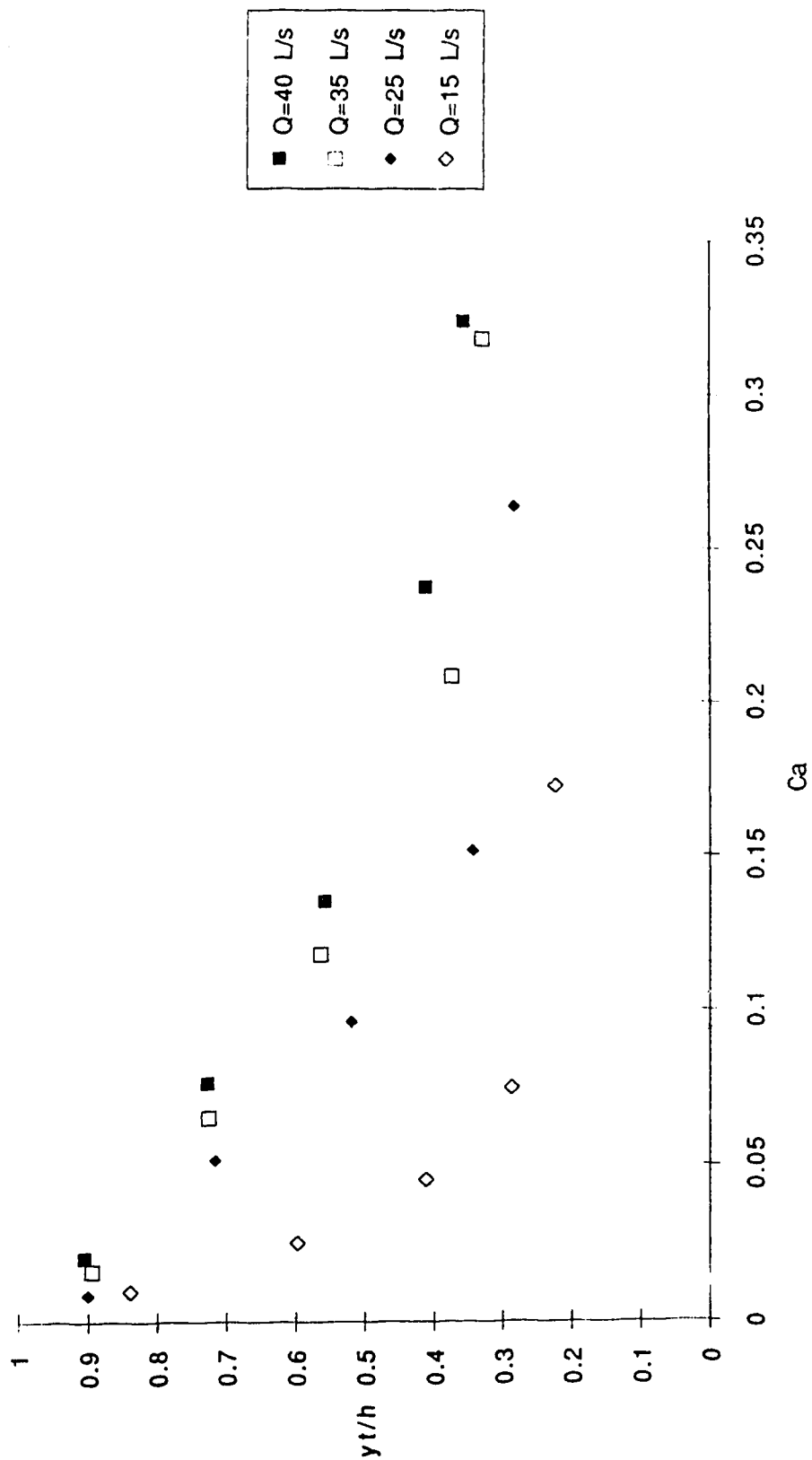
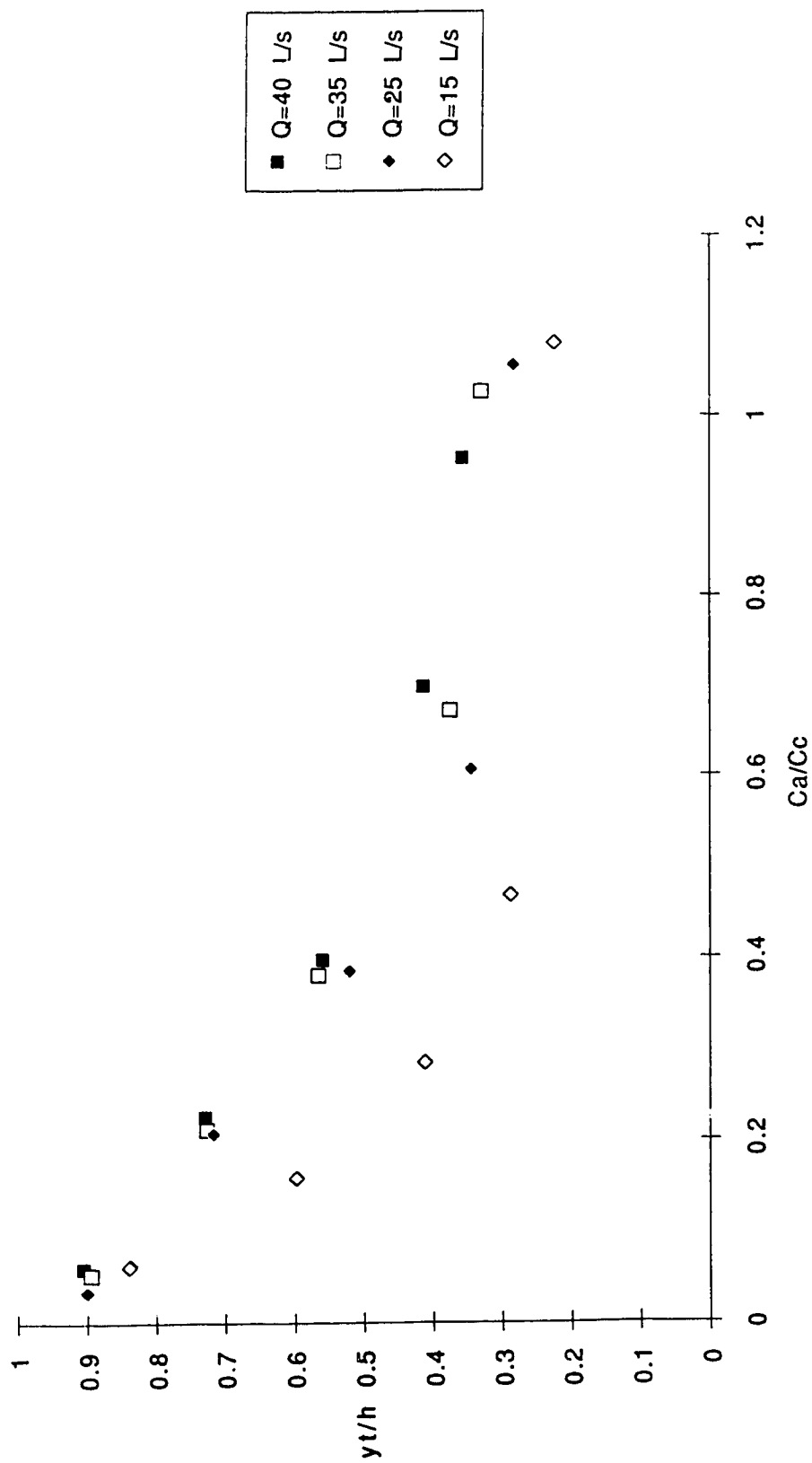


**FIGURE 5.12 Relationship between Tailwater Depth Ratio and Depth Averaged Maximum Mean Air Concentration Ratio**



$$q_a = \int_0^x \omega C dx \quad (5.5)$$

where :  $\omega$  is the rising speed of entrained air bubbles;  
 $dx$  is the increment of horizontal distance.

The size of entrained air bubbles in a plunge pool is usually well mixed. However, an average size of entrained bubbles can roughly be approximated for the experiments by careful observations. The corresponding bubble rising speed in water can thus be obtained according to published results (Clift et.al., 1978).

Figure 5.13 shows the relationship of the air entrainment ratio for the plunge pool regime with the corresponding tailwater depth ratio. As seen from Figure 5.13, the scatter of the data is quite wide and thus another relationship is sought for the air entrainment rates of the plunge pool conditions. Again, using the critical air entrainment rates from Equation 5.4, another ratio is obtained for the air entrainment rates of plunge pool regime. This ratio is called the absolute air ratio,  $A_\beta$ , and is defined as :

$$A_\beta = \frac{q_{ap}}{q_{ac}} = \frac{\beta_p}{\beta_c} \quad (5.6)$$

where :  $q_{ap}$  is the air entrainment rate for plunge pool condition,  
and  
 $\beta_p$  is the air entrainment ratio for plunge pool condition.

FIGURE 5.13 Relationship between Tailwater Depth Ratio and Maximum Air  
Entrainment Ratio in Plunge Pool

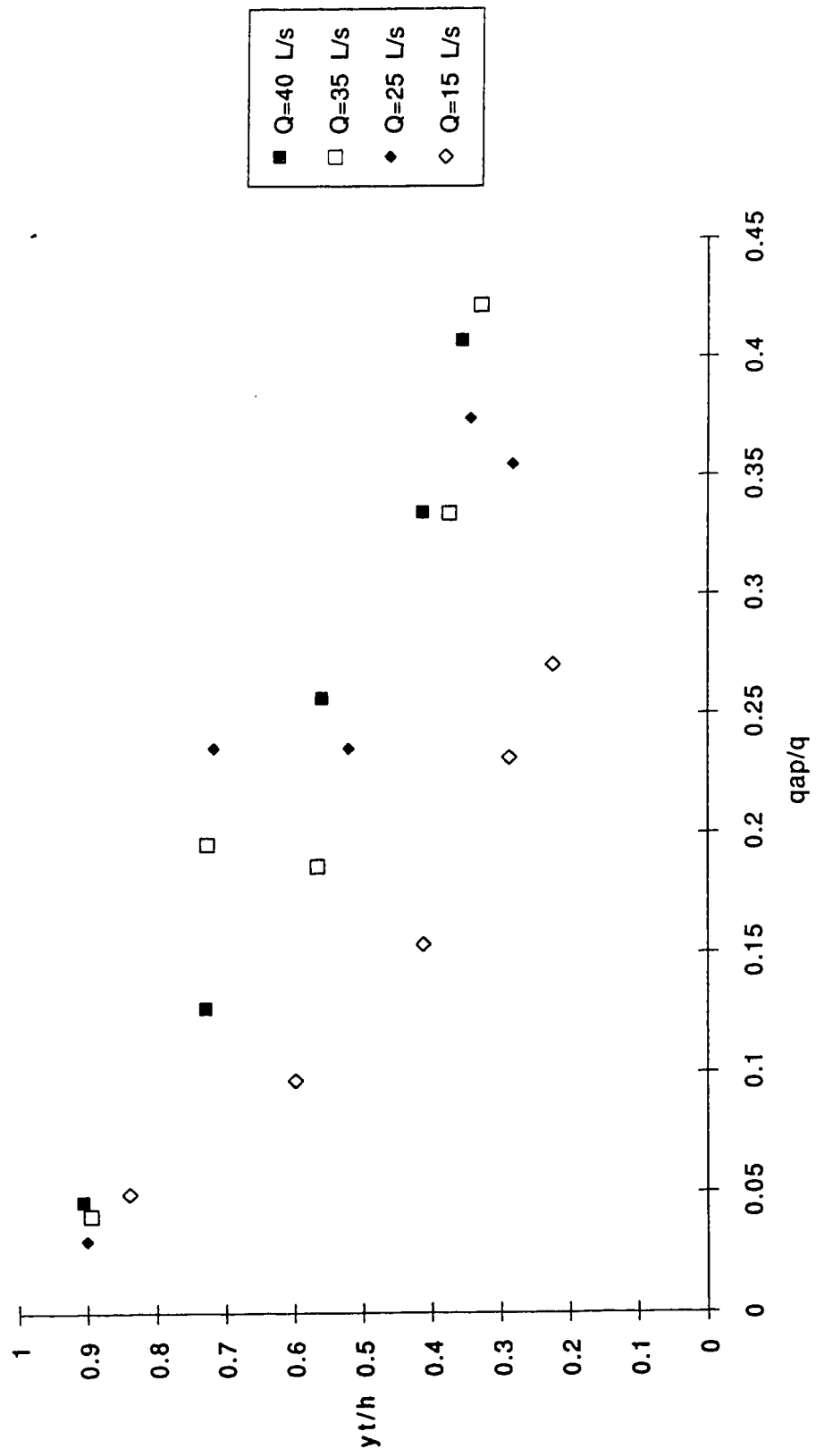


Figure 5.14 shows the corresponding variations of the absolute air ratio with the tailwater depth ratio. A general trend is evident in Figure 5.14 with less scatter than in Figure 5.13.

#### 5.3.2.3 Mean air concentration profiles

Finally, an attempt is made to find a general profile that represents the mean air concentration distribution in the plunge pool regime. A general longitudinal profile will first be developed and the corresponding vertical profile will then be derived from the longitudinal profile.

In order to find the general longitudinal profile, a distance basis is first required to make the measured distance dimensionless. This distance basis is assumed to correspond to the location of maximum mean air concentration in the plunge pool and called the maximum mean air concentration length. The maximum mean air concentrations occur along the downstream face of the plunging jet. Therefore, the maximum mean air concentration length is the same as the jet beginning length at the water surface and equals the bed hitting length at the channel bed. A linear variation from the jump beginning length to the bed hitting length is then assumed for the maximum mean air concentration length within these two limits.

Using the maximum mean air concentration length for the distance basis, the mean air concentrations are then compared to the corresponding depth averaged maximum mean air concentration and the dimensionless longitudinal profiles can be obtained. Figures 5.15 (a) to (d) show typical dimensionless longitudinal profiles for the



FIGURE 5.14 Relationship between Tailwater Depth Ratio and Absolute Air  
Entrainment Ratio

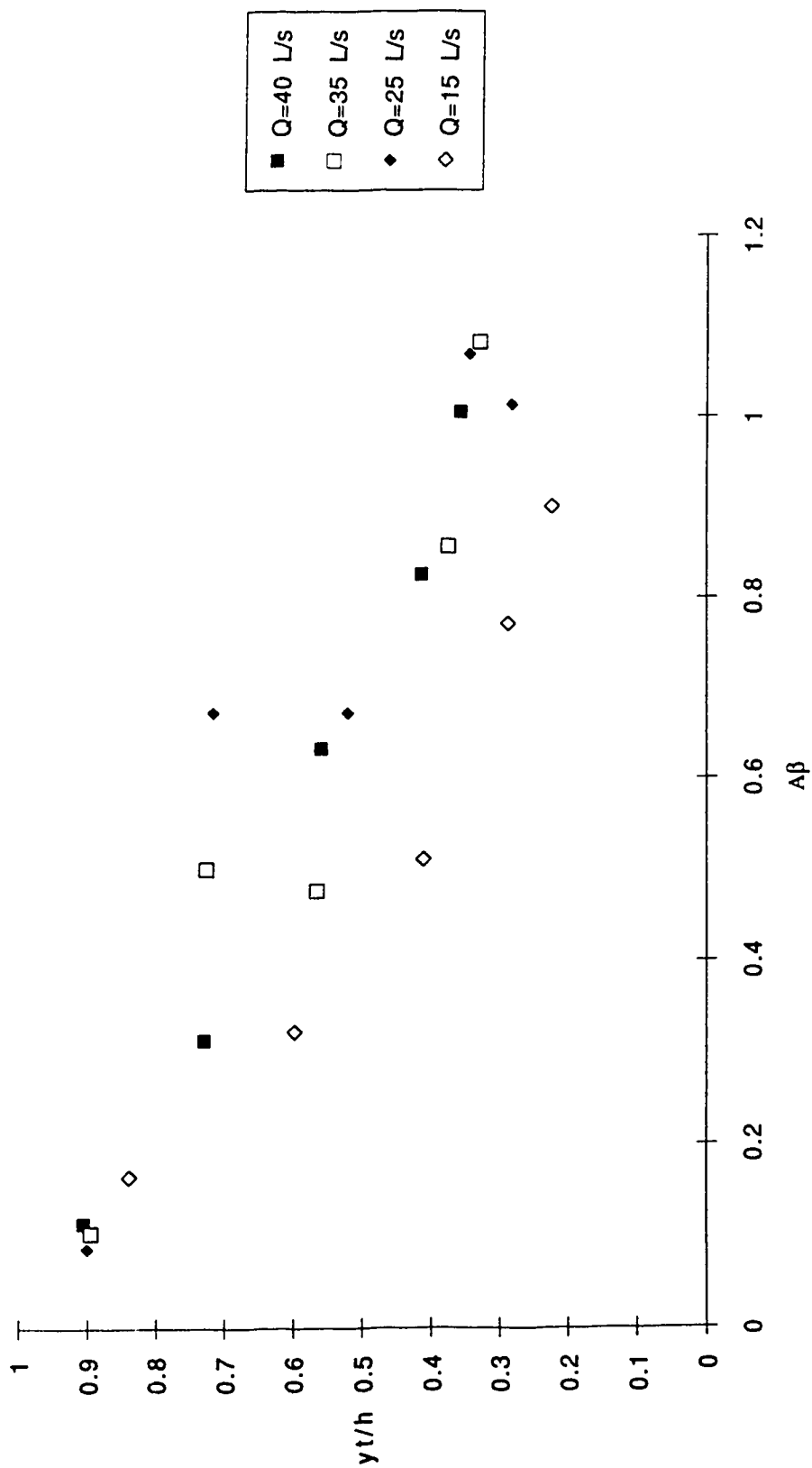


FIGURE 5.15 (a) Dimensionless Longitudinal Profiles with  $Q$  of 40 L/s and  $yt$  of 0.231 m

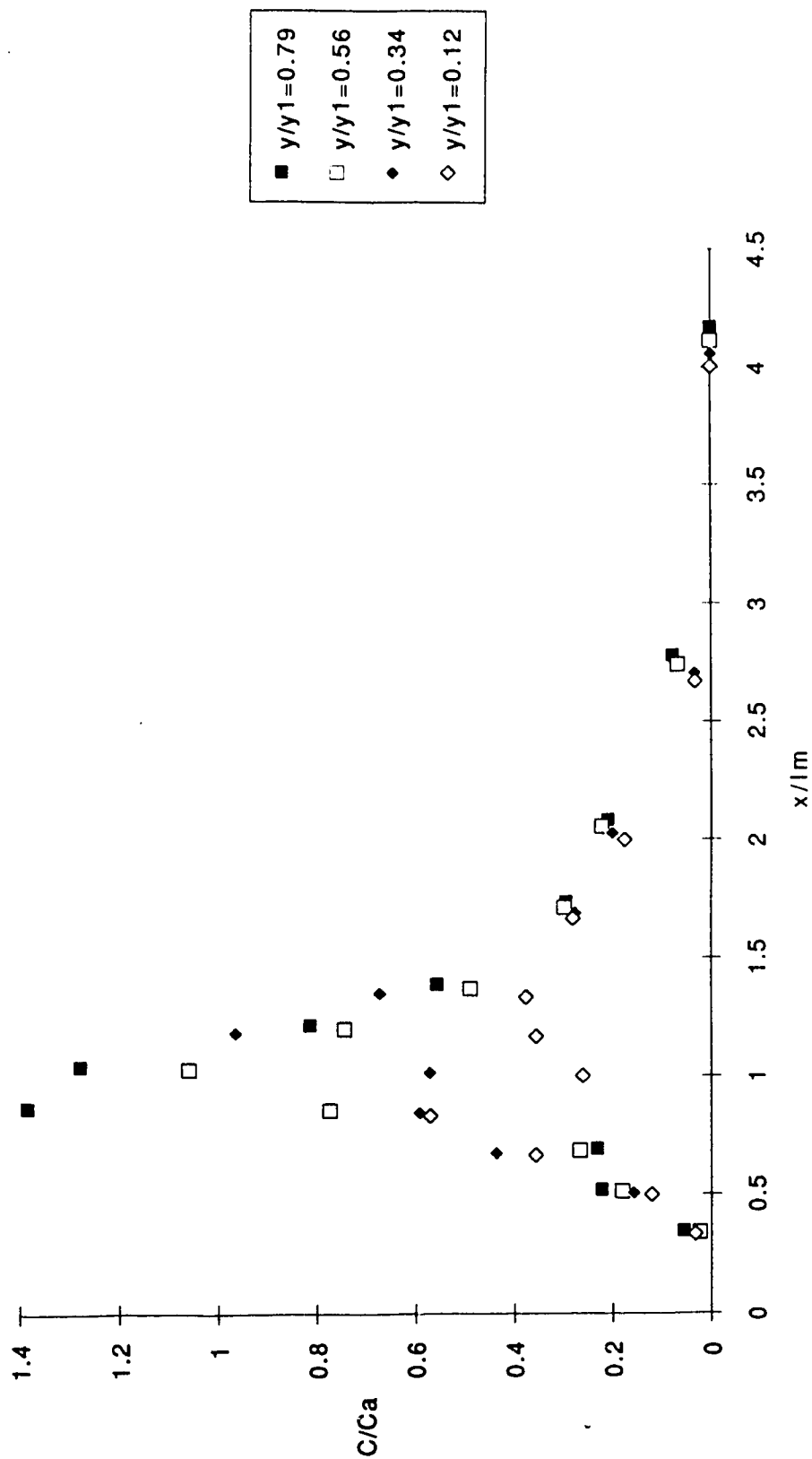


FIGURE 5.15 (b) Dimensionless Longitudinal Profiles with Q of 40 L/s and yt of 0.312 m

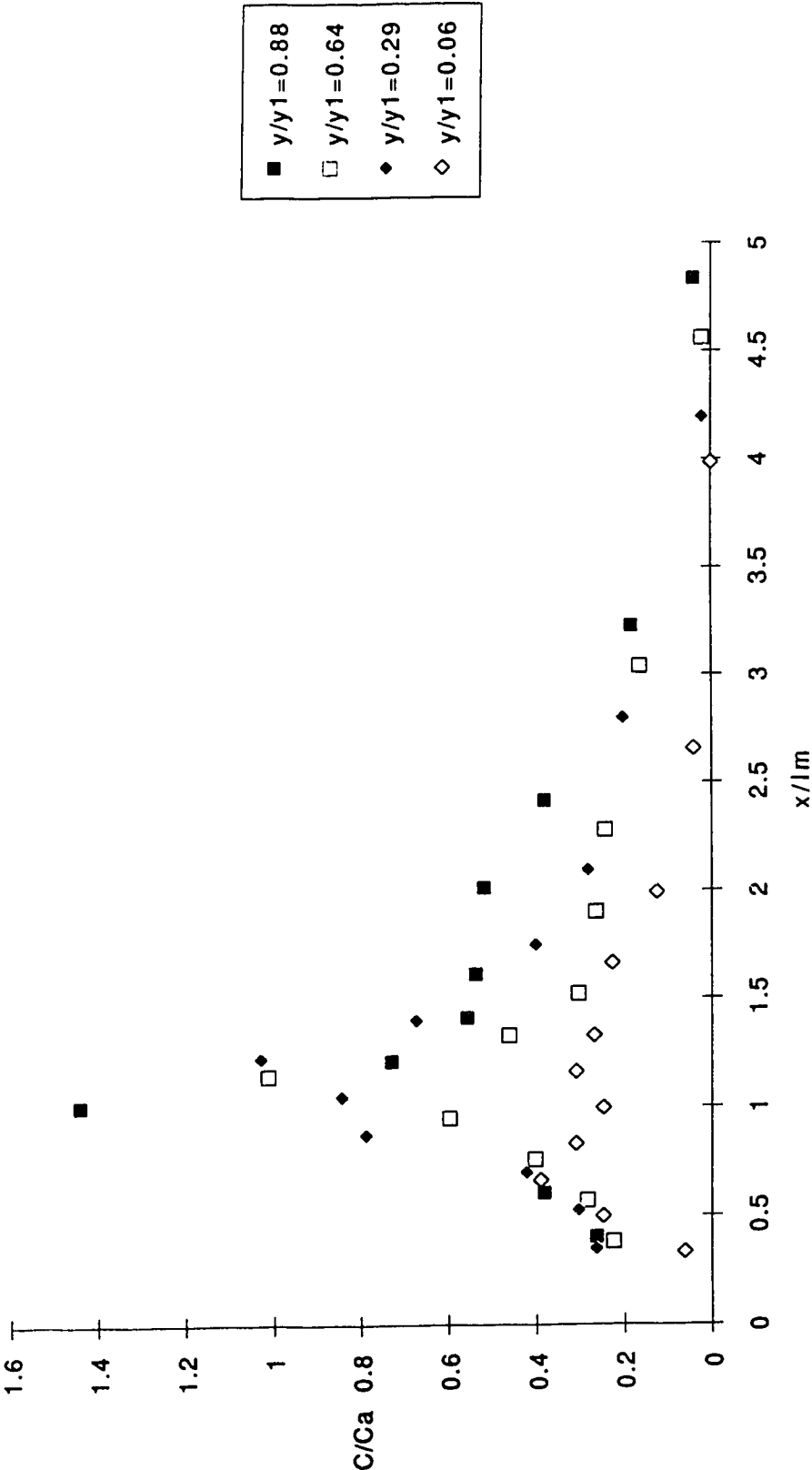


FIGURE 5.15 (c) Dimensionless Longitudinal Profiles with Q of 40 L/s and  $y_t$  of 0.407 m

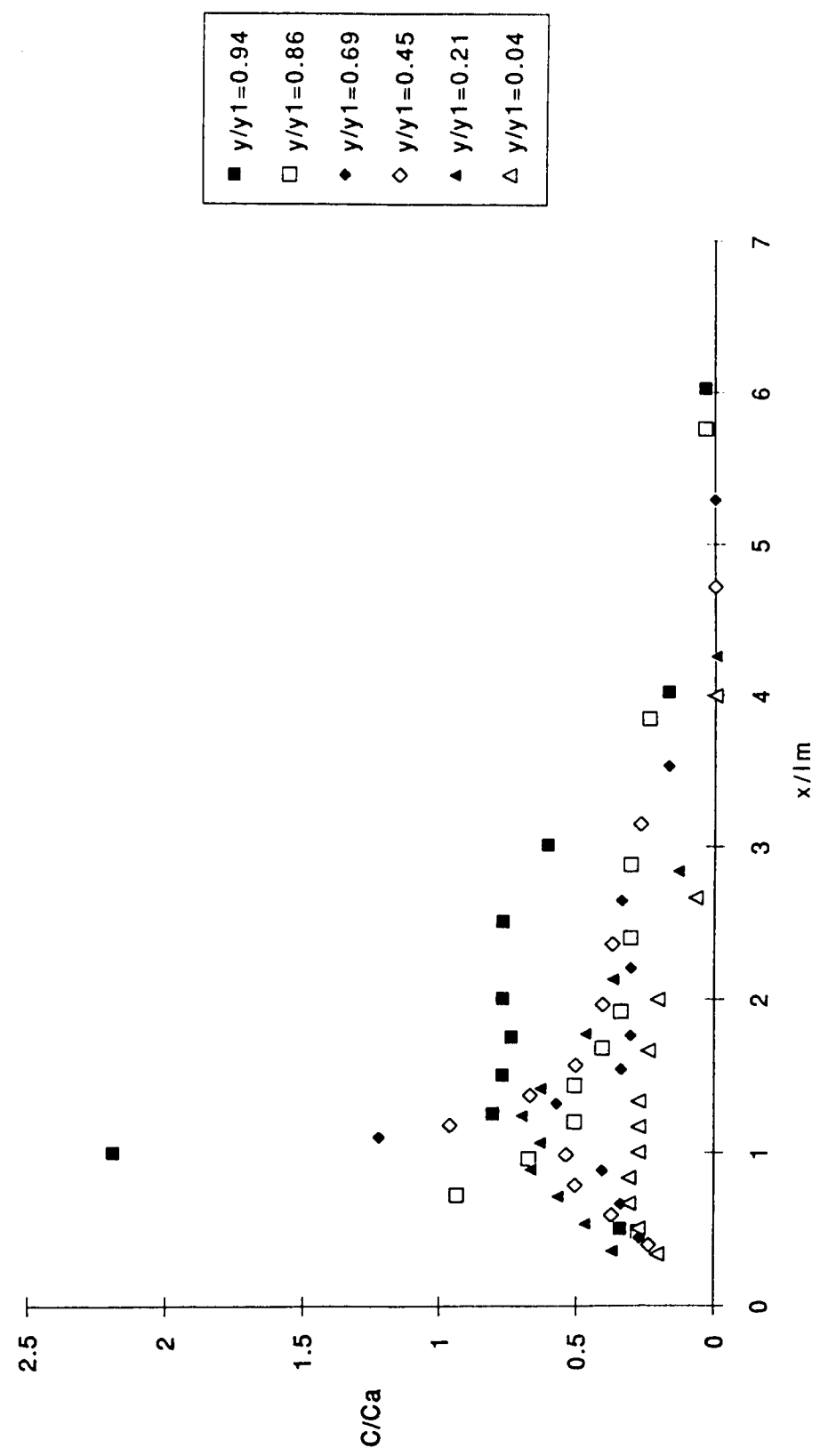
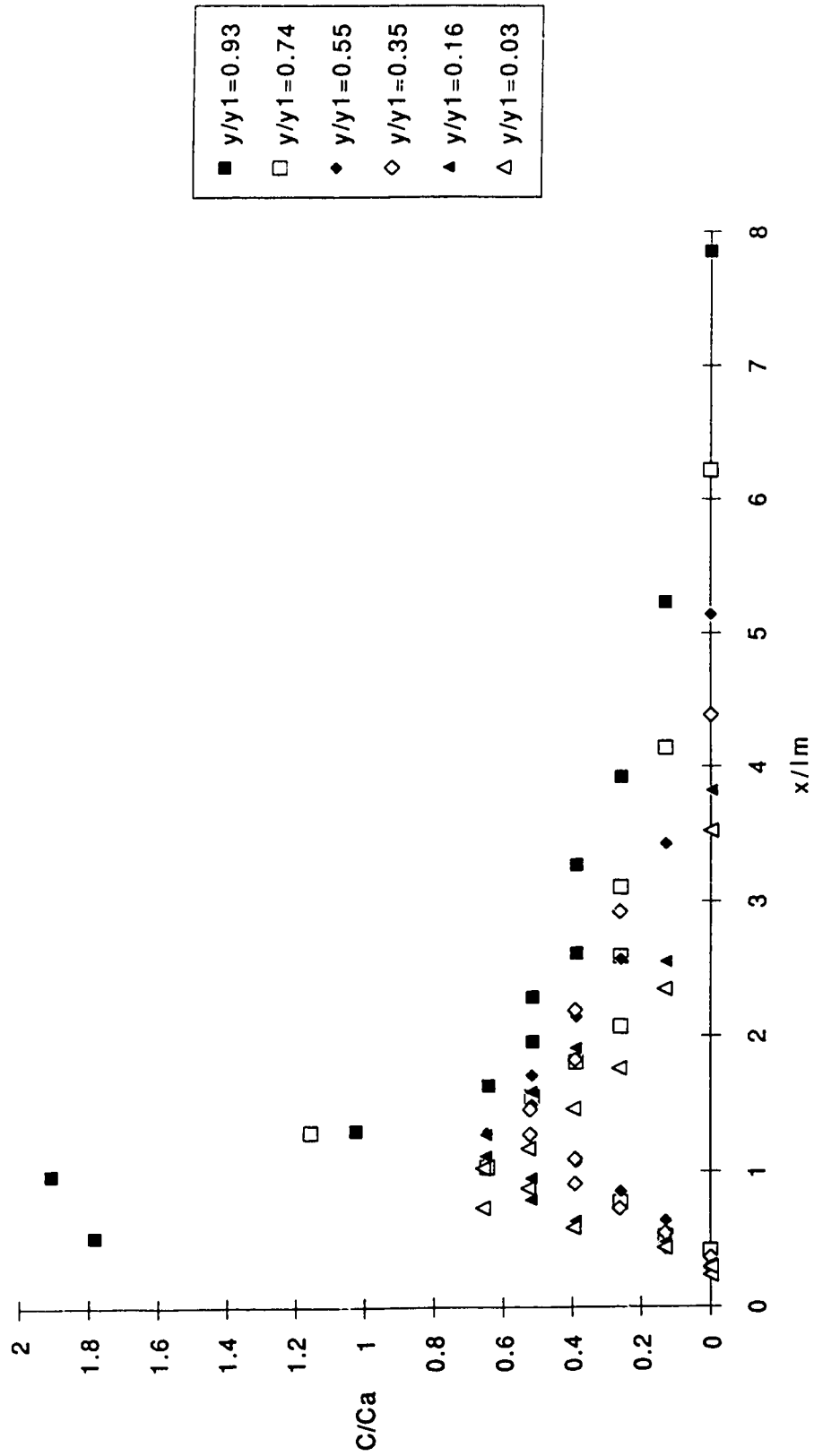


FIGURE 5.15 (d) Dimensionless Longitudinal Profiles with  $Q$  of 40 L/s and  $y_t$  of 0.505 m



different tailwater conditions at the water discharge of 40 L/s.

A remarkably similar trend can be seen in all such profiles which are valid for the depth within 0.2 and 0.8 of the jump beginning depth. This trend shows that a general longitudinal profile describing the mean air concentrations distribution can be found for the main body of the plunge pool. This general profile starts from zero at the brink of the overfall and increases to the depth averaged maximum mean air concentration at the corresponding maximum air concentration length. Then, the mean air concentration decreases gradually to zero again at around four times the maximum mean air concentration length.

Furthermore, the vertical maximum mean air concentration variation can also be derived from the dimensionless longitudinal profiles. Within the lower twenty percent of the jump beginning depth, the maximum mean air concentration will increase roughly in linear fashion. Around twenty percent of the jump beginning depth, the depth averaged maximum mean air concentration is achieved and will remain roughly until the eighty percent depth. From eighty percent to the water surface, the maximum mean air concentration would increase drastically to more than double the value of the depth averaged maximum mean air concentration.

## 5.4 CONCLUSIONS

Using the situation with the hydraulic jump forming at the toe of the falling jet as the critical condition, some generalized relationships have been derived for both the flow and air

entrainment characteristics of free overfalls. Most of these relationships are functions of the tailwater depth ratio especially in the plunge pool situation of the overfall.

In the plunge pool regime, both the jump beginning depth and length ratios have a well defined relationship especially at higher tailwater depth ratio. There exists also two asymptotes for bed hitting length. The first asymptote occurs at the low tailwater depth ratio where the bed hitting length remains constant. The second asymptote is at the onset of breaking surface waves where there is no bed hitting length. Finally, the onset for breaking surface waves occurs when tailwater depth reaches the drop height which showed that the inflow conditions have little influence on the onset of breaking surface waves regime.

A general description of the maximum mean air concentrations can be proposed for free overfall flow. For flow with shooting jet, the maximum mean air concentration will quickly increase to the almost constant value of backpool maximum condition. The critical maximum mean air concentration, which is a function of the Drop number, is then reached for the critical hydraulic jump condition. In the plunge pool regime, the depth averaged maximum air concentration ratio will follow a unique trend with the tailwater depth ratio as shown in Figure 5.12. Finally, at the formation of flow with breaking surface waves, the maximum mean air concentration will again approach zero.

A general description of the air entrainment rate can also be proposed for free overfall. For flow with the supercritical shooting jet, the air entrainment rate will quickly increase to the constant

value of the backpool condition. The critical air entrainment rate, which is also a function of the Drop number, is then reached at the critical hydraulic jump condition. In the plunge pool regime, the absolute air ratio and the tailwater depth ratio will follow the trend shown in Figure 5.14. Finally, at the formation of flow with breaking surface waves, the air entrainment rate will again approach zero.

Finally, a general longitudinal mean air concentration profile has been obtained to describe the main body of the plunge pool. This profile reaches the depth averaged maximum air concentration at the corresponding maximum mean air concentration length. The total length of the profile is about four times the maximum mean air concentration length.

Although the method of analysis may be crude in some areas, the final results still show interesting and useful relationships for both the flow and air entrainment characteristics of the free overfall.



## **CHAPTER 6**

### **CONCLUSIONS**

#### **6.1 REVIEW**

The flow at free overfalls can be subdivided into several flow regimes. These regimes include the supercritical shooting jet, hydraulic jump, plunge pool and breaking surface waves. The studies by Moore, White, Rand and Gill have provided a lot of information especially for the regimes of supercritical shooting jet and hydraulic jump. The concept of Drop number introduced by Rand has been especially useful in summarizing the many flow characteristics for the critical hydraulic jump regime of the overfall.

The air entrainment characteristics of the overfall, on the other hand, have not been studied quite as thoroughly as the general flow characteristics. The current knowledge on air entrainment characteristics is not derived from the free overfall situations but from some related studies only. In summary, minimum amount of air is entrained into the flow for the supercritical shooting jet and breaking surface waves regimes. Air entrainment characteristics have been well studied for the hydraulic jump regime. The air entrainment characteristics for the plunge pool regime have, on the other hand, been an ongoing research topic especially in the recent decades.

The aim of this research was first to study the general flow characteristics of free overfall with emphasis on the plunge pool

situation. Secondly, the air entrainment characteristics for the hydraulic jump and plunge pool situations were studied in order to find its relationship with the free overfall.

### 6.3 PRESENT CONTRIBUTIONS

The flow characteristics of the free overfall depend on the downstream conditions. Moreover, the air entrainment characteristics are related to the flow characteristics as well. Although the main emphasis has been placed on the plunge pool regime, the contributions of present study are summarized according to the flow regimes of free overfall.

In the supercritical shooting jet regime, minimum amount of air is entrained through the action of shooting jet. However, the amount of air entrained through the backpool has been quite considerable. The backpool maximum mean air concentration and the backpool air entrainment ratio have been found to be independent of the upstream influences, and both have shown to have a constant value of about 0.10.

In the hydraulic jump regime, a critical condition is reached when the hydraulic jump forms at the toe of the falling jet. The experimental results for the flow characteristics have shown good agreement with the results of Rand (1955). The critical maximum mean air concentration,  $C_C$ , and the critical maximum air entrainment ratio,  $\beta_C$ , were also found to be functions of the Drop number in the following forms respectively:

$$C_c = 2.087 D^{0.336} \quad (6.1)$$

$$\beta_c = 1.444 D^{0.226} \quad (6.2)$$

In the plunge pool regime, all dimensionless flow characteristics have been shown to have a unique relationship with the corresponding tailwater depth ratio. Flow characteristics such as the jump beginning depth and length ratios have distinct relationships with the tailwater depth ratio. The bed hitting length ratio has also been shown to have two clear asymptotes with the tailwater depth ratio. Similar trends can also be found for the air entrainment characteristics such as the depth averaged maximum mean air concentration ratio and the absolute air ratio. Furthermore, a general longitudinal profile, which can be used to describe most of the plunge pool body, has also been developed.

Finally, in the breaking surface waves regime, minimum amount of air is entrained into the flow. However, the onset of flow with breaking surface waves has a distinct relationship with the tailwater depth ratio and is independent of the upstream conditions. As the tailwater depth ratio approaches one, the formation of flow with breaking surface waves will suddenly set in.

In summary, most of the hydraulic characteristics can be described in a unique manner by the Drop number for the flow regimes of supercritical shooting jet and hydraulic jump of free overfall. On the other hand, most hydraulic characteristics follow a distinct pattern with the corresponding tailwater depth ratio in the flow regimes of plunge pool and breaking surface waves.

## **CHAPTER 7**

### **RECOMMENDATIONS**

#### **7.1 FLOW CHARACTERISTICS**

Although much effort has been spent to study the hydraulics of the free overfall, the researches are far from complete. There are still many areas which require further study. These areas include :

- 1) Energy dissipation for the flow regimes of plunge pool and breaking surface waves;
- 2) General flow characteristics of flow with breaking surface waves; and finally
- 3) Formation of characteristic eddies in flow with plunge pool.

#### **7.2 ENTRAINMENT CHARACTERISTICS**

The air entrainment characteristics of the free overfall have been a complicated topic. Much progress has been made in understanding the air entrainment characteristics of free overfall in this thesis. However, there are still areas where research can be done to improve our current knowledge. Some of the possible topics for further study are :

- 1) Air entrainment characteristics for the breaking surface waves regime;
- 2) Energy dissipation and dissolved oxygen transfer of free overfalls; and finally
- 3) Dissolved oxygen transfer of free overfalls.

## REFERENCES

Amed, A.A.; Ervine, D.A. and McKeogh, E.J. "The Process of Aeration in Closed Conduit Hydraulic Structures". Symposium on Scale Effects in Modelling Hydraulic Structures, International Association for Hydraulic Research, Esslingen, Germany, Paper 4.13, September 3-6 1984.

Babb, A.F. and Aus, H.C. "Measurement of Air in Flowing Water". Journal of the Hydraulics Division, Proceedings of the American Society of Civil Engineers, Vol. 107, HY 12, December 1981, pp 1615-1630.

Bin, A.K. "Air Entrainment by Plunging Liquid Jets". Symposium on Scale Effects in Modelling Hydraulic Structures, International Association for Hydraulic Research, Esslingen, Germany, Paper 5.5, September 3-6, 1984.

Cain, P. and Wood, I.R. "Instrumentation for Aerated Flow on Spillways", Journal of the Hydraulics Division, Proceedings of the American Society of Civil Engineers, Vol. 107, HY 11, November 1981, pp 1407-1424.

Casteleyn, J.A.; Van Groen, D. and Kolkman, D.A. "Air Entrainment in Siphons: Results of Tests in Two Scale Models and an Attempt at Extrapolation". Proceedings of the XVII Congress, International Association for Hydraulic Research, Baden Baden, Germany, November 1977.

Chow, V.T. Open Channel Hydraulics, McGraw-Hill Book Co. Inc., New York, 1959.

Clift, R.; Grace, J.R. and Weber, M.E. Bubbles, Drops, and Particles, Academic Press Inc. (London) Ltd., London, 1978, pp 1-380.

Elsawy, E.M. and McKeogh, E.J. "Study of Self Aerated Flow with regard to Modelling Criteria". Proceedings of the XVII Congress, International Association for Hydraulic Research, Baden Baden, Germany, Paper A60, November 1977, pp 475-481.

Ervine, D.A. and Elsayy, E.M. "The Effect of a Falling Nappe on River Aeration". Proceedings of the XVI Congress, International Association for Hydraulic Research, Sao Paulo, Brazil, Paper C45, July 1975, pp 390-397.

Ervine, D.A. and Himmo, S.K. "Modelling the Behavior of Air Pockets in Closed Conduit Hydraulic Systems". Symposium on Scale Effects in Modelling Hydraulic Structures, International Association for Hydraulic Research, Esslingen, Germany, Paper 4.15, September 3-6 1984.

Ervine, D.A. and Falvey, H.T. "Behavior of Turbulent Water Jets in the Atmosphere and in Plunge Pools". Proceedings of the Institution of Civil Engineers, Part 2, Vol. 83, March 1987, pp 295-314.

Falvey, H.T. "Air-Water Flow in Hydraulic Structures". Engineering Monograph 41, United States Department of the Interior, Bureau of Reclamation, December 1980.

Falvey, H.T. and Ervine, D.A. "Aeration in Jets and High Velocity Flows". Model-Prototype Correlation of Hydraulic Structures, (Ed. Burgi, P.H.), American Society of Civil Engineers, New York, New York, 1988, pp 25-55.

Gill, M.A. "Hydraulics of Rectangular Vertical Drop Structures". Journal of Hydraulic Research, Vol. 17, No. 4, 1979, pp 289-302.

Hager, W.H. "Hydraulics of Plane Free Overfall". Journal of Hydraulic Engineering, American Society of Civil Engineers, Vol. 109, No. 12, December 1983, pp 1683-1697.

Haindl, K. "Aeration at Hydraulic Structures". Developments in Hydraulic Engineering - 2, (Ed. Novak, P.), Elsevier Applied Science Publishers, London and New York, 1984, pp 113-158.

Henderson, F.M. Open Channel Flow, The Macmillan Co., New York, 1966.

Kalinski, A.A. and Robertson, J.M. "Closed Conduit Flow-Entrainment of Air in Flowing Water". Transactions of the American Society of Civil Engineers, Vol. 108, 1943, pp 1435-1516.

Kobus, H. "Local Air Entrainment and Detrainment". Symposium on Scale Effects in Modelling Hydraulic Structures, International Association for Hydraulic Research, Esslingen, Germany, Paper 4.10, September 3-6, 1984.

Lamb, O.P. and Killen, J.M. "An Electrical Method for Measuring Air Concentration in Flowing Air-Water Mixtures". Technical Paper Number 2, University of Minnesota, St. Anthony Falls Hydraulic Laboratory, Minneapolis, Minn., Series B, 1950.

Leutheusser, H.J.; Resch, F.J. and Alernu, S. "Water Quality Enhancement Through Hydraulic Aeration". XVst Congress, International Association for Hydraulic Research, Istanbul, Turkey, September 1973.

McKeogh, E.J. and Elsayy, M.E. "Air Retained in Pool by Plunging Water Jet". Journal of the Hydraulics Division, Proceedings of the American Society of Civil Engineers, Vol. 106, HY 10, October 1980, pp 1577-1593.

Moore, W.L. "Energy Loss at the Base of a Free Overfall". Transactions of the American Society of Civil Engineers, Vol. 108, 1943, pp 1343-1360.

Pan, S. and Shao, Y. "Scale Effects in Modelling Air Demand by a Ramp Slot". Symposium on Scale Effects in Modelling Hydraulic Structures, International Association for Hydraulic Research, Esslingen, Germany, Paper 4.7, September 3-6 1984.

Pinto, N. and Neidert, S.H. "Model-Prototype Conformity in Aerated Spillway Flow". International Conference on Hydraulic Modelling, B.H.R.A., Coventry, England, Paper E6, September 1982, pp 273-284.

Rajaratnam, N. "Hydraulic Jumps". Advances in Hydrosiences, Vol. 4, (ed Chow, V.T.), Academic Press, New York, 1967, pp 197-280.

Rand, W. "Flow Geometry at Straight Drop Spillways". Hydraulics Division, Proceedings of the American Society of Civil Engineers, Vol. 81, Paper 791, September 1955.

Renner, J. "Air Entrainment in Surface Rollers". Symposium of Design and Operation of Siphons and Siphon Spillways, B.H.R.A., London, Paper A4, 1975, pp 49-56.

Rutschmann, P. "Calculation and Optimum Shape of Spillway Chute Aerators". Model-Prototype Correlation of Hydraulic Structures, (Ed. Burgi, P.H.), American Society of Civil Engineers, New York, New York, 1988, pp 118-127.

Salih, A.M.A. "Entrained Air in Linearly Accelerated Water Flow". Journal of the Hydraulics Division, Proceedings of the American Society of Civil Engineers, Vol. 106, HY 10, October 1980, pp 1595-1605.

Sene, K.J. "Air Entrainment by Plunging Jets". Chemical Engineering Science, Vol. 43, No. 10, 1988, pp 2615-2623.

Sene, K.J.; Thomas, N.H. and Goldring, B.T. "Planar Plunge-zone Flow Patterns and Entrained Bubble Transport". Journal of Hydraulic Research, Vol. 27, No. 3, 1989, pp 363-383.

Straub, L.G. and Anderson, A.G. "Experiments on self-aerated flow in open channels". Journal of the Hydraulic Division, Proceedings of the American Society of Civil Engineers, Vol. 84, HY 7, 1958.

Thomas, N.H. "Air Demand Distortion in Hydraulic Models". International Conferences on Hydraulic Modelling, B.H.R.A., Coventry, England, Paper E5, September 1982, pp 253-272.

Van De Sande, E. and Smith, J.M. "Surface Entrainment of Air by High Velocity Water Jets". Chemical Engineering Science, Vol. 28, 1973, pp 1161-1168.

Van De Sande, E. and Smith, J.M. "Jet Break-up and Air Entrainment by Low Velocity Turbulent Water Jets". Chemical Engineering Science, Vol. 31, 1976, pp 219-224.

White, M.P. Discussion of "Energy Loss at the Base of a Free Overfall". Transactions of the American Society of Civil Engineers, Vol. 108, 1943, pp 1361-1364.

Wood, I.R. "Air Water Flows". 21st Congress, International Association for Hydraulic Research, Melbourne, Australia, Keynote Address, August 19-23 1985, pp 18-29.



## **APPENDIX**

### **AERATION OVER HYDRAULIC STRUCTURES**

#### **1. INTRODUCTION**

Aeration is the process of air entrainment into the flow due to the action of turbulence. The aeration phenomenon is especially evident with the 'whiteness' appearance on flow over hydraulic structures. This process has the somewhat negative effects of 'bulking' of the flow depth. However, aeration over hydraulic structures is also an efficient way for oxygen uptake (i.e. increase in dissolved oxygen concentration) in the river. In this environmentally polluted world, oxygen uptake is important for the self-purification process of the river ecosystem.

Consequently, aeration over hydraulic structures has been the on-going topic of research for more than forty years and is one of the important concerns for hydraulic engineers, sanitary engineers, environmental engineers and chemical engineers. Researchers from Great Britain, Holland, United States and Japan have all contributed significantly to our understanding of the aeration process. This thesis is, then, a summary on the aeration process over hydraulic structures. The theory on oxygen transfer is first presented while the many researches in oxygen uptake over hydraulic structures will then be discussed.

## 2. OXYGEN TRANSFER THEORY

### 2.1 Introduction

Some of the physical phenomena on gas transfer such as evaporation and condensation of a water body have been studied well by hydrologists and the general principle applies to gas transfer as well. Gas molecules are thought to be transferring back and forth via a gas-liquid interface depending upon the energy level. In the oxygen uptake situation, the governing factor would be the dissolved oxygen concentration in the river. Gas molecules will generally continue to diffuse into the liquid until an equilibrium is reached. This equilibrium is called the saturated gas concentration in the liquid. The general theory on oxygen transfer over hydraulic structures is derived from the Fick's First Law of Diffusion and governed by the solubility of oxygen in water.

The following sections discuss the solubility of gases, gas transfer equation and gas transfer rate. The equation for the solubility of gases is first derived from the universal gas law and the relationship between concentration equilibrium. The general gas transfer equation will then be derived from the Fick's First Law of Diffusion while the different theories on the gas transfer coefficient will be followed. Finally, the more practical expression on gas transfer rate is defined.

## 2.2 Solubility of gases

In a closed system of body of gases, the total amount of a particular gas existing in this system is governed by the universal gas law (Popel, 1974). The universal gas law states that :

$$p V = n R T \quad (A1)$$

where :  $p$  is the partial pressure of the particular gas in the gas phase (Pa),

$V$  is the volume occupied by the total gas phase ( $m^3$ ),

$n$  is the number of moles of the particular gas contained in  $V$ ,

$R$  is the universal gas constant (8.31 J/K/moles), and

$T$  is the absolute temperature (K).

If the molar concentration of that particular gas is defined as the number of moles over the total volume occupied (i.e.  $n/V$ ), the mass concentration will be obtained when multiplied by its molecular weight. The mass gas concentration is then defined as :

$$C_g = \frac{p W_m}{R T} \quad (A2)$$

where :  $C_g$  is the mass concentration of a particular gas ( $g/m^3$ ),  
and

$W_m$  is the molecular weight of the particular gas  
(g/mole).

In a closed system of gas or mixture of gases and liquid (i.e. air and water), a dynamic equilibrium of particular gas molecules in the gas and liquid phases will be reached if sufficient time is given. This dynamic equilibrium in the liquid phase is called the saturation mass concentration of the gas in the liquid. If higher mass concentration is introduced into the gas phase, higher saturation mass concentration will be resulted in the liquid phase consequently. The saturation concentration and the mass gas concentration can be related with a simple proportional constant. Substituting the expression for mass gas concentration with Equation A2, the saturation concentration can be expressed as :

$$C_s = k_D \frac{p W_m}{R T} \quad (A3)$$

where :  $C_s$  is the saturation concentration of a gas in a liquid  
(g/m<sup>3</sup>), and  
 $k_D$  is the proportional constant.

Equation A3 is another form of the relationship proposed by W. Henry in 1803 (Tchobanoglous and Schroeder, 1985). The relationship, known as Henry's Law, states that the solubility of a gas in liquid is directly proportional to the partial pressure of the gas in the atmosphere above the liquid. This proportionality, which

is called the Henry's law constant, is obviously not dimensionless as seen on Equation A3. Moreover, the partial pressure of the gas in a air-water system should not only be the volumetric portion of the total pressure in the gas phase but also be corrected for the water vapor pressure to the gas in the system as well. Water vapor pressure tends to reduce further the magnitude of the partial pressure of the gas in the system.

The solubility of gases depends also on temperature. A release of energy is caused by the dissolving of gases in liquid. An increase in temperature would, therefore, be associated with a decrease in the solubility because energy is more difficult to be released.

Finally, the solubility of gases depends on the nature of gas and liquid involved. All the relationships derived above are valid for pure liquids only. The presence of impurities in liquid may complex the system further and should be studied on an individual basis.

### 2.3 Gas Transfer Equation

For a quiescent body of liquid with unlimited depth, the solubility of gas in the liquid is governed by Fick's First Law of Diffusion or, more generally, Fick's Law (Avery and Novak, 1978). Fick's Law states that the mass transfer rate is proportional to the concentration gradient and the equation is the following :

$$\frac{dM}{dt} = - D A \frac{\delta C}{\delta x} \quad (A4)$$

where :  $dM/dt$  is the rate of mass transfer (g/s),  
 $D$  is the molecular diffusion coefficient ( $m^2/s$ ),  
 $A$  is the area of contact between gas and liquid ( $m^2$ ), and  
 $\delta C/\delta x$  is the concentration gradient ( $g/m^2/m$ ).

The negative sign in Equation A4 indicates that the direction of mass transfer is from area of high concentration to low concentration.

Figure A1 shows a typical gas-liquid interface. A representative bulk gas concentration can be defined for the bulk gas and liquid phases ( $C_G$  and  $C_L$ ) respectively. Similarly, a representative interface gas concentration can also be defined in the interface area for the gas and liquid phases ( $C_{Gi}$  and  $C_{Li}$ ) respectively as well. Diffusion is thought to be the primary mechanism responsible for the change in concentrations. Two separate equations can then be written using the Fick's Law in the bulk gas to interface area and in the interface to bulk liquid area. Furthermore, the interface gas concentration of the liquid phase is proportional to the interface gas concentration of the gas phase. Combining the above three relationships, a general gas transfer can be obtained as the following :

$$m = \left( \frac{1}{k_L} + \frac{k_D}{k_G} \right)^{-1} A (k_D C_G - C_L) \quad (A5)$$

where :  $m$  is the mass transfer per unit time (g/s),

$k_L$  is the partial gas transfer coefficient for liquid phase  
(m/s),

$k_G$  is the partial gas transfer coefficient for gas phase  
(m/s),

$C_G$  is the gas concentration in the gas phase (g/m<sup>3</sup>), and

$C_L$  is the gas concentration in the liquid phase (g/m<sup>3</sup>).

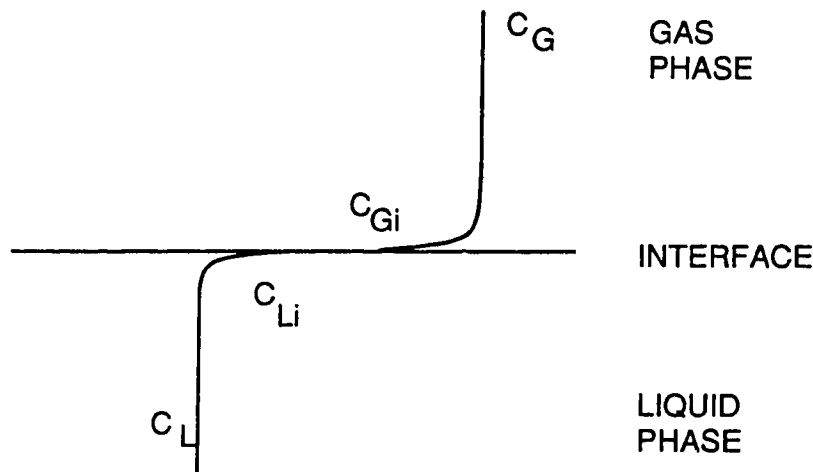


FIGURE A1 Typical gas-liquid interface (from Popel, 1974)

The partial gas coefficients for gases have usually a very small value both in the gas and liquid phases and they are, for example, in the order of  $10^{-5}$  and  $10^{-9}$  magnitude for oxygen in air and water respectively. Consequently, even for a very soluble gas (i.e. high  $k_D$  value), the ratio of the proportional constant over the partial gas coefficient for gas phase (i.e.  $k_D/k_G$ ) is negligible when compared to the inverse of the partial gas coefficient for liquid

phase (i.e.  $1/k_L$ ). For a sparingly soluble gas such as oxygen, the partial gas transfer coefficient in water can certainly be taken as the total gas transfer coefficient. Moreover, applying the saturation gas concentration in the liquid, the gas transfer equation can be written as :

$$m = k_L A (C_S - C_L) \quad (A6)$$

The relationship between the gas transfer coefficient and molecular diffusion coefficient is developed through the different theories on gas transfer mechanism. The common theories on gas transfer mechanism are the film, penetration, surface renewal and film-surface renewal theories (Popel, 1974).

The film theory proposes that gas molecules are being transported to the 'gas film' at the interface area by molecular and eddy diffusion along with mixing action. This gas film is thought to be stagnant and has a interface thickness depending on the level of turbulence in the gas phase. A similar 'liquid film' also exists at the interface area in the liquid phase as well. The main mechanism of gas transport through both films is via the steady state molecular diffusion. The gas transfer coefficient is then a direct proportion to the molecular diffusion.

The penetration theory does not proceed from stagnant films but rather from fluid elements which are briefly exposed to the gas phase at the interface. During this time of exposure, the gas diffuses or 'penetrates' into the liquid body. This process of penetration, in contrast to the film theory, is described by unsteady diffusion



because the time of exposure is too short for steady state to develop. Also because of this briefness for the time of exposure, a roughly constant time of exposure is assumed for all fluid elements. Thus, the gas transfer coefficient is found to be proportional to the square root of the molecular diffusion coefficient.

The surface renewal theory has the same idea of constant renewal of surface with brief time of exposure for unsteady diffusion as the penetration theory. However, the brief time of exposure of fluid elements is not considered to be constant but rather follows a frequency distribution with the ages of the fluid elements. This frequency distribution is called the surface renewal rate. The gas transfer coefficient is, therefore, proportional not only to the square root of molecular diffusion but also to this surface renewal rate as well.

Finally, the film-surface renewal theory attempts to combine the principles of the film and surface renewal theories. The assumption is that the time of exposure of the fluid elements to the gas phase may be sufficiently long for steady diffusion to develop under low turbulence conditions (i.e. stagnant or very slow streaming water) while this time of exposure will follow the frequency distribution of surface renewal rate under high turbulence conditions. The gas transfer coefficient is then found to be proportional to a complex hyperbolic function and the square root of the molecular diffusion with the surface renewal rate.

The difference in the four theories with respect to the mode of diffusion is basically dependent on the hydrodynamic conditions of the fluid. In the case of aeration over hydraulic structures, the

hydrodynamic conditions are too turbulent for steady state diffusion to develop. The film theory is then invalid for this condition. The surface renewal rate is impossible to measure directly and thus makes the surface renewal theory hard to use practically as well. For unsteady diffusion, the penetration theory is more useful and practical because the time of exposure can be estimated from the sizes of air bubbles involved (Pope<sup>1</sup>, 1974).

## 2.4 Practical Gas Transfer Formulation

Even with the many simplifications, the gas transfer equation as in Equation A6 is still difficult to use practically. The determination of the gas transfer coefficient (i.e.  $k_L$ ) from the molecular diffusion coefficient and the time of exposure is, at the best, very crude. The estimation of the contact area (i.e.  $A$ ) is also very difficult especially in the case of aeration over hydraulic structures. Consequently, other practical approaches to the formulation of the gas transfer equation have been proposed and some of the more common practices will be discussed in the following paragraphs.

If a steady state condition can be assumed for the overall aeration process over hydraulic structures, a constant gas transfer coefficient and constant contact area will be the results. The overall gas transfer coefficient (i.e.  $k_2$  or  $k_L a$ ) can then be defined as the product of the constant gas transfer coefficient and the specific surface area which is the constant contact area over the total volume of fluid. This overall gas transfer coefficient is also

known as the atmospheric reaeration coefficient in both environmental and sanitary engineering fields (Tchobanoglous and Schroeder, 1985).

Factors such as temperature, surfactants and turbulence are found to be influencing this overall gas transfer coefficient. Higher temperature will generally produce a higher value for the coefficient. The presence of surfactants, which include hydrophobic constituents and surface active agents, can be manifold and should be studied on an individual basis. Finally, higher turbulence level will also produce a higher value for the coefficient as well (Holler, 1971).

With the use of the overall gas transfer coefficient, the rate of gas concentration transfer (i.e.  $dC/dt$ ) is then the mass transfer per unit time over the total volume of fluid involved (i.e.  $m/V$ ). Integrating the modified gas transfer equation, the gas concentration at any time is the following :

$$C = C_S - (C_S - C_0) e^{-k_2 t} \quad (A7)$$

where :  $C$  is the gas concentration at time  $t$  ( $g/m^3$ ),  
 $C_0$  is the initial gas concentration ( $g/m^3$ ),  
 $k_2$  is the overall gas transfer coefficient ( $1/s$ ), and  
 $t$  is the time of aeration required ( $s$ ).

In 1957, Gameson introduced the use of deficit ratio which is defined as the upstream oxygen deficit over the downstream oxygen deficit. The use of the deficit ratio has since become popular among

the many researchers on aeration over hydraulic structures. The deficit ratio is a general combination of the upstream and downstream dissolved oxygen condition and is easy to use both in the field and the laboratory. The gas transfer equation can also be expressed using the deficit ratio,  $r$ , such as the following :

$$\frac{1}{r} = \frac{C_s - C}{C_s - C_o} = e^{-k_2 t} \quad (A8)$$

Another common parameter used in describing the oxygen uptake over hydraulic structures is the efficiency coefficient or aeration efficiency (Popel, 1974). Since the time of exposure for oxygen uptake is impossible to determine for flow over hydraulic structures, a constant time of exposure is then assumed for the complete aeration process to take place under steady state condition. Consequently, the right hand side of Equation A7 is no longer a time dependant function but a constant instead and is defined as the efficiency coefficient subtracted by one. The efficiency coefficient,  $K$ , is defined as the percentage change in concentration of the initial deficit and has the following relationships :

$$K = 100 \frac{C - C_o}{C_s - C_o} = 100 \left( 1 - \frac{1}{r} \right) \quad (A9)$$

One last parameter which is used extensively only in sewage treatment practice is called the oxygenation capacity (Popel, 1974). Due to oxygen consumption microbes in sewage, aeration process

will only lead to an equilibrium between oxygen supply and oxygen consumption. The oxygenation capacity of an aeration system is then the rate of oxygen transfer at a standard temperature and pressure, and a net driving force of saturated gas concentration. It can be expressed as the following :

$$oc = k_2 C_S' \quad (A10)$$

where :  $oc$  is the oxygenation capacity ( $g\ O_2/m^3s$ ), and  
 $C_S'$  is the oxygen saturation concentration in pure water  
 at  $10\ ^\circ C$  and  $101.3\ kPa$  ( $g/m^3$ ).

Finally, there exists different theoretical studies on the fundamentals of the gas transfer phenomenon (Mastropietro, 1968). However, this thesis is not going to explore this topic area any longer and the readers are welcomed to explore them on their own.

### 3. AERATION RESEARCHES

#### 3.1 Introduction

The studies by Gameson in the 1950's have probably started the parade of the aeration researches. Researchers from England have been contributing significantly to our understanding of this subject ever since the work of Gameson. Later on, the Dutch researchers started in their own studies in late 1960's. During the 1970's, American researchers also produced some important

advances to our understanding in this aeration process. More recently, researchers from Japan have made significant contributions to this subject as well. However, the research in aeration over hydraulic structures is by no means complete. More studies on this aeration process will provide a better understanding in oxygen uptakes.

The researches on aeration over hydraulic structures have been concentrated on providing a reliable equation in predicting the deficit ratio. Many factors have been found to affect the deficit ratio. These factors will first be discussed while the many empirical equations for the deficit ratio will then be summarized.

### 3.2 Aeration Factors

The mechanism of flow over hydraulic structures involves different phases where air entrainment is prominent. The first phase is the falling jet or plunging nappe over the structures. Although air entrainment in this phase is thought to be minimal, the entrainment potential is greatly affected by this phase. The second phase is the plunging nappe into the pool or the formation of hydraulic jump downstream. Since oxygen transfer is believed to be the direct result of the air entrainment process, empirical formulas predicting the deficit ratio has been proposed using the existing parameters of the flow. These parameters include the temperature, water quality, structure types, fall height, discharge, downstream conditions and turbulence.

Temperature has important effect both on the solubility of gases and on the overall rate of gas transfer (Gameson et.al., 1958). According to experiments, the deficit ratio is also found to increase linearly with temperature. However, the maximum range of temperatures in the experiments was from 0 to 40 °C (Department of the Environment, 1973; Tebbutt and Rasaratnam, 1977). Whether the above results would remain in other temperature range is still debatable. Other researchers have proposed other functions to take into the effect of temperature on the deficit ratio (Holler, 1971).

Water quality is also an important factor for oxygen transfer. The presence of high concentrations of dissolved solids, as in sewage outflow, is known to reduce the saturation dissolved oxygen concentration in water and can significantly reduce oxygen transfer as well. The early method to deal with this problem was to use a constant called 'a' which was based mainly on local knowledge and appearance (Gameson, 1957). Avery and Novak (1978) later argued that the effect of pollutants on the liquid film coefficients is negligible in a highly turbulent situation. They then reasoned that the presence of salt in water would produce more significant effect than the pollutants and thus derived a new set of constants accordingly. Other researchers, however, chose to ignore the effect of water quality on aeration completely.

Structure types are another important factor. Many different types of hydraulic structures exist, but most researchers only distinguished between the structures of normal weir, sloped weir and step weir or cascade. A normal weir is defined as a structure that would create a free plunging nappe or free overfall for the flow.

A sloped weir is a structure with a sloping face. A step weir or cascade consists a large number of small steps. The early method was to provide another arbitrary constant called 'b' for the normal weir and step weir only (Gameson, 1957). Later, Van Der Kroon and Schram (1969) made a series of experiment with different weir configurations and found out that the aeration capacity increase significantly from single weir system to the almost constant value of around a three-weir system. However, most researchers derive their equations based on a single free fall only. A sloped weir is found to provide a significantly less aeration capacity than a normal weir (Tebbutt, 1972) and is thus usually ignored by many researchers. As for step weir, some would chose to use the relationship for the single free fall and follow the steps down while others would derive another equation for the step weir based on experiments (Avery and Novak, 1978; Nakasone, 1987). While the types of structures have been extensively studied, the flow regime related to the structure types, which has a more direct effect on the aeration performance, has not been studied at all (Gulliver and Thene, 1988).

Fall height is considered to be the most important factor on the aeration process. The fall height probably relates to the loss of head or the transformation of potential to kinetic energy downstream. Although the precise influence of height on aeration is still unknown, almost all researchers agreed that fall height is directly affecting the capacity of aeration.

Discharge or flow rate is another major factor for aeration over hydraulic structures. Early researches indicated that the effect



of discharge is minimal and usually neglected in their prediction equations. There are, however, indications that a solid free falling jet is essential for good aeration performance. A disintegrated jet is, therefore, not desirable for good aeration result (Avery and Novak, 1977). The combination of fall height and discharge is thus the important factor for maintaining the falling jet not to disintegrate. As a result, the effect of discharge on the deficit ratio is more prominent in recent researches. (Nakasone, 1987)

Downstream conditions are also important for the aeration process. Hydraulic jumps and downstream pools are the two common conditions encountered. The oxygen uptake in a hydraulic jump has not received much attention and only a few experimental results can be found (Holler, 1971; Apted and Novak, 1973; Avery and Novak, 1975). On the other hand, the downstream pool conditions have been studied more extensively than the hydraulic jump conditions. Early experiments indicated that an optimum depth of receiving water will provide maximum benefit from the given conditions (Jarvis, 1970). Later on, the researches have been concentrated on finding an optimum receiving pool geometry instead of the optimum depth alone (Avery and Novak, 1978). As a result, many prediction equations are derived only for the optimal receiving pool conditions (Department of the Environment, 1973).

Finally, turbulence has long been recognized as one of the major contributors to the aeration process. However, the effect of turbulence to the oxygen uptake over hydraulic structures has not been studied much probably because of its complexity.

### 3.3 Deficit Ratio Prediction Equations

Figure A2 shows a typical sketch of flow over hydraulic structures. A substantial number of researches has studied the oxygen uptake over hydraulic structures. As a result, a substantial number of empirical equations have also been proposed to predict the deficit ratio. Table A1 in the following page provides a rough summary of these empirical equations.

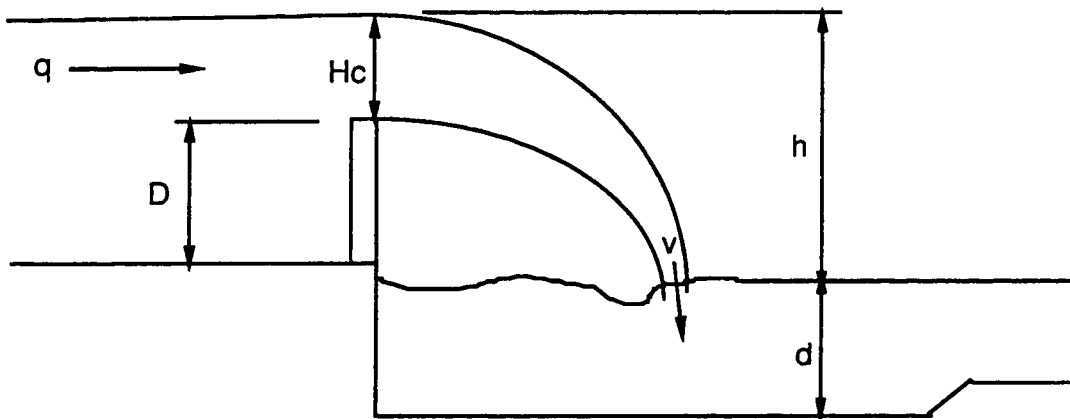


FIGURE A2 Flow over hydraulic structures

| PREDICTION EQUATIONS   | UNITS   | SOURCES            |
|--|---|--------------------|
| Gameson (1957) :<br>$r = 1 + 0.5 a b h$<br>$a = 1.25$ (slight), $1.00$ (moderate), $0.85$ (sewage)<br>$b = 1.0$ (free weir), $1.3$ (step weir)   | h, in meters  | field survey       |
| Gameson, Vandyke and Ogden (1958) :<br>$r = 1 + 0.11 a b (1 + 0.046 T) h$<br>$a = 1.25$ (slight), $1.00$ (moderate), $0.85$ (sewage)<br>$b = 1.0$ (free weir), $1.3$ (step weir)   | h, in feet  | model              |
| Jarvis (1970) :<br>$r(15)^* = 2.05 (h^{0.434})^{**}$   | h, in meters  | model              |
| Holler (1971) :<br>$r(20)^* = 1 + 0.0043 v^2$<br>$r(20)^* = 1 + 0.0010 v^2$<br>$v = (2 g h)^{0.5}$   | v, in ft/s<br>v, in ft/s<br>g, in ft/s <sup>2</sup><br>h, in feet | model<br>prototype |
| Department of the Environment (1973) :<br>$r = 1 + 0.69 h (1 - 0.11 h) (1 + 0.0464 T)^{**}$<br>$r = 1 + 0.38 a b h (1 - 0.11 h) (1 + 0.046 T)^{**}$<br>$a = 1.8$ (clean), $1.6$ (slight), $1.0$ (moderate), $0.65$ (gross)<br>$b = 0.2$ (slope weir), $1.0$ (free weir), $1.3$ (step weir) | h, in meters<br>h, in meters                                      | model<br>prototype |
| Novak (1977) :<br>$\ln r(20)^* = 0.0675 (h^{1.28}) (q^{0.62}) (d^{0.439})$   | d, h, in<br>meters<br>q, in m <sup>2</sup> /hr.                   | model              |
| Avery and Novak (1978) :<br>$r(15)^* = 1 + k (F^{1.78}) (R^{0.53})$<br>or $= 1 + k (h^{1.34}) (q^{-0.36})$   | h, in meters<br>q, in m <sup>2</sup> /s                           | model              |
| Nakasone (1987) :<br>$\ln r(20)^* = C ((D + 1.5 Hc)^x) (q^{(y-1)}) (d^z)$<br>C, x, y, z are constants depends on q and (D + 1.5 Hc)  | D, d, Hc, in<br>m.<br>q, in m <sup>2</sup> /hr.                   | model              |

Notes :

\* deficit ratio at the specified temperature

\*\* for optimum downstream pool depth conditions

**TABLE A1 Summary of deficit ratio prediction equations**

#### 4. CONCLUSIONS

The problem of aeration over hydraulic structures is not only difficult to analyze but also hard to predict. The theory on oxygen uptake over hydraulic structures has been derived mainly from the Fick's Law which is valid for a stagnant body of water only. Furthermore, the many theories predicting the relationship between the diffusion rate and the gas transfer rate are not fool-proof as well. As a result, the theory on oxygen uptake over hydraulic structures can only be a rough guide to the actual process.

Although many prediction equations are available for the deficit ratio, no equation can provide good results in all situations. Many such situations are also site-specific and regime controlled. As a result, a specific prediction relationship is often derived only for the conditions involved. Furthermore, the effect of some existing parameters, such as structure types and turbulence, should be studied in more details in order to provide a better understanding for the oxygen uptake problem.

#### 5. REFERENCES

Apted, P. W. and Novak, P. "Some Studies of Oxygen Uptake at Weirs". Proceedings of the XV Congress, International Association for Hydraulic Research, Paper B23, 1973, pp177-186.

Avery, S. T. and Novak, P. "Oxygen Uptake in Hydraulic Jumps and at Overfalls". Proceedings of the XVI Congress, International Association for Hydraulic Research, Paper C38, 1975, pp 329-337.

Avery, S. T. and Novak, P. "Modeling of Oxygen Transfer from Air Entrained by Solid Jets Entering a Free Water". Proceedings of the XVII Congress, International Association for Hydraulic Research, Paper A59, 1977, pp 467-474.

Avery, S. T. and Novak, P. "Oxygen Transfer at Hydraulic Structures". Journal of Hydraulic Engineering Division, ASCE, Vol. 104, HY11, 1978, pp1521-1540.

Department of the Environment "Aeration at Weirs". Notes on Water Pollution, Number 61, HMSO, 1973.

Gameson, A. L. H. "Weirs and the Aeration of Rivers". Journal of the Institute of Water Engineers, Vol. 11, 1957, pp 477-490.

Gameson, A. L. H.; Vandyke, K. G. and Ogden, C. G. "The Effect of Temperature on Aeration at Weirs". Water Engineering, Vol. 62, 1958, pp 489-492.

Gulliver, J. S. and Thene, J. R. "Gas Transfer at Hydraulic Structures". Proceedings of the 1988 National Conference, ASCE, 1988, pp 985-990.

Holler, A. G. "The Mechanism Describing Oxygen Transfer from the Atmosphere to Discharge through Hydraulic Structures". Proceedings of the XIV Congress, International Association for Hydraulic Research, Paper A45, 1971, pp 373-382.

Jarvis, P. J. "A Study in the Mechanics of Aeration at Weirs". Thesis presented to the University of Newcastle upon Tyne, England, in partial fulfillment of the requirements for the degree of Master of Science, 1970, pp 1-105.

Mastropietro, M.A. "Effects of Dam Reaeration on Waste Assimilation Capacities of the Mohawk River". Proceedings of the 23rd International Waste Conference, 1968, pp 754-765.

Nakasone, H. "Study of Aeration at Weirs and Cascades". Journal of Environmental Engineering Division, ASCE, Vol. 113, No. 1, 1987, pp 1521-1540.

Popel, H. J. Aeration and Gas Transfer. Delft University of Technology, 1974, pp 1-64.

Tebbutt, T. H. Y. "Some Studies on Reaeration in Cascades". Water Research, Vol. 6, 1972, pp 297-304.

Tebbutt, T. H. Y. and Rasaratnam, S. K. "Reaeration Performance of Stepped Cascades". Journal of the Institution of Water Engineers and Scientists, Vol. 31, No. 4, 1977, pp 285-297.

Tchobanoglous, G. and Schroeder, E. D. Water Quality. University of California at Davis, Addison-Wesley Publishing Company, 1985, pp 100-351.

Van Der Kroon, G. T. M. and Schram, A. H. "Weir Aeration - Part I: Single Free Fall". H<sub>2</sub>O(2), No. 22, 1969, pp 528-537.

Van Der Kroon, G. T. M. and Schram, A. H. "Weir Aeration - Part II: Step Weirs or Cascades". H<sub>2</sub>O(2), No. 22, 1969, pp 538-545.